Microglial sialic-acid-binding immunoglobulin-like lectin-H (Siglec-H) and Siglec-11 in neuroinflammation

Dissertation

Zur Erlangung des Doktorgrades (Dr. rer. nat)
der Mathematisch-Naturwissenschaftlichen Fakultät
der Rheinischen-Friedrich-Wilhelms-Universität Bonn

Vorgelegt von

Jens Christopher Kopatz

aus Flensburg

Bonn 2014

Anfertigung mit der Genehmigung der Mathematisch-Naturwissenschaftlichen Fakultät der Rheinischen Friedrich-Wilhelms-Universität Bonn am Institut für Rekonstruktive Neurobiologie.

Datum der mündlichen Prüfung

30.09.2014

Erscheinungsjahr 2015

1. Gutachter Prof. Dr. Harald Neumann

2. Gutachter Prof. Dr. Joachim Schultze

Table of content

Abbreviations

BrdU	Bromodeoxyuridine
CD	Cluster of differentiation
CHO	Chinese ovarian hamster
CNS	Central nervous system
DAMP	Danger associated molecular pattern
DAPI	4',6-diamidino-2-phenylindole
EAE	Experimental autoimmune encephalomyelitis
ESdM	Embryonic stem cell derived microglia
FCS	Fetal calf serum
GAPDH	Glyceraldehyde-3-phosphate dehydrogenase
GFP	Green fluorescent protein
HPLC	High performance liquid chromatography
IFN	Interferon
IL	Interleukin
IgSF	Immunoglobulin superfamily
IPSdM	Induced pluripotent stem cell derived microglia
ITAM	Immunoreceptor tyrosine-based activatory motif
ITIM	Immunoreceptor tyrosine-based inhibitory motif
KDN	2-keto-3deoxy-D-glycero-D-galacto-2-nononic acid
LD50	lethal dose 50%
LPS	Lipopolysaccharide
MAG	Myelin-associated glycoprotein
MTT	3-(4,5-dimethylthiazol-2-yl)-2,5-dipenyl

	tetrasodium bromide
MOG	Myelin Oligodentrocyte Glycoprotein
Neu	Neuraminic acid
Neu5Ac	N-acetylneureminic acid
Neu5Gc	N-glycolylneuraminic acid
NO	Nitric oxide
PAMP	Pathogen-associated molecular pattern
PBS	Phosphate buffered saline
PBST	Phosphate buffered saline tween
PDC	Plasmacytoid dendritic cell
PFA	Paraformaldehyde
PLL	Poly-L-lysine
PMA	Phorbol 12-myristate 13-acetate
PRR	Pattern recognition receptors
PSA	Polysialic acid
ROS	Reactive oxygen species
SAMPs	Self-associated molecular patterns
Siglec	Sialic acid-binding immunoglobulin-like lectins
SHP	Src-homology domain 2-containing phosphatase
SH2	Src homology region 2
SMP	Schwann cell myelin protein
Syk	Spleen-tyrosine-kinase
TBE	Tris-borate-EDTA
TLR	Toll-like receptors
TNF	Tumor necrosis factor

1.Introduction

1.1 Siglecs

1.1.1 The Siglec receptor family

Lectins are carbohydrate-binding proteins that are widespread present in pro and eukaryotic cells. Within mammals they are responsible for functions such as cell-cell interactions, protein trafficking or defense reactions (*1, 2*). Siglecs are a receptor protein subgroup of the immunoglobulin superfamily (IgSF) (*3*). Like most of the lectins the members of this family are linked to the mediation and contribution of various biological processes (*4*). Among others certain members of this family have been shown to recognize complex carbohydrate molecules (*5*). To the first proteins of the Siglec receptor group that were discovered belong sialoadhesin on macrophages and cluster of differentiation (CD) 22 on mature B-cells. Independent work from different groups described an abolishment of sialoadhesin and CD22 mediated cell-cell interactions in cells treated with sialidases (*5-7*). Since the cell surface sialic acids were missing it was concluded that certain sialic acids were ligands for these membrane proteins. Further confirmation of this hypothesis was achieved by experiments with purified sialoadhesin and recombinant forms of CD22 domains (*8, 9*). Based on these findings various groups demonstrated that the structure of the sialic acids is of particular importance for the recognition by cells (*10*). Due to their structural homology CD33, mammalian myelin-associated glycoprotein (*11*) and avian Schwann cell myelin protein (SMP) were later identified to recognize sialic acids as well (*12, 13*). The fact that a group of lectins belonging to the IgSF was able to specifically detect glycan molecules led to the generic name I-type lectin (*14*). Since this name did not allow proper sub-classification of the sialic acid recognizing proteins the term Siglecs was introduced to describe this family of sialic acid binding lectins (*15*).

Sialoadhesin being the first molecule discovered to bind sialic acids received the name Siglec-1. CD22 and CD33 were categorized as Siglec-2 and Siglec-3 while MAG and SMP were put together as Siglec-4a and -4b. Later discovered Siglecs were named in

the order of discovery. For human Siglecs numbers were chosen while rodent Siglecs received capital letters.

1.1.2 The Siglec subfamilies

The Siglec receptors are based on sequence similarity and evolutionary conversion divided in two distinct subfamilies. Siglec-1, 2, 4 and the recently discovered Siglec-15 represent an evolutionary conserved group (*16*). These Siglecs are only distantly related (25-30% sequence identity) and have clear orthologes in all of the Siglec expressing species (*17*).

In contrast, the second group named CD33 related Siglecs is rapidly evolving and presents species dependent divergent features. The CD33 related Siglecs include Siglec-3 (CD33), -5, -6, -7, -8, -9, -10, -11, -12, -14 and -16 in human beings and murine CD33, Siglec-E, -F, -G and –H in mice. The sequence identity within the CD33 related Siglecs is between 50-99% (*17*). In contrast to the conserved group however, these Siglecs are influenced by various gene-altering mechanisms including deletion and exon shuffling. Angata and co-workers hypothesized that this could be the result of an evolutionary arms race between hosts and pathogens within the field of sialic acid recognition (*17*).

Apart from Siglec-4 and -6, the expression of Siglecs is mainly located in cells of the haematopoietic and immune system (*16*). Some of the Siglecs are linked to a specific cell type. Siglec-1 and -2 for example are strictly present on macrophages or B-cells (*18*). However, most of the CD33 related Siglecs are more widespread distributed within the innate immune system. Mouse Siglec-E and human Siglec-9 present a widespread expression pattern on various leukocyte subsets, being so far described on monocytes, macrophages, neutrophiles, dendritic cells and in case of Siglec-E mouse microglia (*19, 20*). Besides T-cells the majority of immune cells express one or several Siglecs (*21*). Especially, cells of the innate immune system are equipped with several Siglecs within their receptor arsenal (*21*). Microglia present the murine Siglec-E, -F and H (*19, 22*) and the human Siglec-3, -11 and -16 on their cell surface (*13, 23, 24*).

1.1.3. Structural features and functions of Siglecs

Siglecs developed 180 million years ago (*25*). Inhibitory Siglecs manifested themselves in greater numbers while only few activating (Siglec-14, 15, 16 in humans) Siglecs can be found. Pressure to de-select the activating Siglecs was coming from the fact that immune reactions would be out of line. Reaching a balance between activation and inhibition was necessary.

A common feature of all Siglecs known to date appears to be that they are single-pass type 1 integral membrane proteins that exhibit an extracellular N-terminal V-set immuneglobulin domain followed by a variable amount of C2-set domains. The V-set domain is considered to be mainly responsible for the ability of the Siglecs to recognize sialic acids while the C2-sets are functioning as spacers. The process of ligand recognition by Siglecs is described in detail in chapter 1.1.4.

Siglec receptor expressing immune cells transmit their intracellular signals via immunoreceptor tyrosine-based activation motif (ITAM) or immunoreceptor tyrosine-based inhibition motif (ITIM) and ITIM-like motif signaling cascades. A line of ITAM-signaling receptors including mouse Siglec-H as well as human Siglec-14, -15 and -16 interact with the ITAM-containing adaptor protein DAP12 via charged amino acids that are located in their transmembrane regions. As a consequence, Src family tyrosine kinases phosphorylate the ITAM protein providing docking sites for Spleen tyrosine kinases (Syk). Subsequently, these kinases activate a line of downstream factors (Figure.1.1) responsible for actions like phagocytosis, cytokine release and cell migration (*26*). The ITAM signaling cascade is counter regulated by ITIM signaling receptors (Figure 1.1). Upon ligand binding these motifs get phosphorylated via Src family tyrosine kinases. As a result, high affinity binding sites for Src homology region 2 domain-containing phosphatase 1 (SHP1) a Src homology region 2 (SH2) containing ubiquitously expressed tyrosine-specific protein phosphatase, are made available. Past activation SHP-1 dephosphorylates key components of ITAM regulated signaling pathways. Important functions of the ITIM mediated effects are the modulation of leukocyte behavior by counteracting ITAM signaling and modulation of anti-inflammatory reactions (*27, 28*).

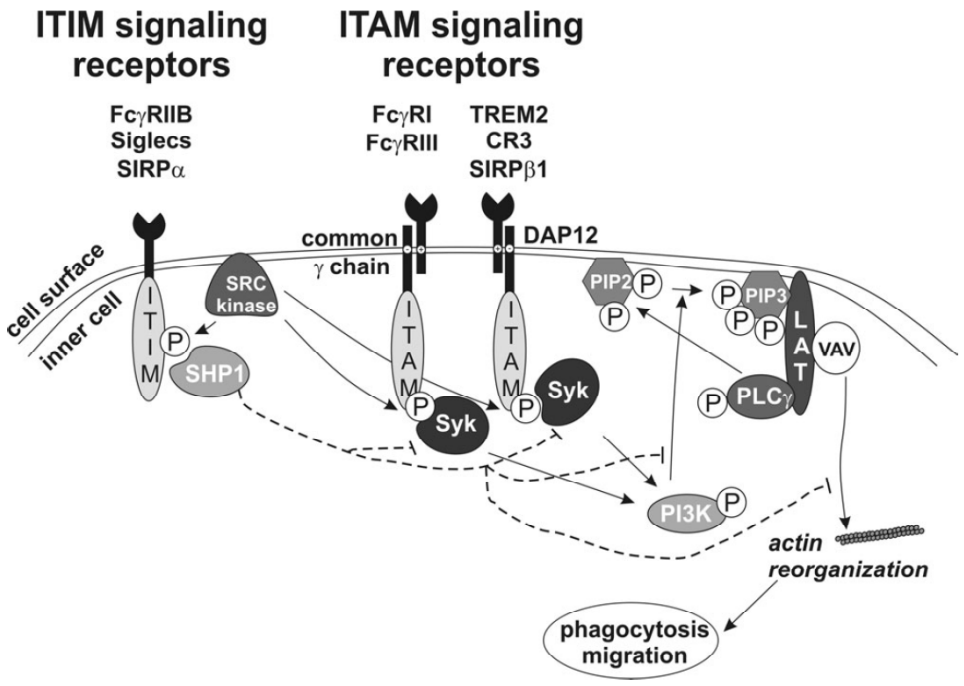

Figure 1.1: Pathway of ITAM and ITIM signaling in immune cells. Past ligand binding ITAM expressing cells execute the phosphorylation of intracellular adaptor proteins. As a consequence syk kinases phosphorylate a line of downstream proteins that orchestrate among others actin reorganization, which is the requirement for migration and phagocytosis. The majority of Siglec receptors are transmitting their signals via the ITAM counter-regulating ITIM pathway. This is done by activation of SHP1, which dephosphorylates and thereby inactivates key elements of the ITAM signaling cascade. Adapted from Linnartz and Neumann, 2013.

The majority of the CD33 related Siglecs plus CD22 act via ITIM signaling cascades while mouse Siglec-H as well as human Siglec-14, -15 and -16 act via the ITAM containing adapter protein DAP12 (*29-31*). Consequently, the functions of the respective Siglecs are determined by their signaling capacities.

A Siglec-E antibody cross-linking experiment revealed an inhibited production of the pro-inflammatory cytokines tumor necrosis factor (TNF)-α and interleukin (IL)-6. Comparable findings were found in Siglec-9 over-expressing macrophages (*32*). Both Siglecs signal via ITIM structures. Furthermore, Toll-like receptors (TLRs) have been shown to up-regulate the Siglec-E expression on macrophages after lipopolysaccharide (LPS) stimulation (*33, 34*). A regulatory feedback mechanism that gets activated in order to control the inflammatory response and prevent harm from sepsis was considered (*34*). On the other hand, the ITAM associated Siglec-14 was

found to be capable to enhance and thereby worsen inflammatory reactions in patients suffering from chronic obstructive pulmonary disease (*35*).
In general, there is a clear connection with ITIM-linked Siglecs counteracting activation signals from ITAM associated cells thereby controlling and modulating various immune and homeostasis relevant processes.

1.1.4 Sialic acid recognition by Siglecs

All nucleated cells are covered on their surface with a dense layer of different sugar chains also referred to as glycans, which in total are called the glycome. In a variety of tissues the outer part of the glycans of the deuterostome lineage of animals (vertebrates and a few higher invertebrates) and of some bacteria is covered by sialic acids (*36*). The different versions of sialic acids form a subclass of the glycome referred to as the sialome. The sialome is defined as the total complement of sialic acid types and linkages (*37*). Sialic acids are derived from the nonulosonic acid family (*38, 39*). They are ubiquitously expressed on the membranes of vertebrate cells. Due to this outermost location the sialic acid containing cell layer is extremely important for cell and tissue interaction. Furthermore, sialic acids are also required during embryonic development (*40*) and for providing signals for self-recognition to complement factors and Siglecs (*41*). Generally, sialic acids are consisting of nine-carbon alpha-keto aldonic acids. They are synthesized by condensation of a neutral six-carbon molecule with a three-carbon pyruvate. While five or six-carbon structures can be found throughout the different species sialic acids are with the exception of a very few bacteria the only occurring nine-carbon sugars in nature (*36*). The C-5 position of the sialic acids can be linked to an N-acetyl group resulting in N-acetylneuraminic (Neu5Ac) or a hydroxyl group resulting in 2-keto-3deoxy-D-glycero-D-galacto-2-nononic acid (Kdn). The 5-N-acetyl group can also be hydroxylated, resulting in N-glycolylneuraminic acid (Neu5Gc). Less commonly, the 5-amino group is not acylated, resulting in neuraminic acid (Neu).
These four sugars (Neu5Ac, Neu5Gc, Kdn, and Neu) represent the main molecules of the sialic acid family which in total includes over 40 neuraminic acid derivatives (*42*). They can be linked in a α2-3, α2-6 or α2-8 manner by sialyltransferases.

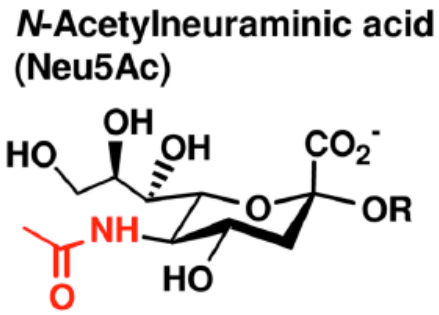

Figure 1.2: Structure of N-acetylneuraminic acid. Located on top of glycans or gangliosides on the surface of cells. When serving as ligand for Siglecs the molecule is linked via its C2 atom with the C3, C6 or C8 atom of its neighboring sialic acid. The kind of linkage of the sialic acids is crucial for the selective recognition by Siglec receptors. Residues at the C5 atom like an acetylated or hydroxylated group determine the basic subgroups of sialic acids (Neu, Neu5Ac, Neu5Gc and Kdn). Adapted from Angata and Varki, 2010.

The most common and most significant member of the family is the Neu5Ac (*42*). Furthermore, the individual Neu5Ac can be connected in a chain up to a length of 180 molecules (Figure 1.2). In some way the majority of the Siglecs recognize Neu5Ac but they differ in their specificity and affinity for type and the linkage of the particular sialic acid molecule. These polysialic acids (PSA) represent therefore endogenous ligands to the Siglec receptors.

The glycan-binding by Siglecs is mediated via their extracellular V-set domain (*3*). Ligand binding depends on several molecular interactions between conserved residues in the V-set domain and the chemical structure of the sialic acids. Certain amino acids of the V-set domain appear to be important for the specific recognition of sialic acids. Of special importance is a conserved arginine residue, which is essential for the binding of the sialic acids to the Siglecs (*21*). This amino acid part is forming a salt bridge with sialic acid carboxylate groups and thereby mediating binding of the sialic acids to the receptor (*42*).

By binding to the respective Siglec receptor sialic acids act as self-associated molecular patterns (SAMPs) (*43*). Recognizing these SAMPs ITIM associated Siglecs act as innate immune modulators that are orchestrating inflammatory reactions in particular after tissue damage (*44*). The ITAM associated Siglecs which are kind of counteracting the effect of the ITIM bearing receptors are considered to be a

evolutionary response of the immune system towards certain bacterial strains that developed the ability to present sialic acids on their surface that can be recognized by ITIM associated Siglecs (*45*).

1.1.5 Siglec-H

A lot of the Siglec related research done so far was aiming at the ITIM linked Siglec receptors. However, to get a more complete idea of how Siglecs work within the immune system it is also important to study the group of ITAM associated Siglecs. The *Siglec-H* gene was discovered in 2006 by a group of investigators that described it to be a cell surface marker on murine plasmacytoid dendritic cells (PDC) (*29, 46*). They also identified the Siglec-H protein on subsets of macrophages in spleen and lymph nodes. However, no expression of Siglec-H on microglia has been reported so far (*47*). Compared to most of the other members of the receptor family Siglec-H is very small and misses its own cytoplasmic signaling domain. Instead, it is linked to the ITAM containing adapter protein DAP12. Until now, no carbohydrate structure that could serve as a potential ligand for Siglec-H has been discovered. Although his exact function is still not clear there is accumulating evidence that Siglec-H might act as an endocytic receptor (*47*). Siglec-H specific engulfment of antigens by plasmacytoid dendritic cells and subsequent presentation to T-cells has been described recently (*48*). Furthermore, extensive involvement of Siglec-H in T-cell immune activation and tumor inhibition has been documented over the past few years as well (*49*). At the moment the overwhelming majority of available data deals with Siglec-H in PDCs but not in the CNS.

1.1.6 Siglec-11

Varki and co-workers first described the CD33 related human Siglec-11 in 2002. The receptor is distinct located in various tissues. Siglec-11 was found in Kupffer cells in the liver, intestinal lamina propria macrophages, microglia cells in the central nervous system (CNS), and perifollicular cells in the spleen, as well as in cells from tonsils and appendix (*23*). The structure of Siglec-11 is composed of five extracellular IgG-like domains, one single-pass transmembrane domain and a cytosolic part that is linked to

ITIM structures (*23*). Intracellular signaling takes place like in the other members of this receptor group via recruitment SHP 1 and 2 units.

Siglec-11 shares over 99% of sequence identity at the first two Ig-like domains to the recently discovered ITAM associated Siglec-16 (*24, 50*). Siglec-16 is likely to have developed by a gene conversion event of the uncharged transmembrane domain and inhibitory cytoplasmic tail of the primordial *Siglec-11* gen. Although it is discussed to be a "paired" Siglec to Siglec-11 that is balancing the functions of microglia there are no functional data on Siglec-16 published at the moment (*24*).

Siglec-E in mice and human Siglec-10 are the functional most similar receptors to Siglec-11 known so far. Siglec-11 shows 90% gene sequence homology to the extracellular domains of Siglec-10. However, while Siglec-10 binds to both α2-3- and α2-6-linked sialic acids, binding of α2.8-linked sialic acid preferentially consisting of three monomers to Siglec-11 has been described (*23*). Since Siglec-11 binds uniquely to α2-8 linked sialic acids the strict focus on this sort of sialic acid distinguishes this receptor from other human Siglecs (*23*). *In vitro* experiments using murine primary microglia that were transduced with a Siglec-11 lentiviral vector revealed neuroprotective and immunomodulating features of Siglec-11. The release of pro-inflammatory cytokines and the phagocytosis of neuronal material were reduced following cross-linking with a flag-specific antibody (*51*). Furthermore, co-culture of Siglec-11 transduced microglia with neurons resulted in significant less neuronal cell death compared to the respective controls (*51*). Therefore, the authors considered Siglec-11 a promising target for further studies and highlighted the potential for therapeutic approaches of this receptor protein after stimulation.

1.2 Microglia within the innate immune system

1.2.1 The innate immune system

The mammalian immune system has developed during evolution to fight off invasions by microorganisms or parasites. Moreover, the elimination of degenerated cells and inhibition of tumor development is another important feature. Through the critically involved cell types and essential mechanisms, the defense system can be divided into innate and adaptive immunity. Innate immunity serves as a first line of defense with

cells rapidly responding to invading microorganisms or abnormal cells/tissues by triggering inflammatory, cytotoxic and phagocytotic reactions. The identification of altered host cells, viral, bacterial, fungal or protozoic pathogens is largely based on critical structural motifs. Innate immune cells express receptors with a broad specificity against these diverse motifs. These structures are referred to as pathogen-associated molecular patterns (PAMPs) (*52*). They represent an assortment of evolutionary conserved structures that are most critical for the vitality of the microbes and thus exert only minor variation. Innate immune cells, in turn, got equipped with complementary receptor systems called pattern recognition receptors (PRRs) that are able to sense such characteristic structures (*52-54*).

The adaptive immune system can recognize, neutralize, eliminate and remember an enormous variety of antigenic structures including tumor cells with a high degree of specificity. Both the innate and adaptive immune systems mutually cooperate to mount and govern efficient host defense activities. Failure in targeting, executing or controlling can either result in insufficient protection and tumor development or autoimmune diseases.

1.2.2 Microglia

Microglial cells are a specialized type of tissue macrophages within the CNS. These cells also known as brain macrophages (*55*) represent an important part of the innate immune system and guarantee its defense capacity. They represent the main part of the innate immune system in the immune privileged area that is the CNS. Del Rio-Hortega first described microglial cells in 1932. The origin of microglial cells was a matter of debate for some time. In 2010 it was shown that in contrast to previous assumptions post-natal hematopoietic progenitors do not significantly contribute to microglia homeostasis in the adult brain compartment. Instead adult microglia derive from primitive myeloid progenitors that arise before embryonic age E8.0 (*56*).

Microglial cells act similar to other kinds of macrophages within the human (and generally the mammalian) body. Their main functions in the adult brain are the homeostatic surveillance and, if required, detection and neutralization of pathogens, support of endangered neurons and phagocytotic clearance of damaged tissue

constituents. Additionally, they can produce and regulate the release of cytokines and chemokines that trigger an inflammatory reaction or attract and activate peripheral immune cells. Microglia, like macrophages are antigen-presenting cells that interact with T cells to recruit the aid of the adaptive immunity (*57*). To execute the various functions, microglial cells need to become activated. Under normal conditions, they are in a resting state, scanning their environment for signs of normal CNS function and integrity (*55*). Upon signs for homeostatic disturbance, they can rapidly transform to an activated state. In their activated form, microglial cells express increased levels of surface structures for cell-cell and cell-matrix interactions, such as major histocompatibility complexes (MHC) class I and II or cell adhesion molecules, as well as an array of receptor proteins for soluble factors (*55*). They can mediate the release of a line of signal and effector molecules, ranging from small lipid mediators to cytokines and enzymes.

Microglia become activated when getting into contact with certain microbial RNA/DNA motifs, cell walls, envelope or surface structures such as lipopolysaccharide (*33*), a cell wall constituent of Gram-negative bacteria. Microglial cells express numerous PRRs, which serve in immune defense by detecting these motifs. The innate immune system replies not only to exogenous but also to endogenous threats. Microglia sense danger associated molecular pattern (DAMP) indicating disorder in host tissues like damaged or mutated cells. They then produce and regulate the release of cytokines and chemokines that trigger an inflammatory reaction or attract and activate peripheral immune cells (*58*). However, microglia are not only screening for pathogens. There is much evidence that they also play a crucial role in tissue repair processes in the brain (*55*). Microglia cells, like other macrophages, reveal a remarkable functional diversity. Their reactions, or reactive phenotypes, depend on the challenging stimulus, the situational context as well as the modulating impact of their environment. Besides others, two very contrary kinds of activation have to be considered in particular. Classical or M1 activation is associated with interferon-γ (IFN) and/or microbial agent, for example LPS driven inflammatory reactions that are often also cytotoxic. The alternative or M2 activation of microglia is strongly related to IL-4 and -13 mediated processes that decrease inflammation and support tissue repair and regeneration (*59*).

These two stages represent the extreme forms of this kind of activation and exhibit a variety of sub-forms in between.

In their IL-4 influenced activated form, alternatively activated microglia express increased levels of surface structures for cell-cell and cell-matrix interactions, such as MHC molecules I and II. Furthermore, they interact with other CNS-resident cells, including neurons, astrocytes, oligodendrocytes, endothelial cells as well as with immune cell populations, ranging from neutrophils to T and B lymphocytes (*55*). These cell-cell communications are essential for the support of neurogenesis and neuroprotection (*55*). In this regard, microglia themselves can orchestrate and become instructed by virtually all of the above cell types. Cellular communication is thereby, not exclusively but essentially, built on the exchange of cytokines and chemokines (*55*). The understanding of signals and mechanisms which initiate, guide and limit microglial activation and activities are gathering more and more attention as these cells seem to be at a key position to maintain CNS health and function.

1.2.3 Microglial cells in pathogenesis

Besides protecting the CNS against invading microorganisms and maintaining its homeostasis microglia are also involved in a series of diseases. A substantial part of the pathogenic processes is linked to neurodegeneration due to miss-regulated activation of microglia. Multiple sclerosis and Alzheimer`s disease but also bacterial and viral infections (*60, 61*) are among the most prominent cases of this phenomenon. The damage done to the neural structures is often due to the unbalanced release of pro-inflammatory cytokines like TNF-α, reactive oxygen species (ROS) or nitrate oxide (NO) (*62*). The consequences are among others loss of neuronal structures or demyelination of nerve fibers (*63*).

Another important finding regarding neuropathology and inflammation is the development of glioma. Microglia have been shown to be substantially involved in growth and progression of this kind of cancer (*64*). Microglia and invading macrophages are the largest fraction of the inflammatory environment that is surrounding the glioma cells. More than 30% of the total tumor mass is finally created by tumor infiltrating microglia and macrophages (*64*). However, instead of initiating

cytotoxic anti-glioma actions the microglia/macrophages get polarized towards a M2 phenotype, which is supporting cell proliferation and therefore tumor progression (*65*). The role of the Siglec receptor family within the field of neuroinflammation and degeneration is not fully understood yet. However, there is increasing evidence that they could be important contributors to these processes.

1.3. Aim of the study

Depending on their structure Siglec receptors can modulate pro- or anti-inflammatory signaling. The aim of the project is to investigate the role of Siglecs on microglia in an inflammatory environment. As model receptors, the ITAM linked Siglec-H and the ITIM linked Siglec-11 were chosen. The regulation of both receptors under different kinds of stimulation as well as their involvement in essential inflammatory processes like phagocytosis or modulation of cytokines will be investigated. While there is no binding partner for Siglec-H known so far Siglec-11 recognizes α2-8 linked oligosialic acids, preferentially consisting of three monomers. Therefore, Siglec-11 stimulation will be used in cell culture and animal systems. The therapeutic potential of both Siglecs will be investigated with respect to pathological processes linked to neuroinflammation.

2. Material and Methods

2.1 Materials

2.1.1 Buffers

10X (0.125M) Phosphate buffered saline (PBS), pH 7.3

Component	Concentration	Company
NaH2PO4*H2O	0.007 M	Roth, Germany
NaH2PO4*7H2O	0.034 M	Roth, Germany
NaCl	0.6 M	Roth, Germany
ddH2O	up to 1 liter	Roth, Germany

10X Tris-borate-EDTA (TBE) buffer

Component	Concentration	Company
Tris-Base	1.78 M	Roth, Germany
Boric Acid	1.78 M	Sigma, Germany
EDTA	0.04 M	Roth, Germany
ddH2O	up to 2 liter	Roth, Germany

PBS-Tween-20 (PBST)

Component	Concentration	Company
Tween-20	500 µl	Sigma, Germany
PBS (1x)	up to 1 liter	

Arsenite buffer

Component	Concentration	Company
Sodium-arsenite	2 %	Sigma, Germany
HCl	0,5 N	Roth, Germany

Thiobarbituric acid buffer

Component	Concentrations	Company
2-Thiobarbituric acid	0,1 M	Sigma, Germany
(adjusted to pH9)		
ddH_2O	100 ml	Roth, Germany

Acid butanol

Component	Concentration	Company
Butan-1-ol	100 ml	Sigma, Germany
HCl	12 N (5% (v/v))	Roth, Germany

Wash buffer (Fusion protein purification)

Component	Concentration	Company
NaH2PO4*H2O (pH 7)	20 mM	Roth, Germany
ddH_2O	up to 1 liter	Roth, Germany

Elution buffer (Fusion protein purification)

Component	Concentration	Company
HCl (pH 2.7)		Roth, Germany
Glycin	0.1 M (up to 1 liter)	Roth, Germany

Storage buffer (Fusion protein purification)

Component	Concentration	Company
TRIS-HCl (pH 9)	1 M	Roth, Germany
ddH_2O	up to 1 liter	Roth, Germany

Borane buffer (BrdU)

Component	Concentration	Company
Borane	0.1 M	Roth, Germany
ddH_2O	up to 1 liter	Roth, Germany

2.1.2 Solutions and reaction mix

4% Paraformaldehyde (PFA), pH 7.3

Component	Amount	Company
PFA	20 g	Roth, Germany
NaOH (1 M)	30 ml	Sigma, Germany
PBS (10x)	50 ml	Roth, Germany
ddH2O	up to 1 liter	Roth, Germany

Reverse transcription mix

Component	Amount	Company
Total RNA	5 µg	
Hexanucleotide Mix (10X)	1 µl	Roche, Germany
dNTP mix (10 mM)	1 µl	Sigma, Germany
DTT mix (10 mM)	2 µl	Invitrogen, Germany
5X RT 1st Strand Buffer	4 µl	Invitrogen, Germany
RT enzyme (200 U/ml)	1 µl	Invitrogen, Germany
ddH2O	up to 20 µl	Roth, Germany

RT-PCR reaction mix (50 µl)

Component	Amount	Company
cDNA (200 ng/µl)	5 µl	
Buffer (10X)	5 µl	Roche, Germany
dNTP mix (10 mM)	2 µl	Sigma, Germany
Primer mix (10 pmol/µl)	2 µl	MWG, Germany
Taq polymerase (5 U/l)	0.2 µl	Roche, Germany
ddH2O	33.8 µl	Roth, Germany

qRT-PCR reaction mix (25 µl)

Component	Amount	Company
cDNA (200ng/µl)	1 µl	
Syber Green Master Mix	12.5 µl	Invitrogen, Germany

Primer mix (10 pmol/µl)	2 µl	MWG, Germany
ddH2O	9.5 µl	Roth, Germany

Polyacrylamide gel

Component	Amount	Company
Acrylamide	12 ml	Roth, Germany
5xTBE buffer	8 ml	Roth, Germany
APS	400 µl	Roth, Germany
Temed	40 µl	Roth, Germany
ddH2O	20 ml	Roth, Germany

1% Agarose gel

Component	Amount	Company
Tris-Base	0.5 g	Biozym, Germany
Ethidium Bromide	5 µl	Roth, Germany
TBE (1x)	50 ml	

2.1.3 Cell culture media and reagents

Basal cell culture medium (for primary microglia)

Component	Concentration	Company
BME	500 ml	Gibco, Germany
Fetal bovine serum	10 %	Gibco, Germany
L-glutamine	1 %	Sigma, Germany
D-glucose (45 %)	1 %	Sigma, Germany
Penicillin/Streptomycin (100X)	1 %	Gibco, Germany

N2 cell culture medium (for iPSdM and ESdM)

Component	Concentration	Company
DMEM/F-12	500 ml	Gibco, Germany
N2 medium	5 ml	Gibco, Germany

Penicillin/Streptomycin (100X)	1 %	Gibco, Germany
L-glutamine	1 mM	Gibco, Germany
D-Glucose (45 %)	1.7 ml	Sigma, Germany

DMEM cell culture medium (for HEK 293 t/ft)

Component	Concentration	Company
DMEM high glucose	500 ml	Gibco, Germany
Fetal calf serum	10 %	Gibco, Germany
Penicillin/Streptomycin (100X)	1 %	Gibco, Germany
L-glutamine	1 %	Gibco, Germany
Na-pyruvate	4 mM	Gibco, Germany
Non-essential amino acids	0.1 mM	Gibco, Germany

Advanced DMEM cell culture medium (for transfection)

Component	Concentration	Company
Advanced DMEM	500 ml	Gibco, Germany
Fetal calf serum	3 %	Gibco, Germany
Penicillin/Streptomycin (100X)	1 %	Gibco, Germany
L-glutamine	1 %	Gibco, Germany

DMEM cell culture medium (for glioma cells)

Component	Concentration	Company
DMEM F/12	500 ml	Gibco, Germany
Fetal calf serum	10 %	Gibco, Germany
Penicillin/Streptomycin (100X)	1 %	Gibco, Germany

RPMI cell culture medium (for THP-1 cells)

Component	Concentration	Company
RPMI	500 ml	Gibco, Germany
Fetal calf serum	10 %	Gibco, Germany
Penicillin/Streptomycin (100X)	1 %	Gibco, Germany
Pyruvate	1 %	Gibco, Germany

Other reagents

10x4 ligase	Roche Diagnostics, Germany
Bgl II	Roche Diagnostics, Germany
Chloroquine diphosphate salt	Sigma, Germany
DNA ladder	Invitrogen, Germany
EcoRV	Roche Diagnostics, Germany
Hexamer random primers	Roche Diagnostics, Germany
Latex Beads (PE)	Polyscience Inc., Germany
Latex Beads (FITC)	Polyscience Inc., Germany
Lipofectamine 2000 reagent	Invitrogen, Germany
LPS	Roche, Germany
	Enzo, Germany
Mouse Interferon-alpha	Hycult Biotech, Netherlands
Mouse Interferon-Gamma	R&D Systems, Germany
Mouse TNF-alpha	R&D Systems, Germany
MVP Total RNA, human brain	Agilent Technologies
N-Acetylneuraminic Acid	Nacalai Tesque inc, Japan
Polyethylenglycol 6000	Roth GmbH, Germany
Polysialic acid	Lipoxen, UK
	Carbosynth, UK
Puromycin	PAA, Germany
Phorbol 12-myristate 13-acetate	PAA, Germany
Stains all solution	Sigma, Germany
Trypsin-EDTA (0,025%)	Gibco, Germany
Zeocin antibiotic	Roth GmbH, Germany

2.1.4 Cells and animals

Cell lines

Cell line	Company
293 FT HEK cells	Invitrogen, Germany

Chinese ovarian hamster cells	Invitrogen, Germany
E.coli Top10	Invitrogen, Germany
Embryonic stem cell derived microglia (ESdM)	Generated by our lab
GL261 glioma cells	Provided by Prof. Herrlinger/Dr. Glas, University of Bonn
Induced pluripotent stem cell derived microglia (iPSdM)	Generated by our lab
Primary mouse derived microglia	Obtained from C57/Bl6 newborns
SMA glioma cells	Provided by Prof. Herrlinger/Dr. Glas, University of Bonn
THP-1	ATCC TIB-202, USA

Animals

Mouse strain	Company
C57/Bl6/6J mice	Charles River Laboratories, Germany
B6D2 F1/C57/Bl6/6J Siglec-11 transgenic mice	University of Bonn, Germany

2.1.5 Antibodies

Primary antibodies and isotype controls

Antibody	Host	Reactivity	Conj.	Company
Anti-BrdU	mouse			BD Systems, USA
CD16/32 (Fc block)	rat	mouse		BD Pharmingen, Germany
Fc detection	rat	mouse	FITC	BD Pharmingen, Germany
$IgG_{2b,\kappa}$ Isotype control	rat	/	biotin	BD Pharmingen, Germany
IgG_2 Isotype control	goat	/	biotin	Abcam, Germany
Siglec-H	rat	mouse	biotin	Hycult biotech, Germany
Siglec-11	goat	human	biotin	R&D, Germany
Siglec-11 4c4	mouse	human		Prof A. Varki, USA

Secondary antibodies

Antibody	Host	Reactivity	Conj.	Company
PE	/	mouse	streptavidin	BD Pharmingen,
IgG	rat	mouse	Cy3	Jackson, USA
IgG	goat	mouse	Alexa 488	Jackson, USA

2.1.6 Primer

qRT and RT-PCR (all purchased from MWG, Germany)

Gene	Orientation	Sequence
Human GAPDH (qRT)	forward	5'- CTGCACCACCAACTGCTTAG-3'
	reverse	5'- TTCAGCTCAGGGATGACCTT-3'
Human TNF-α (qRT)	forward	5'- GACAAGCCTGTAGCCCATGT-3'
	reverse	5'- AGGACCTGGGAGTAGATGAGG-3'
Mouse GAPDH	forward	5'- ACAACTTTGGCATTGTGGAA-3'
(RT/qRT)	reverse	5'- GATGCAGGGATGATGTTCTG-3'
Mouse IL-1 β (qRT)	forward	5'- CTTCCTTGTGCAAGTGTCTG -3
	reverse	5'- CAGGTCATTCTCATCACTGTC -3'
Mouse TNF-α (qRT)	forward	5'- TCTTCTCATTCCTGCTTGTGG-3'
	reverse	5'- AGGGTCTGGGCCATAGAACT-3'
Siglec-H (RT/qRT)	forward	5'-GTGACAGACCTCACTCACAGCCC-3'
	reverse	5'-GGTCGTGGGGCCCAGGGATA-3'
Siglec-H fusion protein	forward	5'-ATAAGATCTGGTGACATTGAGCTG
(RT)		GATAG-3'
	reverse	5'-CATAAGGTTCTGGAAACTGCTTTA
		TTCTC-3'
Siglec-11 I (RT)	forward	5'- ACAGGACAGTCCTGGAAAACCT-3'
	reverse	5'- AGGCAGGAACAGAAAGCGAGCAG -3
Siglec-11 genotyping	forward	5'- GGAGATGTCAGGGATGGTTC-3'
	reverse	5'- AGCAGCGTATCCACATAGCGT-3'
Siglec-11 II (qRT/RT)	forward	5'-CACTGGAAGCTGGAGCATGG-3'

reverse	5’-ATTCATGCTGGTGACCCTGG-3’

2.1.7. Consumables, equipment and software

Consumables

6-well culture plates	VWR International, Germany
15 ml tubes	VWR International, Germany
50 ml tubes	Sarstedt, Germany
5 ml, 10 ml, 25 ml pipettes	Sarstedt, Germany
75 ml, 175 ml culture flasks	Sarstedt, Germany
5 ml polystyrene round-bottom tubes	BD Falcon, Germany
3 cm, 5 cm, 10 cm culture dishes	Sarstedt, Germany
500 µl, 1000 µl plastic tubes	Eppendorf, Germany
PCR tubes	Biozym Diagnostics, Germany
10 µl, 100 µl, 1000 µl tips	Eppendorf, Germany
5 ml, 10 ml syringes + needles	Braun, Germany
Filters (0.45 µm, 0.2 µm pore)	Sarstedt, Germany

Equipment

ABI 5700 Sequence Detection System	PerkinElmer, USA
Centrifuges	Megafuge, 1.OR. Heraeus, Germany
	Biofuge Fresco, Heraeus, Germany
Electrophoresis	Peqlab, Germany
Mastercycler realplex 4	Eppendorf, Germany
Flow cytometer	FACS Calibur, BD Bioscience, Germany
NanoDrop ND-1000 spectrophotometer	Peqlab, Germany
Envision Multiplate Reader	Perkin Elmer, USA
HRP sepharose anion-exchange column (53ml)	GE Healthcare, Germany

Software

Cellquest Pro	BD Biosciences, USA
CorelDRAW	Graphics Suite 11, Germany
Openlab4.0.1	Improvision, Germany
EndNote X	Thomson ISI ResearchSoft, USA
FlowJo 6.4.7	Tree Star, USA
ImageJ 1.44p	National Institute of Health, USA
Microsoft Office 2004	Microsoft, USA
Realplex 4	Eppendorf, Germany
Wolframalpha	Wolfram Research, USA

2.1.8 Kits

Bradford protein assay	Sigma, Germany
Colorimetric (MTT) Kit for cell survival and proliferation	Millipore, Germany
RNeasy Mini Kit	Qiagen, Germany
RNeasy Mini Kit for lipid tissue	Qiagen, Germany
RNAse free DNAse Kit	Qiagen, Germany
QIAprep Plasmid Miniprep	Qiagen, Germany
Endofree Plasmid Maxiprep	Qiagen, Germany
Red Extract-N-Amp Tissue PCR Kit	Qiagen, Germany

2.2 Methods

2.2.1 Cell culture

Primary microglia were prepared from brain tissue of newborn (P3-P4) C57Bl/6 mice. In brief, the pubs were decapitated and scull bone and meninges were removed. Brain tissue was dissociated mechanically by trituration. Cells from the hippocampus and cortex regions were taken for culture in 75 ml flasks. After 14-21 days in basal medium the cells formed a confluent layer of glial cells. For harvesting the flasks were shaken on a rotary shaker for 3 hours at 350 rpm and detached microglia were plated onto

poly-L-lysine (PLL)-coated cell culture dishes. All cell lines used were kept on 10 or 15 cm culture dishes under normal conditions at 37 °C and 5 % CO_2. Cell culture media were utilized as indicated in chapter 2.1.3. Splitting was done via trypsin treatment for 5 minutes subsequent centrifugation and seeding on new culture dishes.
The human monocyte line THP-1 was cultured in 75 ml cell culture flasks. For differentiation of human tissue macrophages the line was cultured for 3 hours in the normal cell culture medium containing 0.5 µM phorbol 12-myristate 13-acetate (PMA). Medium was changed into PMA free culture medium and the cells were cultured for 24 hours to allow differentiation into mature macrophages.

2.2.2 RT- and quantitative RT-PCR

RNA was isolated from cultured cells or tissue samples by using the RNeasy Mini and RNeasy for lipid tissue Kit. Reverse transcription of the RNA (5 µg/sample) was performed using Super Script III reverse transcriptase and hexamere random primers. The concentration of the samples was determined via NanoDrop spectrophotometer and diluted to 200 ng/µl past transformation into cDNA. Siglec-11 genotyping of the transgenic mice via PCR was done over 30 cycles (initial denaturation 95 °C for 3 minutes, denaturation 95 °C for 30 seconds, annealing 60 °C for 40 seconds, extension 72 °C for 50 seconds, final extension 72°C for 10 minutes). The other RT-PCR products were amplified for 35 cycles but Siglec-H (initial denaturation 94 °C for 10 minutes, denaturation 94 °C for 90 seconds, annealing 65,5 °C for 60 seconds, extension 72 °C for 60 seconds, final extension 72 °C for 10 minutes), Siglec-11 I (initial denaturation 94 °C for 2 minutes, denaturation 94 °C for 90 seconds, annealing 62.5 °C for 60 seconds, extension 68 °C for 60 seconds, final extension 68 °C for 10 minutes) and Siglec II (initial denaturation 94 °C for 5 minutes, denaturation 94 °C for 60 seconds, annealing 60 °C for 60 seconds, extension 72 °C for 60 seconds, final extension 72°C for 10 minutes) required different conditions. All qRT-PCR reactions were running for 40 cycles if not indicated otherwise (initial denaturation 95 °C for 8.30 minutes, denaturation 95 °C for 15 seconds, annealing 60 °C for 30 seconds, extension 72 °C for 30 seconds, stepwise to 95 °C over 20 minutes). Ethidium bromide agarose gels of 1 % were used for visualization of PCR products.

Gene transcripts of the housekeeping gene glyceraldehyde-3-phosphate dehydrogenase (GAPDH) were applied as internal control. Quantitative RT-PCR with specific oligonucleotides was performed with SYBR Green PCR Master Mix using the ABI 5700 Sequence Detection System and amplification protocol for the ABI 5700 Sequence Detection System. Amplification specificity was confirmed by the analysis of the melting curves. Results were analyzed with the ABI 5700 Sequence Detection System version 1.3. Oligonucleotides used for PCR amplification are listed in chapter 2.1.6. The δδCT method with GAPDH as internal standard was performed for real-time PCR quantification

2.2.3 Bromo Deoxyuridine (BrdU) cell proliferation assay

Cell proliferation was assayed via detection of BrdU incorporation into the cells during mitosis. Microglia cells were transduced with a green fluorescent protein (GFP) expressing construct (kindly provided by the groop of Prof. Oliver Brüstle) prior to the experiments. In brief, the two glioma cell lines SMA560 and GL261 were mono- or co-cultured with IFN-γ activated GFP-expressing microglia (10^4 cells from each type) on four-well chamber slides for 24 hours. BrdU was added to glioma cells in a concentration of 10 µM. After time intervals of 0.5, 1, and 2 hours the cells were fixed with 4 % PFA and washed with PBS. Membrane permeabilization was achieved by 30 minutes incubation with 0.5 % Triton X-100 (Sigma-Aldrich) and subsequent DNA denaturation by incubation in 2 M HCl for 10 minutes. For the neutralization of the acid, 0.1 M borane buffer was used for another 10 minutes. Extensive washing with PBS was performed in-between each of the respective steps. Following 15 minutes of blocking (5 % FCS/0.1 % Triton X-100/ PBS) a monoclonal mouse anti-BrdU antibody (3 % FCS/0.1 % Triton X-100/ PBS) was added. The samples were washed with PBS and a Cy3-conjugated rat-anti-mouse secondary antibody was added (3 % FCS/0.1 % Triton X-100/ PBS). Before mounting, the nuclei were stained for 2 minutes with 4',6-diamidino-2-phenylindole (DAPI) in a dilution of 1:10000. Subsequently, analysis by confocal microscopy was performed. For quantification at least three pictures of each condition per experiment were taken. Using ImageJ software the ratio of BrdU-positive

plus GFP-negative glioma cells to the total number of GFP-negative glioma cells in mono- and co-culture was determined.

2.2.4 Generation of the Siglec-H fusion protein

For the creation of the Siglec-H fc fusion protein a commercially obtained fc part containing pFUSE-hIgG1e3-Fc2 (IL2ss) backbone plasmid was used. The extracellular part of the Siglec-H receptor was purified via RT-PCR from a mouse IRAVp968D06168D full-length cDNA clone (ImaGenes). For the assembling the restriction enzymes Bgl II and EcoRV (1 hour at 37 °C) and 10x T4 ligase (16 °C over night) were used according to the manufacturers instructions. 100 to 500 ng of the plasmid were put via transformation into competent cells (E.coli Top10). The cells were plated on antibiotic resistant culture dishes and incubated at 37 °C over night. Colonies were picked and grown in antibiotic (Zeocin) containing LB-medium. Glycerol stocks were created from the successfully grown cultures.

2.2.5 Production of viral particles and the Siglec-H fusion protein

The plasmids for the murine Siglec-H knock-down (TRCN0000068083, Target sequence: 5'-GCCCAAATTAACATTAGAGAA-3') were a kind gift from Prof. Veit Hornung from the University of Bonn. A pLKO.1 puro non targeting control vector (Sigma, Catalog Nr. SHC002) was used as control.

Plasmids were transfected into FT293 HEK cells via a $CaCl_2$ based protocol. In brief, 6.5 x 10^6 cells were plated on 15 cm cell culture dishes. Regular cell culture medium was changed directly before the procedure to MEF medium with 5 % FCS. The vector plasmid (25 µg) was put together with 37.5 µg of packaging plasmids (25 µg 3rd generation: pMDL gag/pol PRE + 12.5 µg pRSV-Rev) and 15 µg of envelope plasmid. 1.125 ml of sterile H_2O and 125 µl of $CaCl_2$ (2.5 M) was added to the plasmids and incubated for 3 minutes. 1.25 ml of 2x HBS was added and the solution was mixed properly. Afterwards, an incubation period of 25 minutes was given. Finally, the solution was added to the HEK 293 FT cells and over night incubation at 37 °C and 5 % CO_2 was performed. Next morning the medium was changed and the viral particles

were harvested after 24 and 48 hours (with another medium change after 24 hours in between). The viral particle-containing medium was mixed 1:1 with the regular culture medium and added for 72 hours in total to the microglial cells. Positive selection of the transduced cells was achieved by adding Puromycin (25 µg/ml, PAA) to the cells after the medium was changed. The efficiency of the respective treatment was determined via flow cytometry.

Plasmids for lentiviral knock-down of human Siglec11 (shRNASig11: TRCN0000062841, Open Biosystems) were obtained from a knock-down library in a human pLKO.1 lentiviral shRNA target gene set backbone (Open Biosystems). A pLenti 6.2/V5_DEST Gateway Vector (Life technologies) without target gene served as control vector. Here, for production of lentiviral particles a different protocol than for the Siglec-H knock-down was used. PLL coated HEK 293 FT cells were transfected with the targeting and packaging plasmids pMD2.G and psPAX2. Two hours before transfection the cell culture medium was changed from regular MEF to an advanced MEF medium. For transfection of an 80 % confluent 10 cm culture dish lentivector (18.5 µg), helper (9.25 µg) and envelope plasmid (9.25 µg) were mixed together with 61.5 µl 2.5 M $CaCl_2$ and filled up with distilled water to 600 µl total volumes. After 5 minutes of incubation, 600 µl of 2xHBSS was added. 15 minutes of incubation was given subsequently to allow formation of complexes. In the meantime 25 µM/ml chloroquine was added to the cells to increase transfection efficiency. Medium was changed 5 hours post-transfection back to the regular MEF medium to remove the chloroquine and a second time, 12 hours later. Supernatant was then collected 48 and 72 hours after transfection. For precipitation the viral particle containing supernatant was incubated for 1.5 hours with 8.5 % Polyethylenglycol, 0.3 M NaCl and PBS at 4 °C. Subsequently the solution was centrifuged with 4500 g at 4 °C for at least 30 minutes. The viral particle-containing pellet was resuspended in 1 ml of 1xPBS and added to the target cells. After 72 hours of incubation transduced cells were selected by addition of 1 µg/ml puromycin. The knock-down efficiency was determined by qRT-PCR and flow cytometry.

The Siglec-H fc fusion protein plasmid was transfected into chinese ovarian hamster cells in a similar way to the plasmids coding for viral particles except that a low IgG FCS containing cell culture medium was used. The protein containing supernatant was

directly taken for purification via a protein-G sepharose column designed to detect the fc tag of the protein. The purification procedure was carried out according to the manufacturers instructions. The concentration of the elution fractions was determined via a Bradford protein assay. 50 µl of fraction was diluted with reagent solution in a ratio of 1:16 and incubated for 10 minutes at room temperature. To determine the concentration, the solution was measured at a wavelength of 465 nm with a reference wavelength of 595 nm against a standard. The Siglec-H fusion protein was stored at -80 °C.

2.2.6 Bead phagocytosis assay

For investigation of phagocytosis activity microglial cells and macrophages were plated on 6 well plates in a concentration of 2,5 x 10^5 cells per well. The cells were stimulated depending on the experiment 24 hours prior to the addition of the beads if not indicated otherwise. For the Siglec-H related experiments FITC fluorescent streptavidin coated beads were pre-incubated with biotin linked primary Siglec-H or Isotype control antibodies (500 ng/ml) for 1 hour at 4 °C to increase the uptake specificity. Incubation with the beads (1 µl beads/ml medium) was performed for 1h under regular cell culture conditions (37 °C, 5 % CO_2). For analysis the media was removed and cells were treated for 1-2 minutes with trypsin (0.025 %) in order to get rid of beads sticking to the surface of the microglia. Afterwards the cells were washed 3x with PBS before being detached mechanically. Fluorescence intensity of 3 x 10^4 cells per sample was measured via the FL-1 channel by flow cytometry.

For the Siglec-11 related phagocytosis experiments PE labeled latex beads were used in a concentration of 1 µl beads/ml medium. The cells were stimulated for 24 hours and beads were added for 1 hour. All steps were performed under regular cell culture conditions (37 °C, 5 % CO_2). For analysis fluorescence intensity of 3 x 10^4 cells per sample was measured via the FL-2 channel by flow cytometry.

2.2.7 Flow cytometry

The mouse microglia cells (ESdM and primary microglia) were harvested mechanically and diluted to a concentration of 1 x 10^6 cells per ml. The samples were washed 3 times with PBS via centrifugation. A rat anti-mouse CD16/CD32 fc blocking antibody (0.5 mg/ml, 1:100 dilution) was added 5 minutes prior to staining with the biotin labeled Siglec-H primary antibody. The incubation time for the primary antibodies was 1 hour at 4 °C. Streptavidin linked PE serving as secondary antibody was added for 30 minutes at 4 °C (0.5 mg/ml, 1:200 dilution). For analysis 3x10^4 cells per sample were measured via a FACS Calibur flow cytometer. Primary microglia derived from the Siglec-11 transgenic mice were stained with a non-commercial 4c4 Siglec-11 antibody on ice (1:10 dilution). The secondary antibody was an alexa 488-conjugated goat IgG2 directed against mouse (1:200 dilution) that was added for 30 minutes on ice as well.
Human microglia cells were immunostained with biotin-conjugated Siglec-11 specific antibodies followed by streptavidin-PE. An irrelevant isotype antibody was used as control. Cells were analyzed by flow cytometry like the mouse microglia. The THP-1 cells were stained the same way like the microglia. The fusion protein was taken instead of the primary antibody (25 µg/ml) and a FITC linked antibody (0.5 mg/ml, 1:100 dilution) directed against the fc-tag of the protein was used for detection. The incubation time for both steps was 1 hour at 4 °C.

2.2.8 Purification of polysialic acid (PSA)

As a preparative step the samples were heated at 65 °C for 90 minutes to break the long chained PSA down into smaller peaces. For separation of the fragments PSA (250 mg) was subjected to a 53 ml HRP sepharose anion-exchange column and separated via a high performance liquid chromatography (HPLC) system. The flow-through was collected in 80 fractions with a respective volume of 8 ml. To get rid of buffer residues the samples were lyophilized and the yield solved in PBS or distilled water. To increase the sample concentration 3-4 fractions of interest were pooled together. Samples of the fractions were loaded on a polyacrylamide gel separated for 4 hours and stained with stains all solution for size determination. Using the Thiobarbituric acid based method published by Aminoff et al. in 1961 (*66*) the

quantification of the fractions was performed. Commercially obtained Neu5Ac served as standard to determine the respective concentrations. The standard and test samples are treated with 25 µl of 25 mM periodic acid in 0.125 M H_2SO_4 and incubated at 37 °C for 30 minutes. Past the incubation step 20 µl of 2 % sodium arsenite solution (in 0.5 N HCl) was added to each sample in order to reduce the excess of periodate. After 2 minutes at room temperature 200 µl of 2-thiobarbituric acid (0.1 M, pH 9) was given to the samples. Subsequently, a heating step (7.5 minutes at 99 °C) was performed that caused the formation of a red colored complex. The solution was cooled on ice for 5 minutes and afterwards shaken with 500 µl/sample acid butanol (butan-1-ol plus 5 % of 12 N HCl). A rapid centrifugation supported the separation of the phases. The intensity of the colorful upper phase was measured via spectrometer at 549 nm. Quantification was afterwards performed based on the NANA standard. Past the quantification the PSA samples were diluted to a stock concentration of 1 mg/ml and sterile filtered (0,2 µm).

2.2.9 Size determination of PSA

To determine the size of the purified PSA polyacrylamide gel based chromatography was performed. The gel-based analysis was done via native 18 % and 20 % Tris-Glycine polyacrylamide gels. The running time of the gels was 2.5 hours at 120 V for the 18 % gels and 3.5 hours for the 20 % gels. Subsequently, the gels were stained via a protocol from Goldberg and Warner (*67*) for at least 2 hours at room temperature with stains-all solution (30 mM Tris, 25 % isopropanol, 7.5 % formamide and 0.025 % (w/v) stains all at a pH of 8.8). Afterwards, the gel was washed 3 to 4 times for 10 minutes with 25 % isopropanol to clear the background.

2.3.1 Cell proliferation and metabolic activity assay

Metabolic activity was assayed via a colorimetric (3-(4,5-Dimethylthiazol-2-yl)-2,5-diphenyltetrazolium bromide (MTT) assay (Millipore). The mitochondria mediated cleavage of MTT by cells leads to the formation of formazan crystals. Cells (10^4 per well) were seeded on a 96 well plate in a volume of 100 µl/well and treated for 24 hours with different concentrations of distinct sialic acid chain lengths at standard

culture conditions (5 % CO_2, 37 °C). After 20 hours of stimulation with different kinds of sialic acids 10 µl of MTT (stock 5 mg/ml) were added and cells were cultured for another 4 hours. To dissolve the formazan crystals 100 µl of isopropanol with 0.04 N HCl were added to each well. The light absorbance of the purple formazan dye was determined by a spectrophotometer at a wavelength of 570 nm with a reference wavelength of 630 nm. Microglia that were plated and stimulated under exact identical conditions were detached by trypsin treatment and counted via a Neubauer cell chamber. Measured absorbance values were divided through the number of cells per well to determine the turnover per single cell. All values were compared to unstimulated control cells to receive the relative changes of cell proliferation and metabolic activity.

2.3.2 Experimental animal models

A Siglec-11 transgenic mouse line generated by Dr. Yiner Wang (*107*) was used for the *in vivo* experiments. For the investigation of Siglec-11 in inflammation a LPS induced model of systemic inflammation was chosen. The genotyping of the Siglec-11 mice was done as described in chapter 2.2.2. In case of the LPS injection model C57/Bl6/6J mice or C57/Bl6/6J Siglec-11 transgenic mice were injected with either 4x 1 µg LPS/g body weight or PBS for 5 days. PSA-20 was always injected in a concentration of 4x 1 µg/g body weight parallel to LPS or PBS.

3. Results

3.1 Siglec-H in neuroinflammation

3.1.1 Detection of Siglec-H transcripts in microglia

Siglec-H was initially found to be present on PDCs. In order to confirm that Siglec-H was expressed not only by PDCs but also on microglial cells RT-PCR and qRT-PCR was performed. Therefore, primary microglia and ESdM a mouse microglia cell line were taken for the experiments. PDC rich mouse spleen was used as positive control for the PCR experiments. A H_2O control was included on a regular basis to all experiments as well.

The Siglec-H receptor is linked to the ITAM associated transmembrane adapter protein DAP12 that is capable of transmitting pro-inflammatory signals. To study the Siglec-H regulation the microglia were challenged with a line of pro-inflammatory cytokines. IFN-α, IFN-γ, LPS, or TNF-α were chosen for a 24 hours lasting challenge of the cells. Results RT-PCR experiments revealed that Siglec-H is not notably expressed on primary microglia or ESdM in an unstimulated state. Treatment with IFN-α, LPS, or TNF-α did not have a detectable effect either. However, IFN-γ stimulation led to a detectable increase of the Siglec-H transcription (Figure 3.1 A)

A

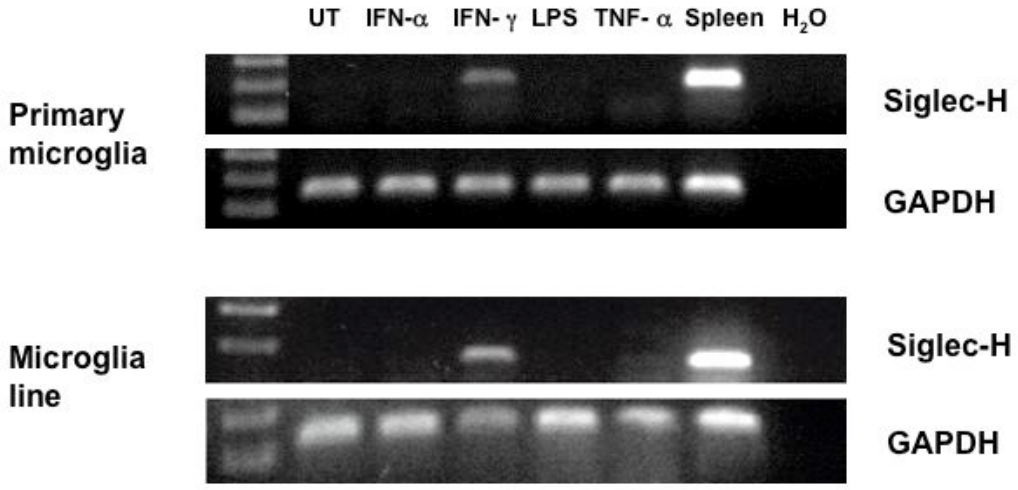

B

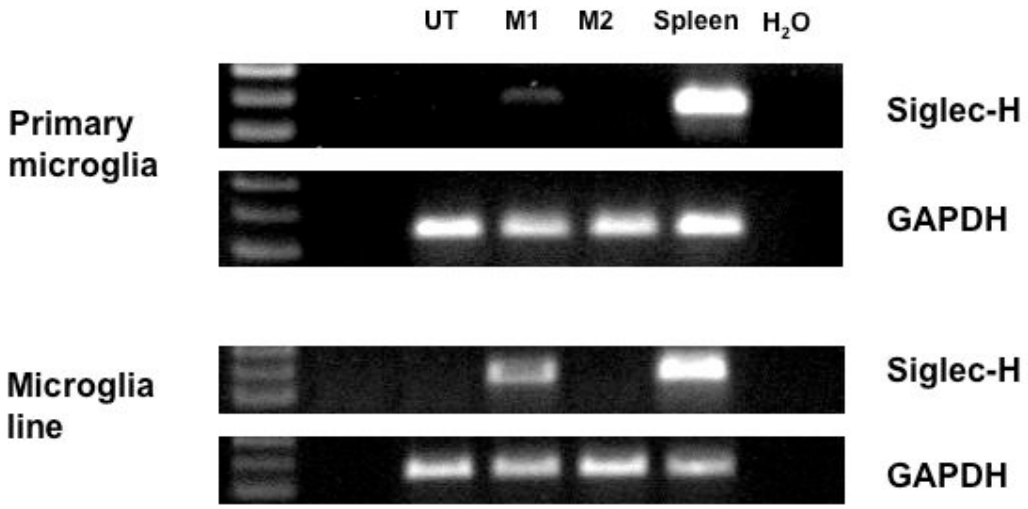

C

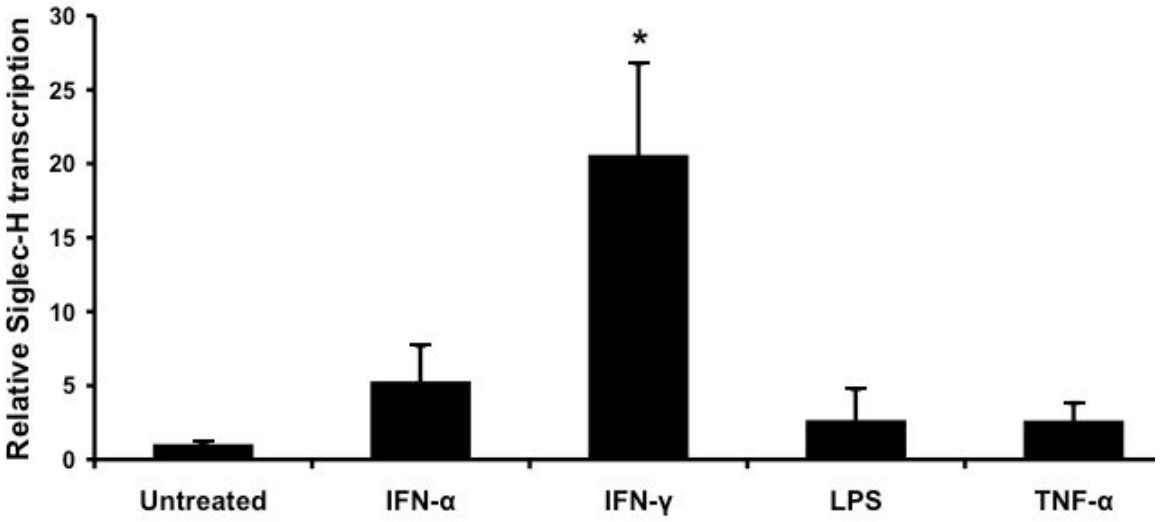

Figure 3.1 Detection of Siglec-H transcripts on microglia: A Detection of Siglec-H transcripts in microglia via RT-PCR. Cells were stimulated for 24 hours with IFN-α (1000 U/ml), IFN-γ (100 U/ml), LPS (500 ng/ml), or TNF-α (20 ng/ml). The regulation of Siglec-H was compared to an untreated sample using GAPDH as internal control. During the RT-PCR experiments only IFN-γ led to increased transcription of Siglec-H in the microglia cells. The data represent the outcome of 3 individual experiments. **B** Detection of Siglec-H transcripts in M1 but not M2 polarized microglia via RT-PCR. Cells were stimulated for 24 hours with a combination of IFN-γ (100 U/ml) and LPS (500 ng/ml) for M1 and IL-4 (20 ng/ml) for M2 polarization. The regulation of Siglec-H was compared to an untreated sample using GAPDH as internal control. Only the combination of the pro-inflammatory molecules LPS and IFN-γ led to a detectable signal. The data represent the outcome of 3 individual experiments. **C** Quantification of

Siglec-H RNA levels in a microglia line via qRT-PCR. Cells were stimulated for 24 hours with IFN-α (1000 U/ml), IFN-γ (100 U/ml), LPS (500 ng/ml), and TNF-α (20 ng/ml). The regulation of Siglec-H transcripts was compared to an untreated sample using GAPDH as internal control. Via qRT-PCR, only stimulation of the cells with IFN-γ led to a statistical relevant change in the expression of Siglec-H. Values are given as mean plus SEM with 4 individual experiments. Statistical analysis of the qRT-PCR derived data was done by SPSS software. Anova Bonferroni was chosen as test (✶≤p<0.05). Adapted and modified from Kopatz et *al*. 2013.

Furthermore, the regulation of Siglec-H was also investigated in M1 and M2 polarized cells. The M1 polarization was achieved via a combination of LPS and IFN-γ while IL-4 stimulation was chosen for the M2 polarization. Here again only stimulation of the microglia cells with IFN-γ in combination with LPS as used for the M1 polarization delivered a signal. As expected the treatment with IL-4 was not having any effect (Figure 3.1B). A quantification of the ESdM RNA levels via qRT-PCR showed that again LPS and TNF-α failed to mediate a noteworthy up-regulation of Siglec-H. In contrast, IFN-γ stimulation increased the regulation of Siglec-H to a significant extent (20.55+/-6.28 fold, p=0.043). The effect of IFN-α to the cells was found to be not significant (Figure 3.1 C). In PDCs the expression of Siglec-H is known to be constitutive. The results from the microglia confirm the presence of Siglec-H on RNA level. However it is inducible and not constitutive expressed.

3.1.2 Detection of Siglec-H on the cell surface of microglia

To confirm the presence of Siglec-H not only on the RNA but also on the protein level microglia were investigated via flow cytometry. Stimulation with the different pro-inflammatory cytokines IFN-α, IFN-γ, LPS, or TNF-α was done over a period of 24 hours. Furthermore, consequences of M1 and M2 polarization with respect to Siglec-H regulation were investigated as well. Primary microglia and cells of the microglia cell line were studied. The stimulation with IFN-γ revealed a notable increase in Siglec-H expression the cell surface of the primary microglia. LPS, IFN-α and TNF-α were not showing any positive signal and were comparable to the unstimulated control cells. In the microglia line the IFN-γ induced increase in Siglec-H expression was even more intense than in the primary microglia.

A

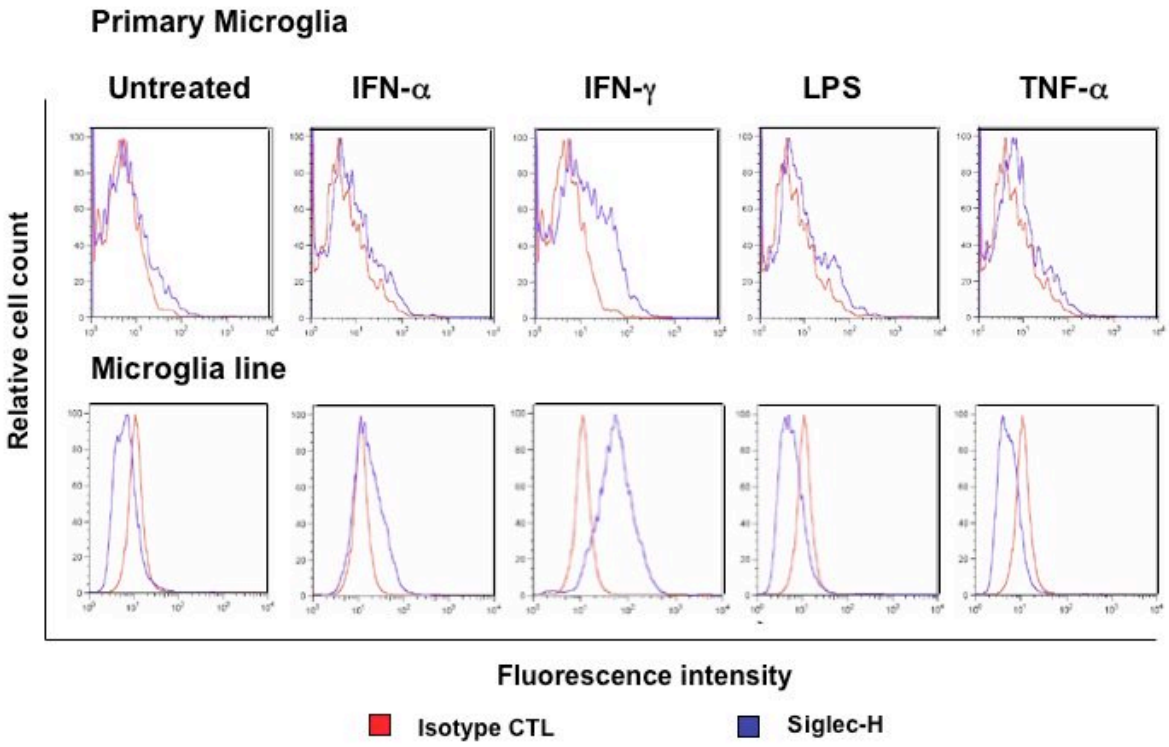

B

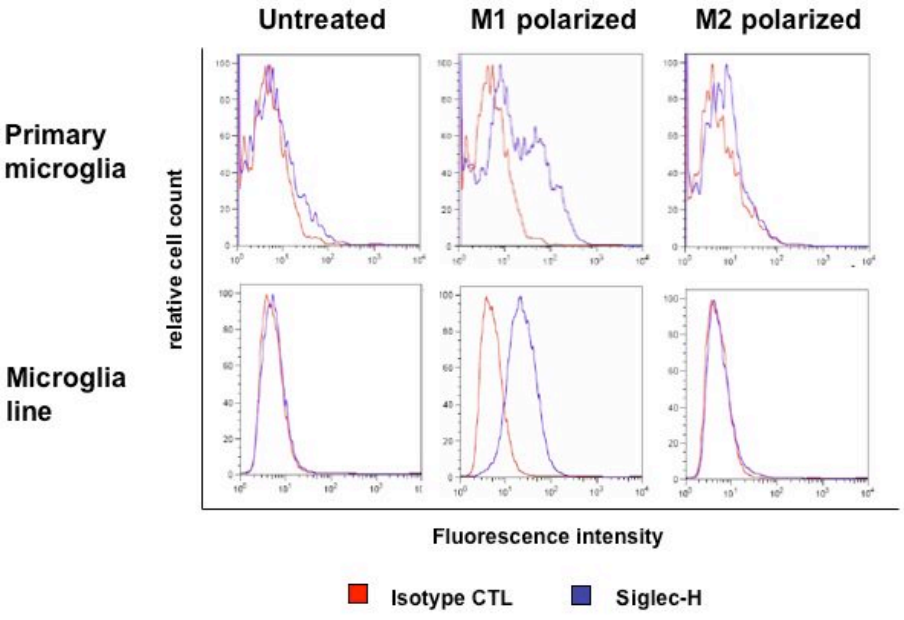

Figure 3.2 Detection of Siglec-H on the cell surface of microglia: A Siglec-H is up-regulated on the protein level after IFN-γ and IFN-α treatment. Primary microglia and cells of the microglial line were

stimulated with IFN-α (1000 U/ml), IFN-γ (100 U/ml), LPS (500 ng/ml) or TNF-α (20 ng/ml). IFN-γ led to a strong increase in Siglec-H protein expression in both types of microglia. IFN-α showed a slight increase in the microglia line but not in the primary microglia. The data represent the outcome of 4 individual experiments. **B** Siglec-H is up-regulated on protein level after M1 polarization via IFN-γ/LPS co-treatment. The data represent the outcome of 3 individual experiments. Adapted and modified from Kopatz et *al*. 2013.

Also a slight increase was mediated by IFN-α however it was no were reaching the intensity of the IFN-γ treatment. Furthermore, no effect of the LPS and TNF-α stimulation was detected (Figure 4 A). Generally, the findings were in line with those obtained from the RT- and qRT-PCR experiments. The results gained after M1 and M2 stimulation were also following the pattern seen on RNA level. IL-4 was without any effect whereas the M1 polarization led to a notable increase of Siglec-H presence on both kinds of microglia cells (Figure 4 B).

3.1.3 Lentiviral knock-down of Siglec-H

To knock-down Siglec-H of microglia a lentiviral mediated transduction of sh-RNA was performed. The efficiency of the respective treatments was tested via flow cytometry. In accordance with the previous findings no Siglec-H was detected on microglia when they were unchallenged or treated with the virus alone. Therefore, a 24 hours stimulation interval with IFN-γ was introduced before the determination of the knock-down efficiency. In parallel to the Siglec-H knock-down, a second group of cells was challenged with a control plasmid. Less than 1 % of the untreated control microglia showed positive staining for Siglec-H. After IFN-γ treatment nearly 85 % of the control microglia were positive for Siglec-H. Virus transduced microglia were presenting 1.2 % positive cells without stimulation and 5.86 % positive cells past IFN-γ administration (Figure 3.3).

When comparing IFN-γ treated wild type microglia with the virus treated cells a 90 % reduction of Siglec-H on the cell surface was found. Therefore, the cells were found suitable for further experimental usage.

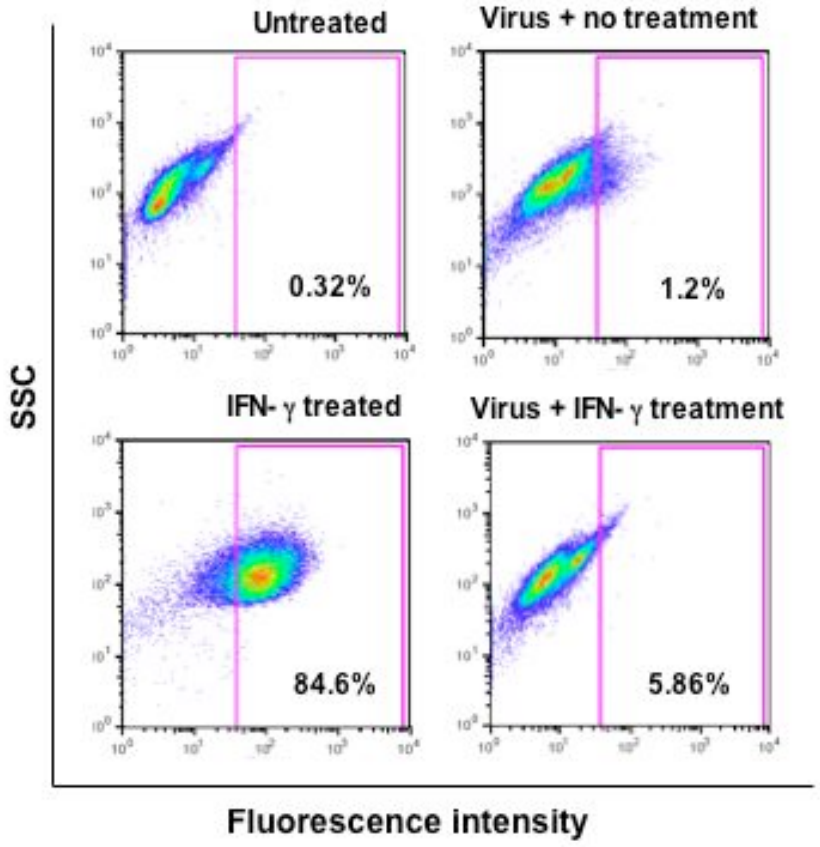

Figure 3.3 Lentiviral knock-down of Siglec-H: Sh-RNA mediated knock-down of Siglec-H in the microglial line. The effect on the protein level was determined via flow cytometry on untreated cells or after 24 hours IFN-γ challenge (100 U/ml). The calculated knock-down efficiency was around 90%. The data represent the outcome of 3 individual experiments. Adapted and modified from Kopatz et *al*. 2013.

3.1.5 Microglia specifically engulf Siglec-H

So far, the role of Siglec-H within the immune system is not well defined. There are data that are suggesting a connection of Siglec-H with endo- and phagocytosis (*47*). To follow up this idea, different samples of wild type and sh-RNA transduced cells from the microglia line (one plasmid targeting Siglec-H and one control sh-RNA plasmid) were prepared and partly pretreated for 24 hours with IFN-γ. Subsequently, the cells were incubated for 1 hour with fluorescent latex beads. To distinguish between Siglec-H mediated and unspecific engulfment the beads were coated with either a Siglec-H detecting antibody or an isotype control antibody. The degree of bead uptake was determined via flow cytometry.

The phagocytosis assay revealed no difference of uptake between Siglec-H coated beads (13.47+/-0.59 %) and control beads (13,07+/-0.84 %) without stimulus. The engulfment of Siglec-H antibody coated beads in IFN-γ stimulated microglia cells was significantly increased (28.77+/-2.25 % p=0,001) compared to the corresponding control microglia cells (12.77+/-1.04 %).

The knock-down of Siglec-H had a notable effect on the IFN-γ pretreated microglia. Treatment with sh-Siglec-H reduced the uptake of Siglec-H antibody coated beads in a way that no difference was detectable any more between sh-Siglec-H (14.22+/-2.82 %,) and sh-control treated (12.35+/-2.43 %, p=1.000) microglia. The control sh-RNA carrying microglia showed no unspecific knock-down effects. The difference of Siglec-H bead phagocytosis between the IFN-γ stimulated sh-Siglec-H or control sh-RNA microglia and knock-down microglia was found to be significant (p=0.005) as well (Figure 3.4 A+B).

A

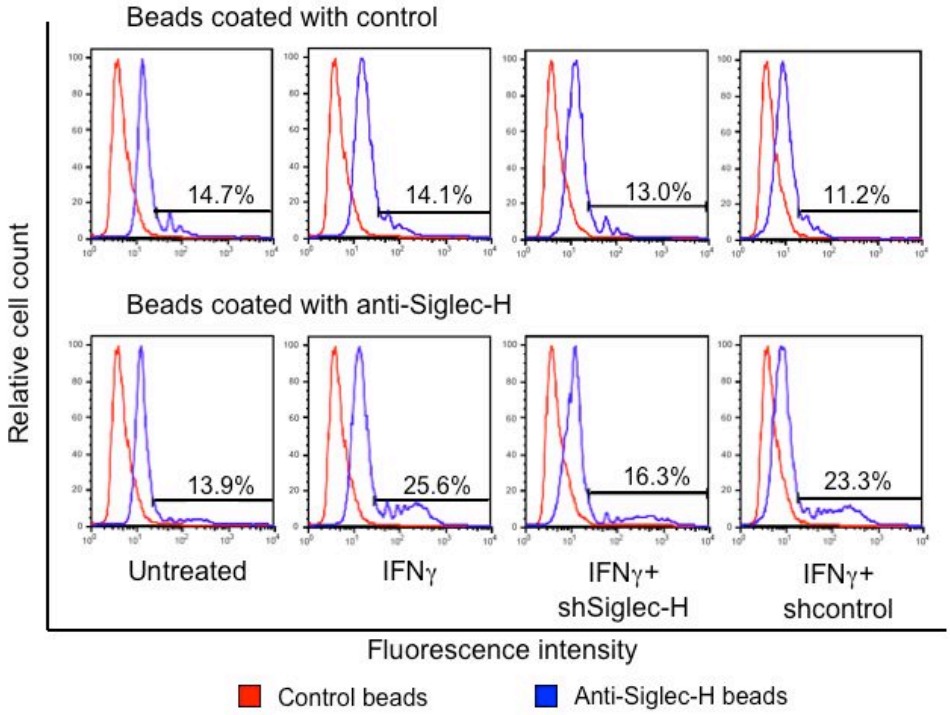

B

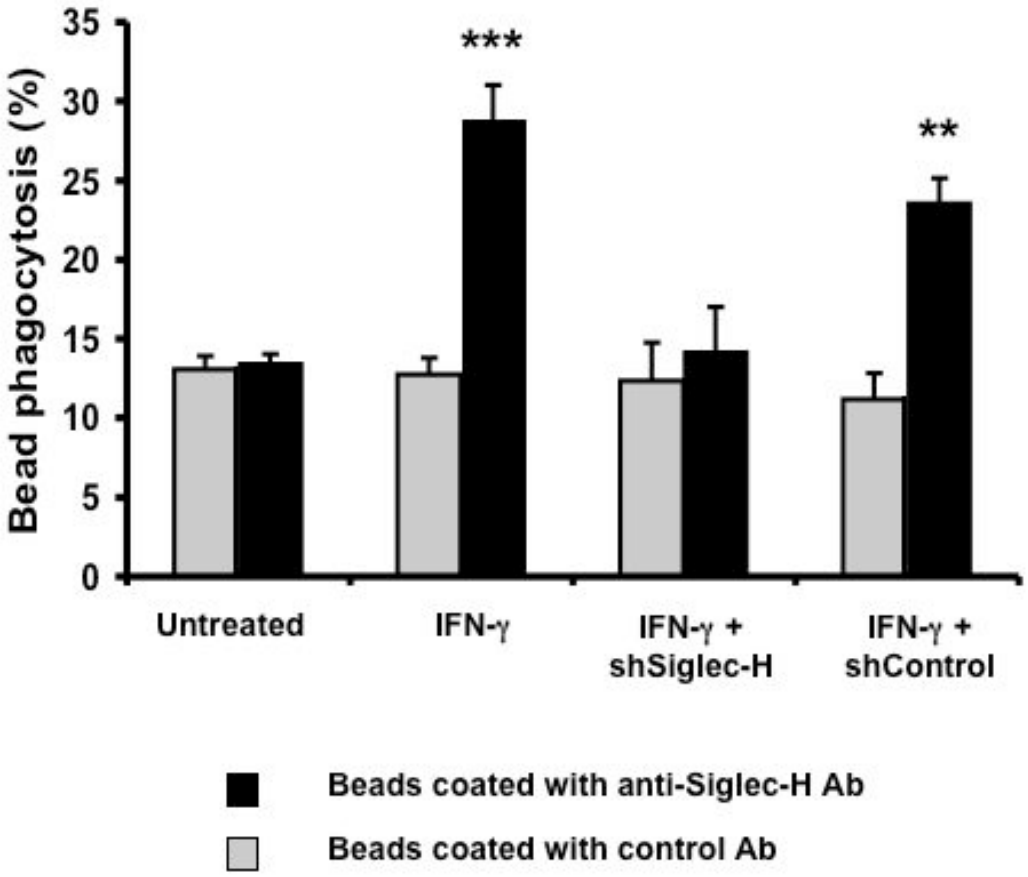

Figure 3.4 Microglia especially engulf Siglec-H: **A** Bead phagocytosis of antibody coated latex beads by microglia. Coating of the beads with Siglec-H did not change uptake behavior in untreated cells. IFN-γ (100 U/ml) stimulated cells showed an increase of Siglec-H coated bead uptake in comparison to control beads. Samples treated with sh-RNA were less effective in taking up the Siglec-H coated beads. Cells carrying the control sh-RNA revealed the same phagocytosis pattern as the just IFN-γ treated cells. **B** The anti Siglec-H sh-RNA significantly reduced the bead phagocytosis in IFN-γ stimulated microglia compared to the wild type and controls sh-RNA samples. Statistical analysis of the experiments was performed using SPSS software and Anova Bonferroni as test. The values are given as mean plus SEM of 3 individual experiments (✶✶=p≤0.01, ✶✶✶=p≤0.001). Adapted and modified from Kopatz et *al*. 2013.

3.1.6 Glioma cells are recognized by a Siglec-H Fc fusion protein

So far, no ligand for Siglec-H is known. To investigate whether Siglec-H recognizes certain pathological structures on glioma cells, but leaves normal cells unaffected,

various cells were incubated with a Siglec-H fusion protein. For this purpose a Siglec-H FC fusion protein (linking the extracellular domain of Siglec-H to the Fc part of human IgG1) was constructed.

The two murine glioma cell lines SMA560 and GL261 were compared to control cells. As controls murine fibroblast, astrocytes and spleenocytes were used. While the control cells showed no notable binding of the Siglec-H Fc fusion protein to structures on the cell surface, the Siglec-H Fc fusion protein bound to the two tested glioma cell lines (Figure 3.5).

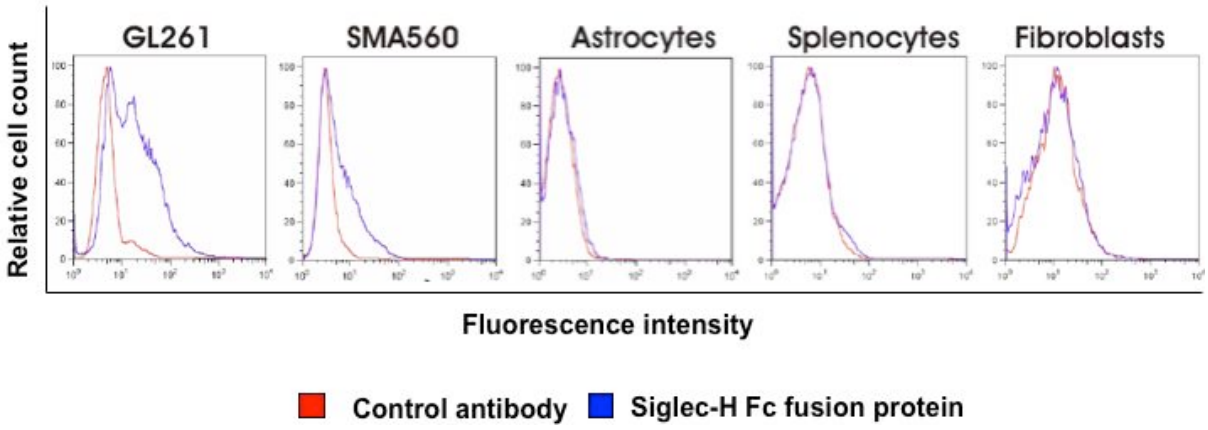

Figure 3.5 Glioma cells are recognized by a Siglec-H Fc fusion protein: Flow cytometry analysis of Siglec-H Fc fusion protein binding capacity. The Siglec-H Fc fusion protein (25 µg/mL) bound to both GL261 and SMA560 glioma cells (kindly provided by Prof. Herrlinger and Dr. Glas, University of Bonn), but not to astrocytes, splenocytes or fibroblasts derived from normal C57Bl/6 mice. Data were generated in collaboration with Dr. Janine Claude and Johannes Ackermann. Representative data out of 3 independent experiments are shown. Adapted and modified from Kopatz et *al*. 2013.

3.1.7 No alteration of proliferation speed in glioma cells co-cultured with microglia

Since the Siglec-H receptor bound to certain structures on glioma cells it was interesting to test whether a co-culture of glioma cells and activated Siglec-H expressing microglia would alter the proliferation rate of the cancer cells. To investigate this question a BrdU assay was performed. Therefore, IFN-γ activated microglia were co-cultured with SMA560 and GL261 glioma cells for 24 hours. To

distinguish the microglia from the glioma cells they were transfected with a GFP construct in advance. The co-culture was compared regarding proliferation to glioma cells that were cultured alone. Afterwards the percentage of glioma cells that incorporated BrdU over a 0.5, 1 or 2 hours time period was determined. No effect of activated microglia cells on the glioma cell proliferation rate of SMA560 and GL261 was observed at any of the tested intervals (Figure 3.6).

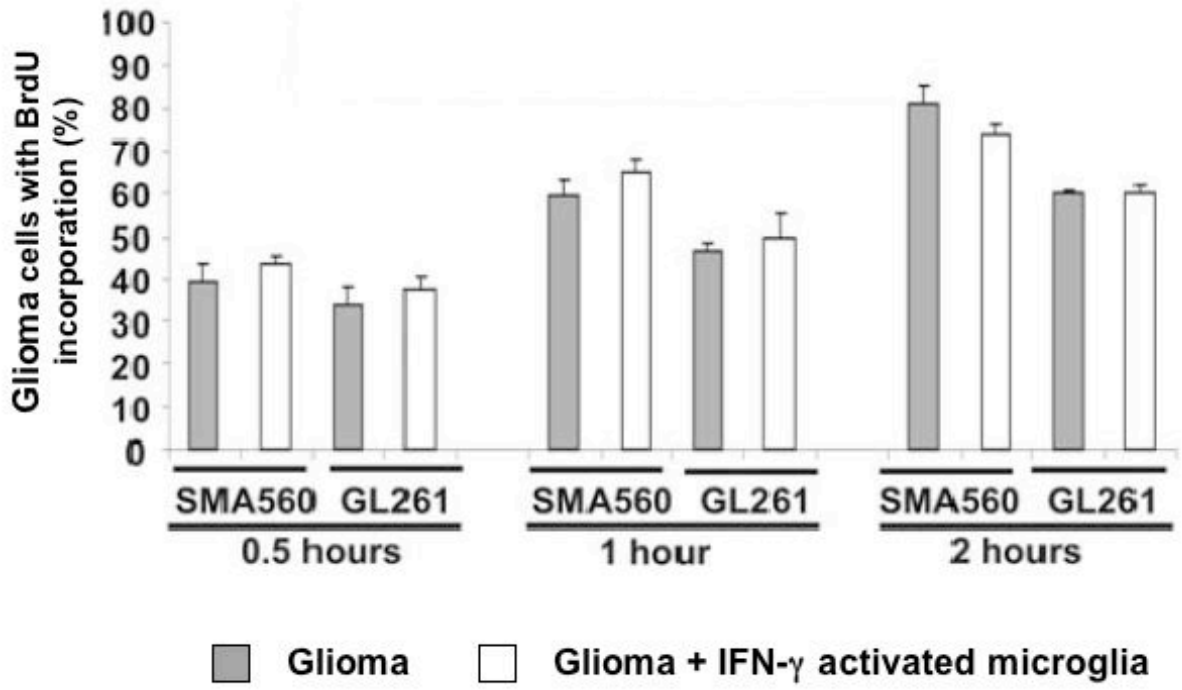

Figure 3.6 No alteration of proliferation speed in glioma cells co-cultured with microglia: Determination of glioma proliferation by incorporation of BrdU after co-cultured with GFP transduced microglia. The glioma lines SMA560 and GL261 (kindly provided by Prof. Herrlinger and Dr. Glas, University of Bonn) were either cultured alone or co-culture for 24 hours with activated microglia before addition of BrdU. Cells were fixed 0.5, 1, or 2 hours after challenge with BrdU. No significant differences were detected among the different groups. Data are presented as mean plus SEM of 3 independent experiments. Statistical analysis of the experiments was performed using SPSS software and Anova Bonferroni as test. Adapted and modified from Kopatz et *al*. 2013.

3.2. Siglec-11 in neuroinflammation

3.2.1 Detection and regulation of Siglec-11 in human microglia cells

The expression of Siglec-11 in human microglia was discovered recently (*23*). To confirm its presence in the human microglia cell line (iPSdM-L1) RT-PCR, qRT-PCR as well as flow cytometry analysis was performed. For the experiments the cells were tested for Siglec-11 without further treatment. For the RT-PCR experiments DNA originating from human brain tissue was used as positive control. Transcripts of Siglec-11 were found to be constitutive expressed by untreated microglial cells (Figure 3.7 A). For further investigation the human microglia were stimulated with LPS, TNF-α, IFN-γ and IL-4. The Siglec-11 regulation was determined on RNA and protein level using a time frame of 24 hours of stimulation. All of the compounds used, up-regulated Siglec-11 transcription of the human microglia. TNF-α (2.28+/-0.31 fold) and IFN-γ (2.08+/-0.3 fold) had a significant impact on the gene transcription and protein expression. The effect of LPS (1.41+/-0.37 fold) and IL-4 (1.31+/-0.18 fold) treatment on the Siglec-11 transcription was notably weaker. However, both caused higher Siglec-11 levels then the untreated control sample (Figure 3.7 B).

A

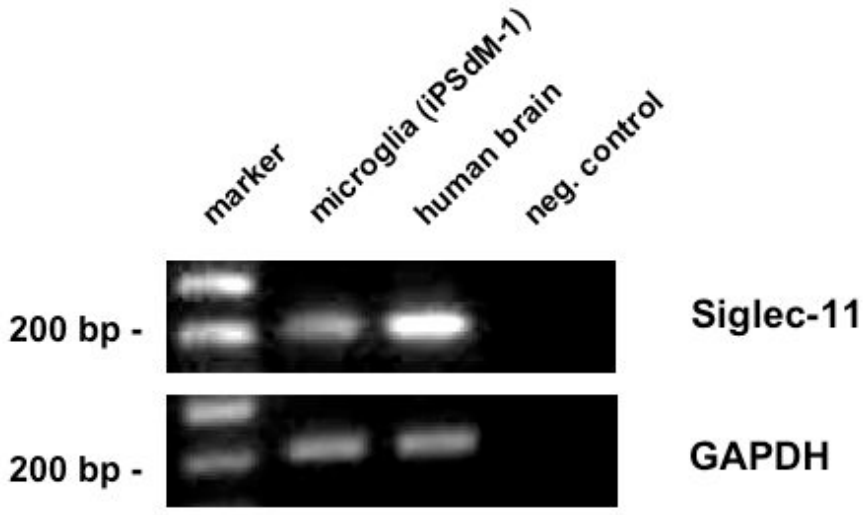

B

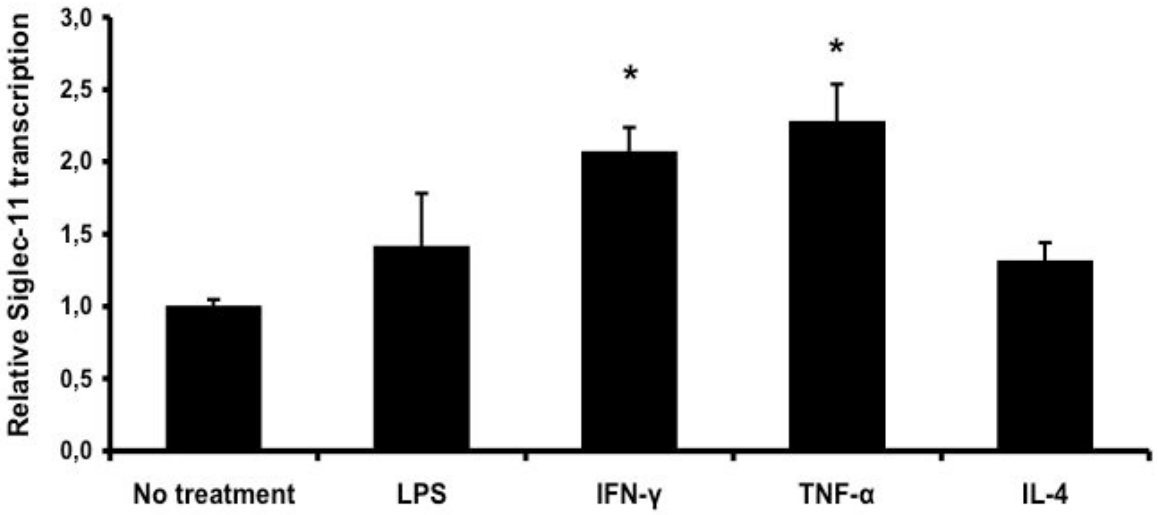
Relative Siglec-11 transcription
3,0
2,5
2,0
1,5
1,0
0,5
0,0
*
*
No treatment
LPS
IFN-γ
TNF-α
IL-4

C

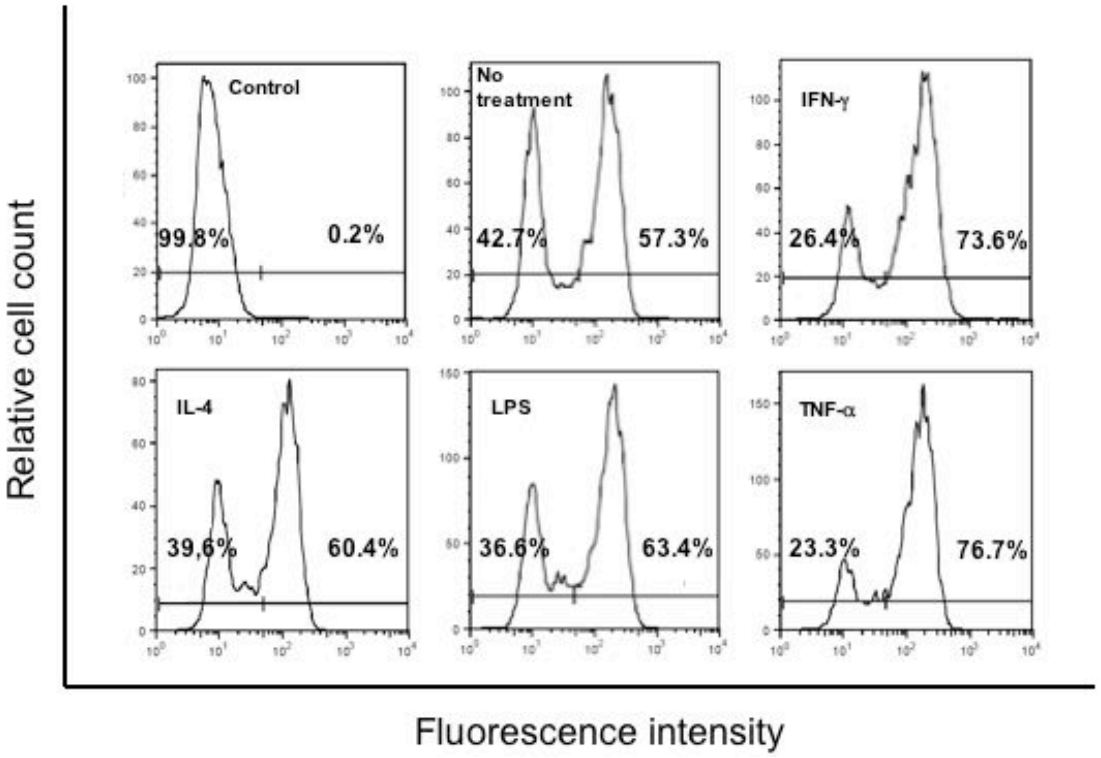
Relative cell count
Control
99.8%
0.2%
No treatment
42.7%
57.3%
IFN-γ
26.4%
73.6%
IL-4
39.6%
60.4%
LPS
36.6%
63.4%
TNF-α
23.3%
76.7%
Fluorescence intensity

D

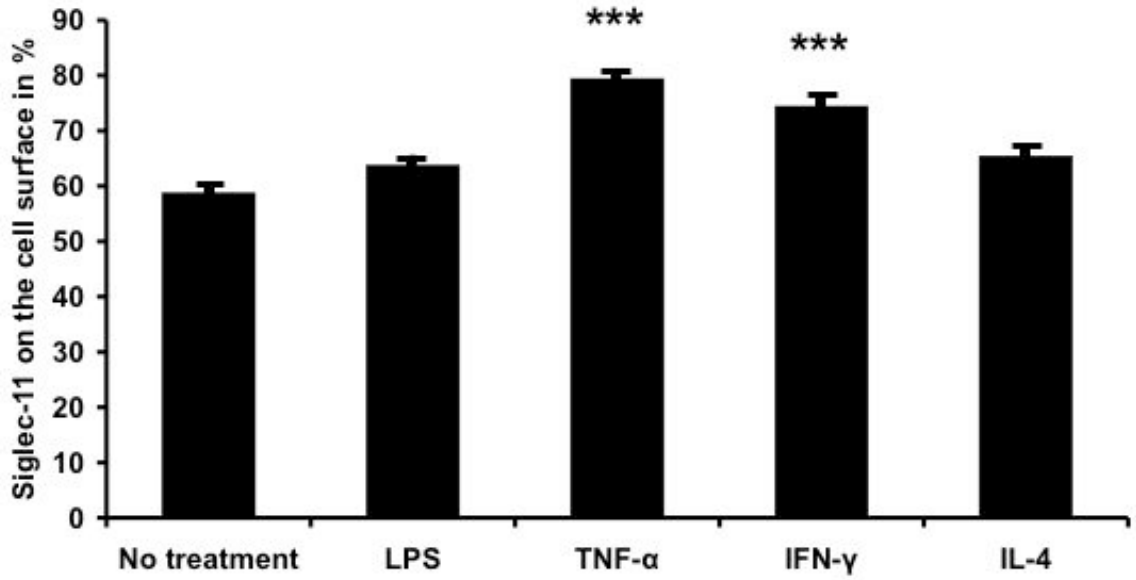

Figure 3.7 Detection and regulation of Siglec-11 on human microglia cells: A Determination of Siglec-11 transcription on RNA level in cells of the microglia line. GAPDH served as internal control. **B** Regulation of Siglec-11 on RNA level via qRT-PCR in human microglia after stimulation. For 24 hours. Cells were treated with IFN-γ (1000U/ml), LPS (1µg/ml) IL-4 (20ng/ml) or TNF-α (20ng/ml). GAPDH served as internal control. Siglec-11 transcription is up-regulated under every condition tested. The strongest increase in transcription was found under IFN-γ and TNF-α treatment. The values are given as mean plus SEM of at least 4 individual experiments. Statistical analysis was done using SPSS software. Anova Bonferroni was chosen as test (✶=p≤0.05). **C** Determination of Siglec-11 regulation on the cell surface of microglia via flow cytometry. Cells were stimulated with IFN-γ (1000 U/ml), LPS (1 µg/ml) IL-4 (20 ng/ml) and TNF-α (20 ng/ml). The graphs show Siglec-11 positive stained microglia cells. The strongest increase is detected after IFN-γ and TNF-α stimulation. The results shown in the graph are representative for 3 individual experiments. **D** Quantification of Siglec-11 expression on the cell surface of microglia. Treatment with TNF-α and IFN-γ significantly increased the Siglec-11 presence on the cells. The values are given as mean plus SEM of 3 individual experiments. Statistical analysis was done using SPSS software. Anova Bonferroni was chosen as test (✶✶✶=p≤0.001). Adapted and modified from PCT/EP2014/055445, Neumann *et al*, 2014.

Untreated microglia showed positive staining for Siglec-11 on the protein level. Past 24 hours of stimulation the amount of Siglec-11 in all tested types of microglia cells was increased. Compared to the untreated control (58.77+/-1.09 %) the values for TNF-α (79.4+/-1.45 %, p=0.001) and IFN-γ (74.43+/-1.2 %, p=0.001) treated cells were significantly increased. The ratios of Siglec-11 up-regulation on protein level were

similar to the data obtained from the Siglec-11 transcription level. None of the tested compounds down regulated the receptor indicating a permanent presence of Siglec-11 on microglia independent of a pro- or anti-inflammatory environment (Figure 3.7 C and D).

3.2.2 Detection and regulation of Siglec-11 in human macrophages

The expression of Siglec-11 was not only found on microglia cells but also on macrophages (*23*), therefore it was an interesting question whether the receptor was regulated on macrophages in the same way as in microglia. In order to investigate this point the human macrophage cell line cell line THP1 was chosen. RNA transcription of Siglec-11 was detectable by RT-PCR in unstimulated macrophages similar to microglia (Figure 3.8 A).

Up-regulation of transcription and protein expression was found in all tested conditions in the macrophages. Regulation of Siglec-11 was however not identical compared to the microglia cells. In the macrophages LPS led to the strongest increase of transcription and expression. TNF-α and IFN-γ that caused the most notable up-regulation in microglia were less effective than LPS. IL-4 stimulation created a reaction that was close to the IFN-γ one. In detail 7.05 +/-1.72 fold for LPS, 2.27 +/- 0.42 fold for TNF-α, 3.7 +/- 0.34 fold for IFN-γ and 2.96 +/- 0.22 fold for IL-4 (Figure 3.8 B).

A

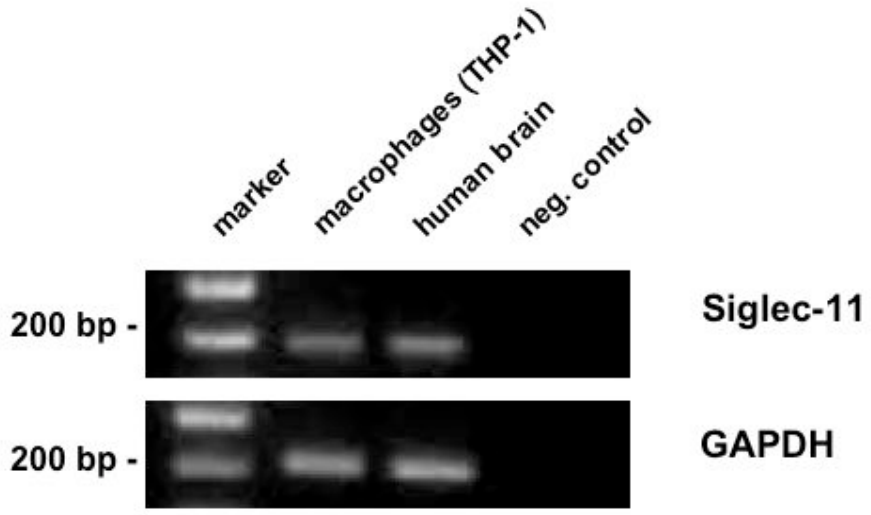

B

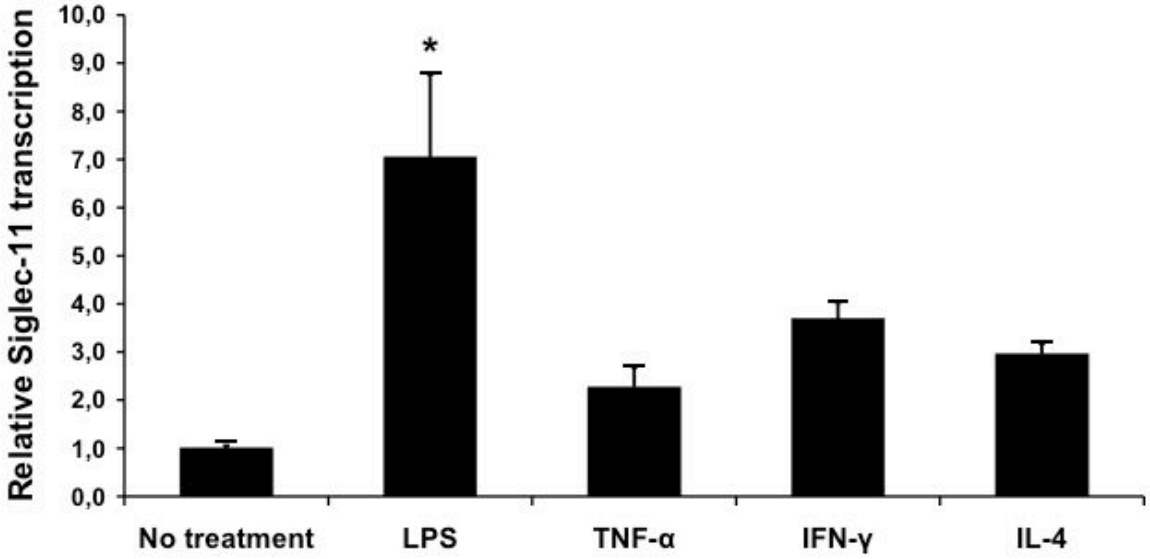
Relative Siglec-11 transcription
10,0
9,0
8,0
7,0
6,0
5,0
4,0
3,0
2,0
1,0
0,0
*
No treatment
LPS
TNF-α
IFN-γ
IL-4

C

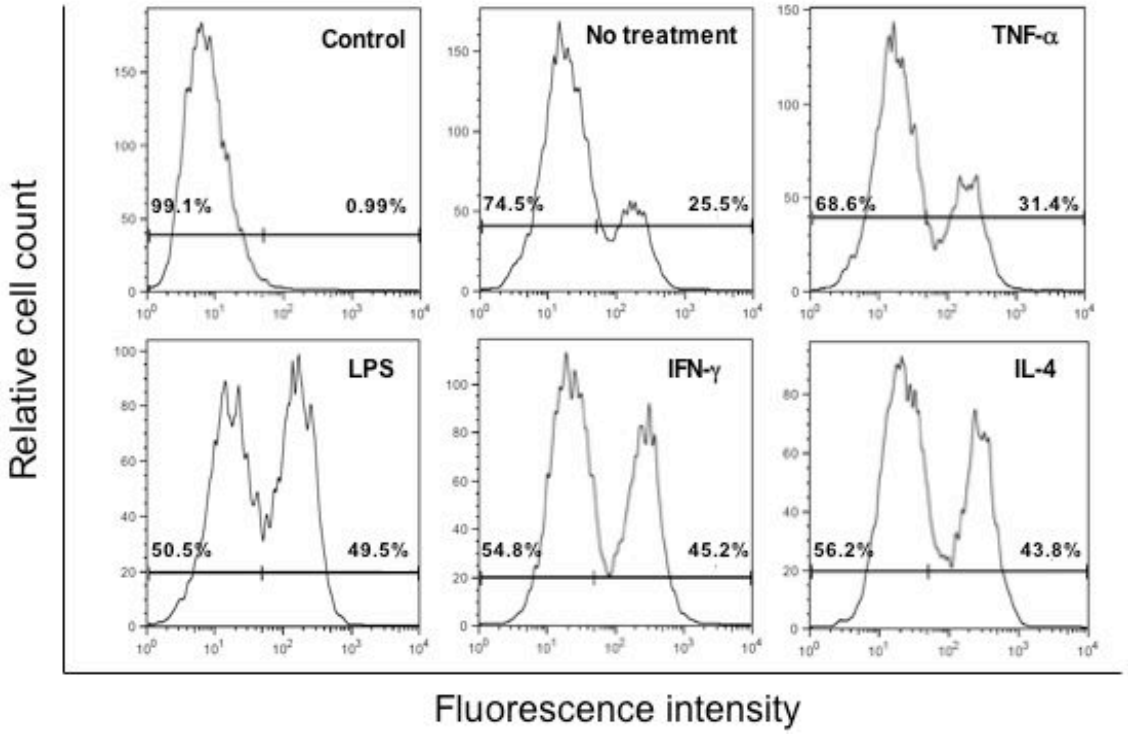
Relative cell count
Control
99.1%
0.99%
No treatment
74.5%
25.5%
TNF-α
68.6%
31.4%
LPS
50.5%
49.5%
IFN-γ
54.8%
45.2%
IL-4
56.2%
43.8%
Fluorescence intensity

D

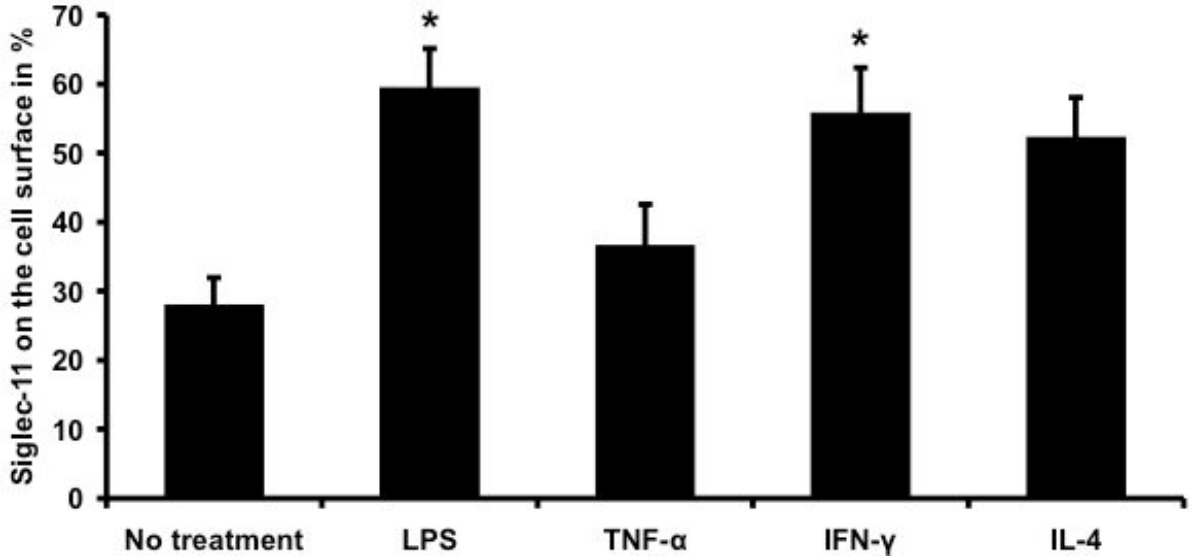

Figure 3.8 Detection and regulation of Siglec-11 in human macrophages: A Determination of Siglec-11 expression on RNA level in cells of the human macrophage line. GAPDH served as internal control. **B** Regulation of Siglec-11 on RNA level via quantitative RT-PCR in human macrophages after stimulation under different conditions for 24 hours. Cells were treated with IFN-γ (1000 U/ml), LPS (1 µg/ml) IL-4 (20 ng/ml) and TNF-α (20 ng/ml). GAPDH served as internal control. The values are given as mean plus SEM of at least 3 individual experiments. Statistical analysis was done using SPSS software. Anova Bonferroni was chosen as test (✶=p≤0.05). **C** Determination of Siglec-11 regulation on the cell surface of macrophages via flow cytometry. Cells were stimulated with IFN-γ (1000 U/ml), LPS (1 µg/ml) IL-4 (20 ng/ml) and TNF-α (20 ng/ml). The graphs show Siglec-11 positive stained macrophage cells. The strongest increase is detected after IFN-γ and LPS stimulation. The results shown in the graph are representative for at least 3 individual experiments. **D** Quantification of Siglec-11 expression on the cell surface of macrophages. Treatment with LPS and IFN-γ significantly increased the Siglec-11 presence on the cells. The values are given as mean plus SEM of at least 3 individual experiments. Statistical analysis was done using SPSS software. Anova Bonferroni was chosen as test (✶=p≤0.05). Adapted and modified from PCT/EP2014/055445, Neumann *et al*, 2014.

Flow cytometry experiments revealed a comparable regulatory pattern on the protein level of the macrophages following 24 hours of stimulation. Like the microglia a subpopulation of cells was found positive for Siglec-11 (27.93+/-4.0 %) without stimulation. Treatment with LPS (59.43+/-5.67 %, p=0.01), TNF-α (36.53+/-6.58 %), IFN-γ (55.77+/-6.03 %, p=0.04) or IL-4 (52.23+/-5.89 %) all increased the amount of

Siglec-11 on the macrophages similar to the ratios found on transcription level (Figure 3.8 C and 3.8 D).

3.2.3 Purification of defined fractions of PSA for Siglec-11 stimulation experiments

To get a more detailed idea about the effects of the sialic acids on Siglec-11 expressing immune cells it was necessary to stimulate the Siglec-11 receptor not only with a reagent consisting of molecules of various chain lengths (not separated PSA) but with fractions of more defined size. Therefore, the PSA was separated via an ion exchange column and subsequently investigated via polyacrylamid gel chromatography. The intention was to receive fractions with an average length of 20, 60 and 180 sialic acid chains. Gel chromatography showed a successful separation of PSA and provided molecules of different sizes (Figure 3.9 A).

A

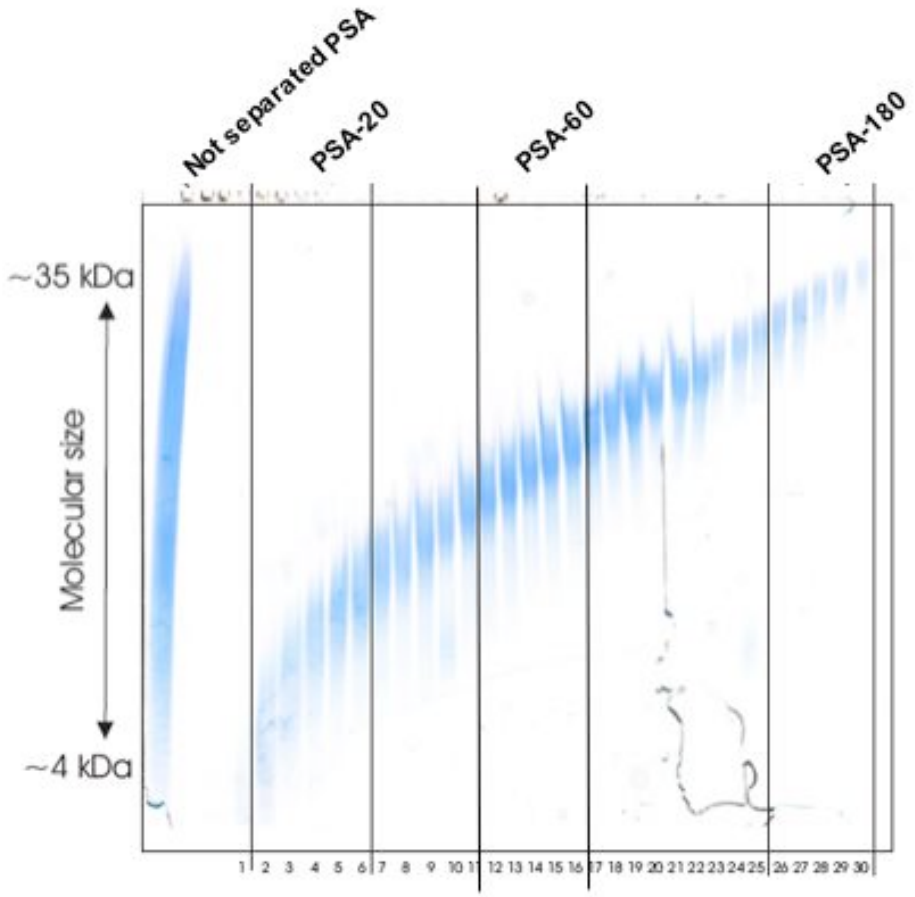

B

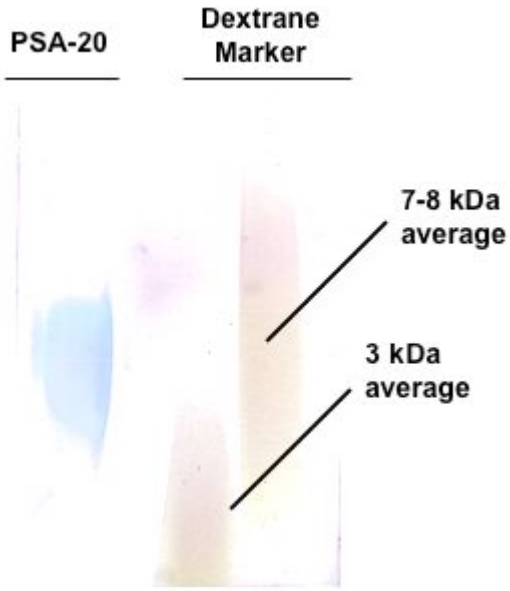

Figure 3.9 Purification of defined fractions of PSA for Siglec-11 stimulation experiments:
A Separated fractions of PSA after lyophilization and solving in PBS on a polyacrylamide gel. The first middle and last 10-20% of the fractions were considered low (PSA-20), medium (PSA-60) and high molecular weight (PSA-180) PSA respectively and taken for experiments. The data were created in cooperation with Dr. Kappler and Norbert Rösel of the Biochemistry Department of the University of Bonn. **B** Size determination of PSA-20 against commercially available dextranes of known size. Fractionated PSA (Fractions 2-6) with an estimated average size of 7kDa (equal ≈ 20 chains) was collected and polyacrylamide gel based chromatography was performed. The PSA showed an average size of around 6-7 kDA therefore receiving the name PSA-20. Adapted and modified from PCT/EP2014/055445, Neumann *et al*, 2014.

The first, middle and last 10-20% of the fractions received were taken for further experiments. The created groups were named PSA-20, -60 and -180 and represent low molecular weight, medium molecular weight and high molecular weight PSA. The effects of those different sized PSA molecules on Siglec-11 exhibiting cells on human microglia were of high interest for further experimental testing.
The PSA with an average of 20 chains of sialic acid was further characterized by using Tris-Glycin gel chromatogrphy. Sulfated dextranes of known size were used as markers. PSA from fractions 3-5 presented an average size of 6-7 kDa. Since the molecular weight of a single sialic acid is known to be at 309 Da this result fitted well with our considered size of 20 sialic acid chains/molecule in average (Figure 3.9 B).

3.2.4 PSA treated microglia show size dependent alterations in cell proliferation and metabolic activity

To test whether the application of PSA can be harmful to Siglec-11 expressing cells, various size lengths of sialic acids (mono-, tri- or hexa-sialic acid plus PSA-20, -60 and 180) were added to cultured human microglia. The cells received different concentrations for 24 hours. Changes in proliferation and turnover per single cell were investigated. Proliferation of cells slightly increased under the impact of stimulation with commercial available mono-, tri- or hexa-sialic acid and PSA-20. Treatment with PSA-60 and -180 showed no difference of the values compared to the control cells. None of the differences found in proliferation between mono-, tri- or hexa-sialic acid and PSA-20, -60, -180 treated cells were significant (Figure 3.10 A). The metabolic activity of the cells was affected in a more notable way. Interestingly, stimulation with the shorter sialic acid molecules resulted in an increase of cellular turnover that was significant higher than that of the untreated control (tri-sialic acid 0.5 µM p=0.017 and 1.5µM p=0.04, PSA-20 0.5 µM p=0.014 and 1.5 µM p=0.033). Concentrations of PSA-60 and -180 showed in general MTT turnover values that were lower than those of mono-, tri- or hexa-sialic acid and PSA-20 stimulated cells. Furthermore, 1.5 µM of PSA-60 (0.7+/-0.05, p=0.012) and PSA-180 (0.74+/-0.04, (p=0.021) showed a significant lesser turnover value then the untreated control cells (Figure 3.10 B).

A

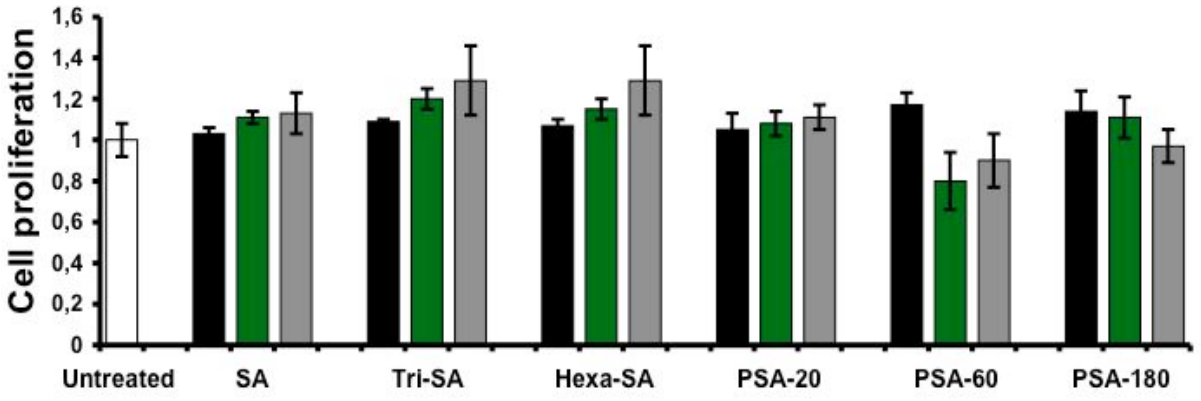

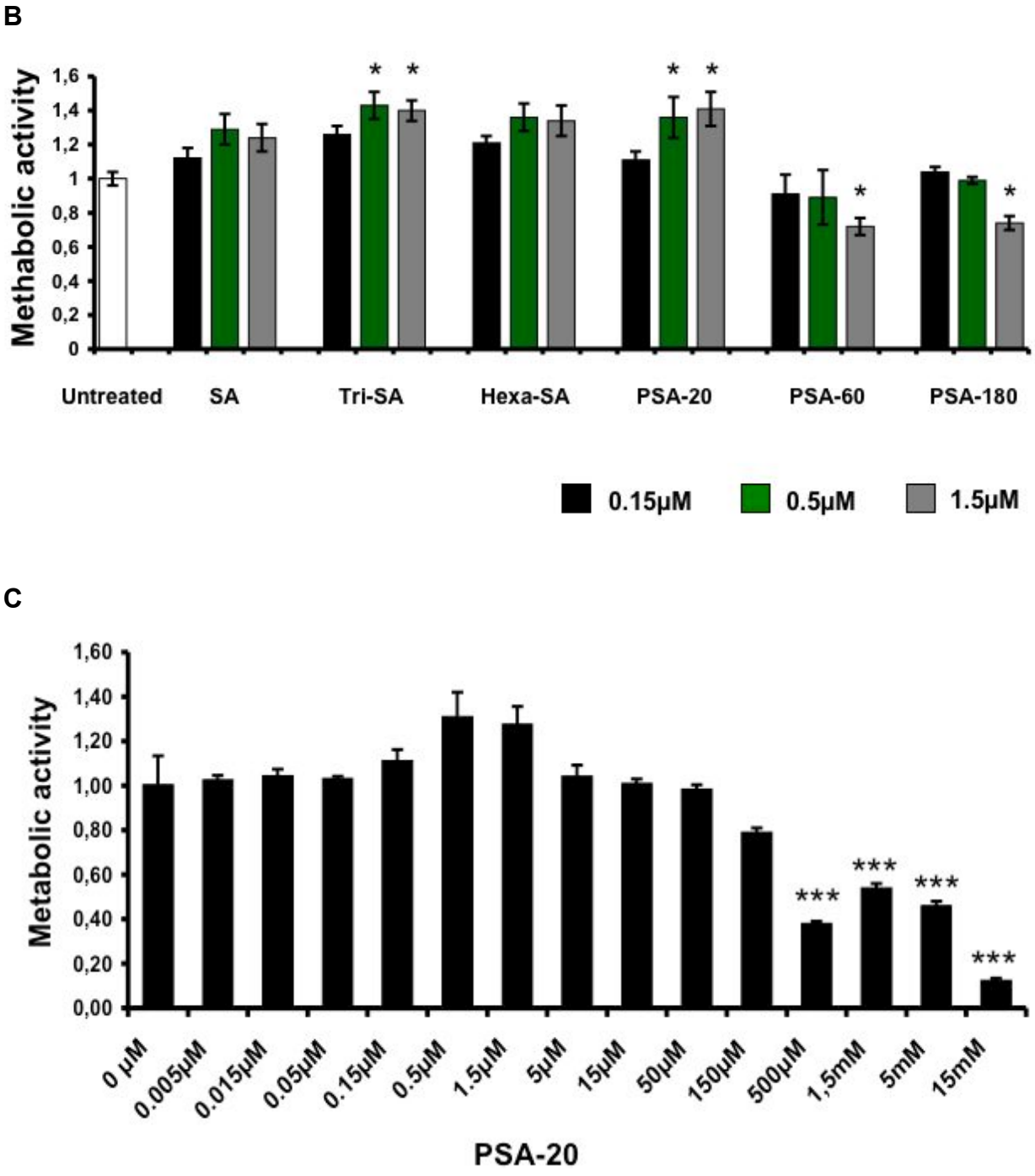

Figure 3.10 PSA treated microglia show size dependent alterations in cell proliferation and turnover: A Effect of different sizes of sialic acid in concentrations of 0.15, 0.5 and 1.5 µM on the proliferation of human microglia. 10^4 cells were stimulated for 24 hours with different kinds of sialic acids. Cells were counted via Neubauer chamber and normalized to control cells. The stimulation with the different kinds of sialic acids did not alter the cell proliferation of the microglia cells. **B** Effect of different sizes of sialic acid in concentrations of 0.15, 0.5 and 1.5 µM on metabolic activity. 10^4 cells

were stimulated for 24 hours with different kinds of sialic acids and metabolic activity was determined using an MTT assay system. Calculation was done with respect to the untreated control cells. Mono-,tri- and hexa-sialic acids as well as PSA-20 increased the metabolic activity of the microglia. PSA-60 and 180 showed a decrease of the metabolic activity. **C** Determination of the toxic dose of PSA-20 for cultured human microglia. Concentrations from 0.005µM to 15mM were administered for 24 hours. Calculation was done with respect to the untreated control cells. Concentrations of 500 µM to 15 mM of PSA-20 decreased the metabolic activity of the microglia significantly. The values for A, B and C are given as mean plus SEM with at least n= 3 for all experiments. Statistical analysis was done using SPSS software. Anova Bonferroni was chosen as test (✶=p≤0.05, ✶✶p≤0.01, ✶✶✶=p≤0.001). Adapted and modified from PCT/EP2014/055445, Neumann *et al*, 2014.

Based on the findings, PSA-20 was chosen for further cell culture experiments since it was showing no immediate negative effects on the microglia. To discover the limitations for cell culture experiments, cells were treated with a concentration gradient of PSA-20 reaching from 0.005 µM to 15 mM. Significant harmful effects were measured at 500 µM (0.38+/-0.01, p=0.001), 1.5 mM (0.54+/-0.02, p=0.001), 5 µM (0.46+/-0.02, p=0.001) and 15 mM (0.12+/-0.01, p=0.001). Interestingly, it required a total of 15 mM of PSA-20 to reduce the microglia turnover to a degree were no normal cell activity was left (Figure 3.10 C). With the generated data the half lethal dose (LD50) for PSA-20 was calculated for the human microglia by using Wolframalpha software. Via regression calculation the LD50 was found to be at 1724,73 µM of PSA-20.

3.2.5 PSA treated microglia show reduced TNF-α transcription after stimulation with LPS

To test whether purified fractions of PSA could be used to stimulate the Siglec-11 receptor, mono-, tri- or hexa-sialic acid plus PSA-20, -60 and 180 were added in three different concentrations (0.15, 0.5, and 1.5 µM) to cultured microglia cells. Since an immune modulating effect was expected from the ITIM linked Siglec-11 receptor LPS induced release of the pro-inflammatory cytokine TNF-α was chosen as readout of the PSA effect. Oligosialic acids consisting of 1, 3 or 6 chains of sialic acids and PSA-20, -60 and -180 in combination with LPS were compared to LPS treated cells without sialic acid treatment (3.11+/-0.12 fold). None of the smaller molecules was showing a

significant reduction of the TNF-α levels past co-stimulation. Medium sized PSA-20 abolished the LPS effect significantly at concentrations of 0.5 and 1.5 µM (0.5 µM = 1.52+/-0.09 fold, and 1.5 µM = 1.23+/-0.08 fold). Also the PSA-60 stimulation of the microglia cells provided comparable results. Here a concentration of 0.15 µM showed significant differences (0.15 µM = 1.36+/-0.16 fold). Stimulation of microglia with both kinds of PSA molecules counteracted the LPS induced TNF-α release notably more efficient then the remaining variants of sialic acid. Treatment of the microglia with PSA-180 also showed a suppression of TNF-α transcript however, without reaching significant levels (Figure 3.11 A). No significant effect of PSA-20 on TNF-α transcription by itself was found in additional control experiments with microglia (1.5 µM PSA-20 = 1,16+/-0.14 fold, p = 1,000, data not shown). The results from the MTT and qRT-PCR experiments highlighted PSA-20 as most suitable form of sialic acids for further studies. Therefore, various concentrations of PSA-20 were administered to human microglia in order to study the ligand/receptor interaction in more detail.

A

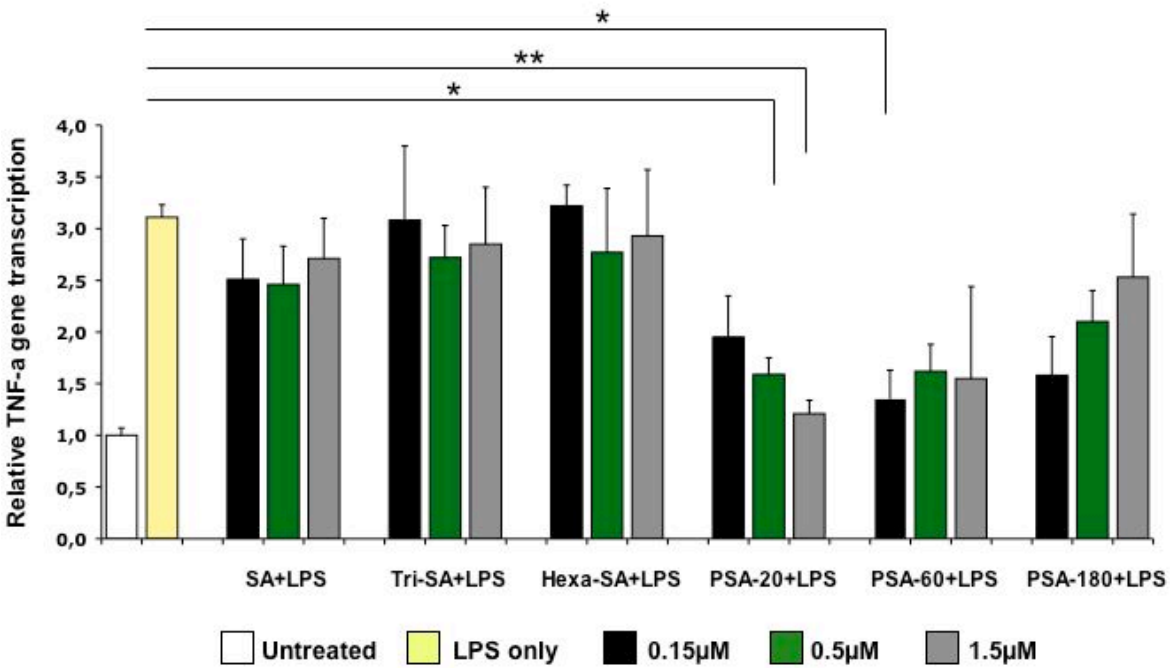

B

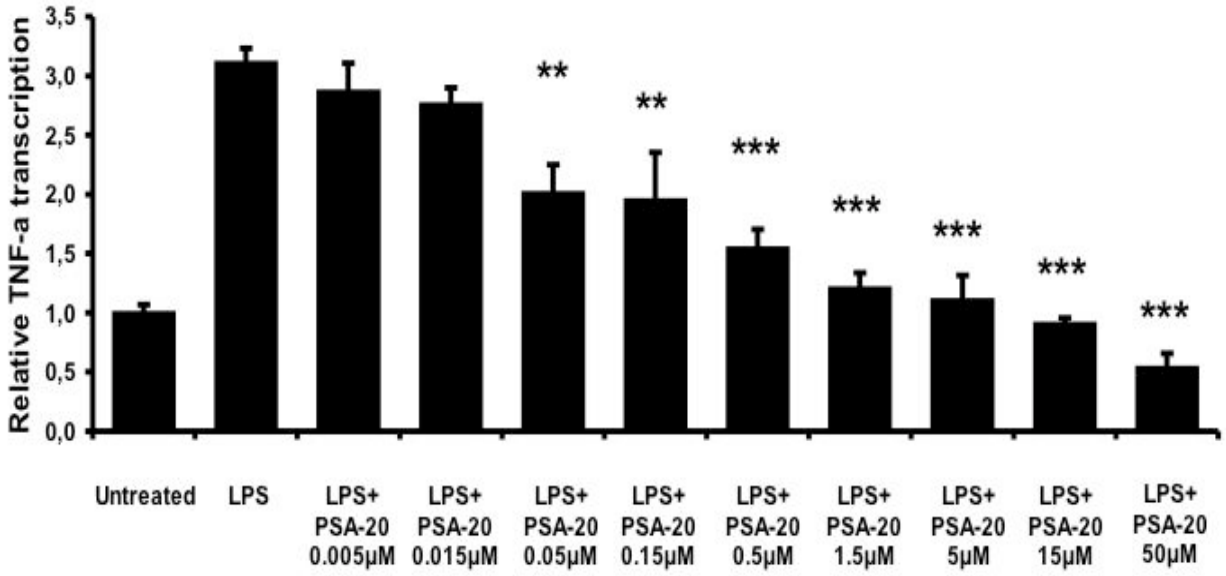

Figure 3.11 PSA treated microglia show reduced TNF-α transcription after stimulation with LPS: A Modulating effect of PSA of different sizes on the transcription of the pro-inflammatory cytokine TNF-α in human microglia. A human microglia cell line was treated with LPS (1 µg/ml) and mono, tri, hexa sialic acid or PSA (0.15, 0.5, 1.5µM) for 24 hours. **B** Effect of PSA-20 on human microglia tested for a wide range (0.005-50 µM) of concentrations. All PSA-20 concentrations were added in combination with 1µg/ml LPS to the cells. Gene transcripts for TNF-α were determined by quantitative RT-PCR and normalized to GAPDH for all data shown. The values for A and B are given as mean plus SEM of at least 3 experiments. Statistical analysis was done using SPSS software. Anova Bonferroni was chosen as test (✶=p≤0.05, ✶✶p≤0.01, ✶✶✶=p≤0.001). Calculations of statistics were done with respect to the LPS control. Adapted and modified from PCT/EP2014/055445, Neumann *et al*, 2014.

In total nine different concentrations ranging from 0.005 µM to 50 µM were chosen. Tested concentrations of PSA-20 showed significant reduced levels of TNF-α transcripts starting at 0.05 µM or higher (Figure 3.11 B).

Based on these findings the half maximal inhibitory concentration (IC50) was calculated via Wolframalpha software. The IC50 was determined by regression calculation to be at 0.09 µM of PSA-20. Taken together with the LD50 (1724.73 µM) from the cell metabolic activity experiments the therapeutic index of PSA-20 was calculated as LD50/IC50 = 19163,7 µM.

3.2.6 Siglec-11 knock-down in microglia shows an impaired PSA-20 effect

To verify that the observed down-regulation of TNF-α transcripts was exclusively due to an interaction of PSA-20 with the Siglec-11 receptor on the human microglia a sh-RNA mediated knock-down of the receptor was introduced.

A

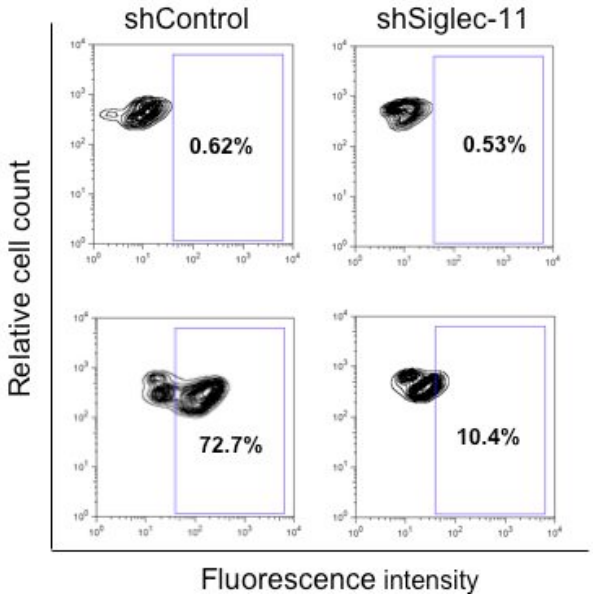

B

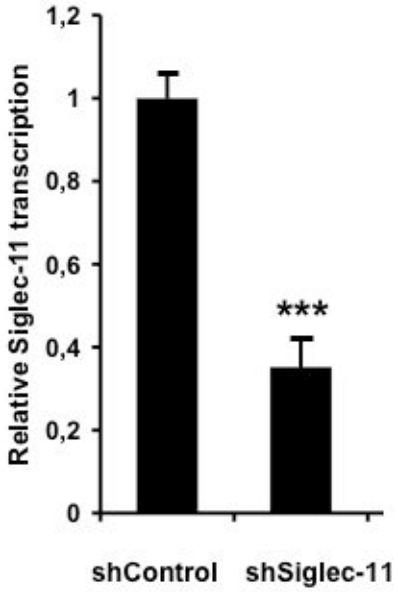

C

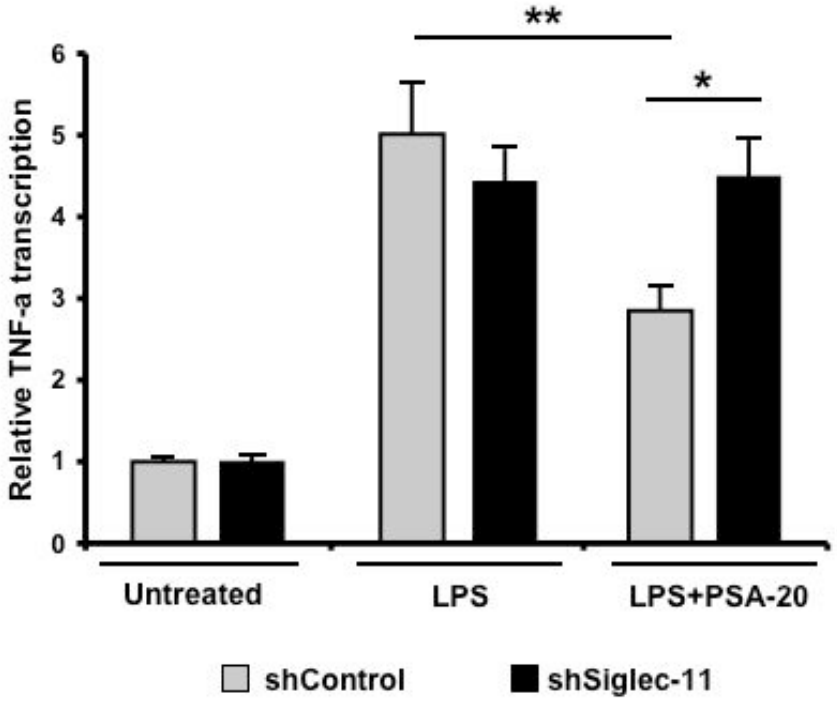

Figure 3.12: Siglec-11 knock-down microglia show an impaired PSA-20 effect: A Determination of Siglec-11 reduction on the cell surface of human microglia via flow cytometry. The knock-down cells show around 85% less Siglec-11 presence than the control microglia. Data are representative for 3 independent experiments. **B** Determination of the reduction of Siglec-11 transcription via qRT-PCR. Transcription level of Siglec-11 in the knock-down microglia are significantly reduced. Values are given as mean plus SEM of at least 3 experiments. Statistical analysis was done using SPSS software. The chosen test was a t-test of independent values (✶✶✶=p≤0.001). **C** Determination of the PSA-20 mediated modulation of the TNF-α transcription via qRT-PCR. No significant PSA-20 effect was detectable anymore in Siglec-11 knock-down microglia. Values are given as mean plus SEM of at least 3 experiments. Statistical analysis was done using SPSS software. Anova Bonferroni was chosen as test (✶=p≤0.05, ✶✶p≤0.01, ✶✶✶=p≤0.001).

Efficiency determination revealed that on the cell surface of the microglia the presence of Siglec-11 was reduced by 85% (Figure 3.12 A). On RNA level around 65 % lower amounts of Siglec-11 transcripts were measured. The knock-down of Siglec-11 transcription was significant in the microglial cells (0.35+/-0.07 fold, p=0.001), (Figure 3.12 B). After successful confirmation of the knock down the microglia were co-stimulated with PSA-20 and LPS and compared to control cells transduced with a non-

targeting vector plasmid. To determine the effect of the knock-down, qRT-PCR tested modulation of TNF-α transcription was chosen. The control cells showed increased TNF-α transcription level after addition of LPS (5.01+/-0.63 fold) and significant reduced values after LPS/1.5 µM PSA-20 co-stimulation (2.85+/-0.28 fold, p=0.006). The LPS/PSA-20 treated knock-down cells showed no reduction of TNF-α transcription compared to the LPS stimulated knock-down microglia. The difference in TNF-α transcription between LPS/PSA-20 stimulated knock-down (4,49+/-0.45 fold) and control microglia (2.85+/-0.28 fold) was significant as well (p=0.018). Without sufficient amounts of the Siglec-11 receptor present the PSA-20 mediated effect was hardly detectable in the microglia (Figure 3.12 C).

3.2.7 Human macrophages show reduced TNF-α transcription after stimulation with LPS/PSA-20

Since the low molecular weight PSA-20 reduced the LPS-induced gene transcription of TNF-α at a concentration of 0.15 µM, 0.5 µM and 1.5 µM in the human microglia very effectively the same paradigm was tested with the human macrophages. LPS induced increase of TNF-α in macrophages (3.57+/-0.06 fold) similar to microglia levels. Two of the three tested LPS/PSA-20 concentrations showed a significant down-regulation of TNF-α transcripts (0.15 µM = 2.36+/-0.24 fold, p=0.022 and 1.5 µM = 2.31+/-0.4 fold, p=0.016) when compared to LPS alone.

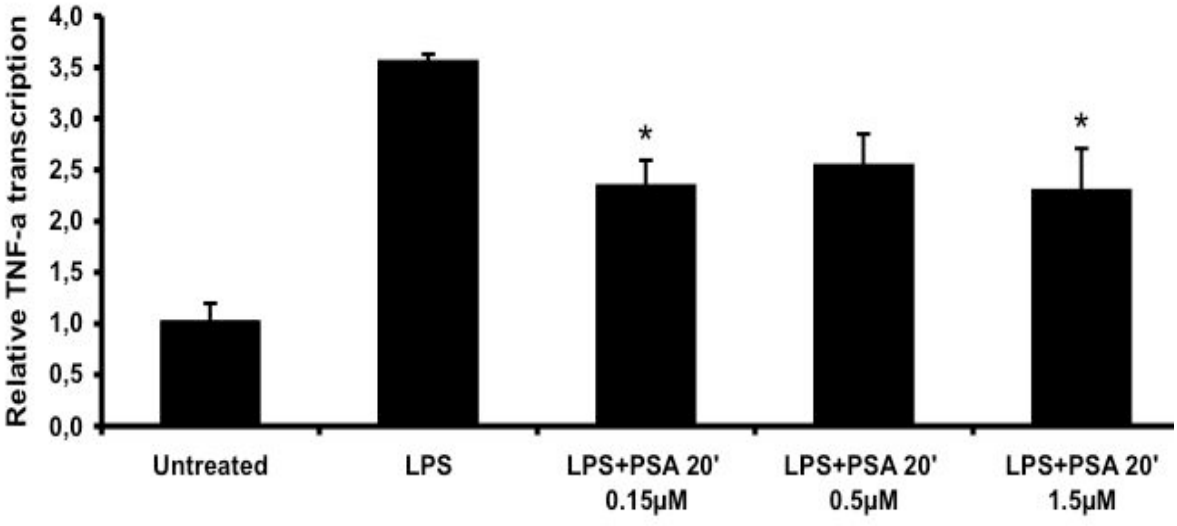

Figure 3.13 Human macrophages show reduced TNF-α production after stimulation with LPS/PSA-20: Effect of low molecular weight PSA (PSA-20) on the pro-inflammatory cytokine TNF-α in human macrophages. The human macrophage cell line THP-1 was treated with LPS (1 µg/ml) and PSA-20 (0.15 µM, 0.5 µM, 1.5 µM) for 24 hours. Gene transcripts for TNF-α were determined by quantitative RT-PCR and normalized to GAPDH. Compared to LPS, the TNF-α transcription was significantly reduced when co-treated with LPS and 0.15 µM or 1.5 µM PSA-20. Values are given as mean plus SEM of 4 independent experiments. Statistics were performed using SPSS software. Anova Bonferroni was chosen as test (✶=p≤0.05). Adapted and modified from PCT/EP2014/055445, Neumann *et al*, 2014.

Values of 0.5 µM PSA-20/LPS co-stimulation were not found to be significantly lower than the LPS reference (Figure 3.13). The results were quite comparable to those received from the human microglia experiments.

3.2.8 PSA-20 modulates phagocytosis in Siglec-11 positive microglia and macrophages

Phagocytosis is one of the key features performed by activated macrophages and microglia. Therefore, it was an interesting question whether PSA-20 would be capable of modulating phagocytosis in LPS treated cells. Macrophages and microglia were challenged with the same LPS/PSA-20 co-stimulation procedure as before and the phagocytosis capacity was determined via uptake of fluorescent latex beads.

No activating effect of PSA-20 on bead uptake was found in additional control experiments with microglia cells (1.5 µM PSA-20 = 87.45+/-0.74 % of control, data not shown). The stimulation with LPS increased the bead phagocytosis of microglia (141.63+/-4.93 %) and of macrophages (145.03+/-6.08 %) compared to untreated control cells. Both cell types showed less uptake when co-treated with LPS and PSA-20 compared to the LPS control. Microglia bead phagocytosis was 124.86+/-7.21%, 122.8 +/-8.62 % and 108.05+/-1.32 % for 0.15, 0.5 and 1.5 µM PSA-20/LPS treatment (Figure 3.14 A). Macrophages showed 118.39+/-4.34 %, 107.27 +/-6.34 % and 104.55+/-2.95 % of phagocytosis for 0.15, 0.5 and 1.5 µM PSA-20/LPS stimulation respectively (Figure 3.14 B). Engulfment of beads was significantly decreased at 1.5 µM PSA-20 (p=0.004) in microglia. In macrophages stimulation with 0.15 µM (p=0.022), 0.5 µM (p=0.002) and 1.5 µM PSA20/LPS (p=0.001) led to significant lower phagocytosis levels as well.

A Human microglia

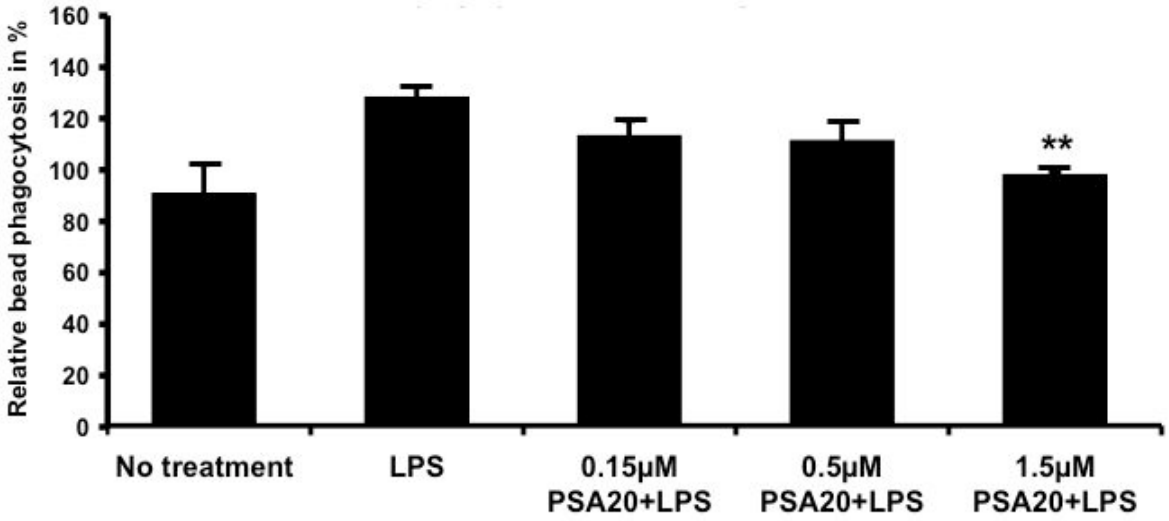

B Human macrophages

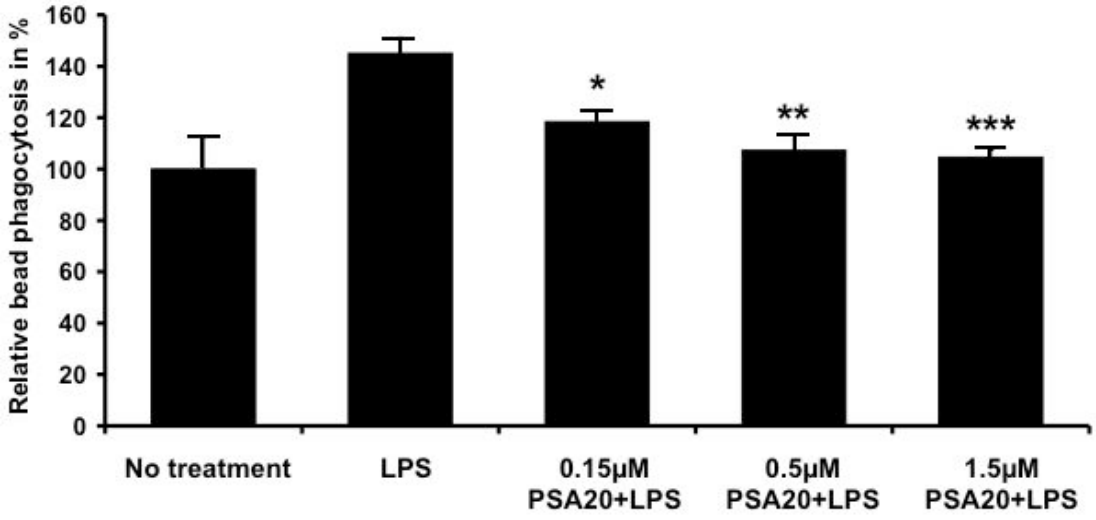

Figure 3.14 PSA-20 modulates phagocytosis in Siglec-11 positive microglia and macrophages: Engulfment of fluorescent latex beads by human microglia **(A**) and macrophages **(B)**. The cells were treated for 24 hours with either LPS or LPS in combination with different concentrations of PSA-20. The beads were added for 1 hour before measurement. The values of the untreated samples were normalized to 100% serving as reference for all other groups. In microglia combination of 1.5 µM PSA-20/LPS led to significant reduced levels of bead engulfment compared to LPS. In macrophages all tested LPS/PSA-20 combinations were showing significant lower levels of bead phagocytosis. Data for A and B are shown as mean plus SEM with n=4 independent experiments for microglia and n= 3

independent experiments for macrophages. Statistics were performed using SPSS software. Anova Bonferroni was chosen as test (✶=p≤0.05, ✶✶p≤0.01, ✶✶✶=p≤0.001).

3.2.9 Siglec-11 expression in a transgenic mouse model

To investigate the effect of human Siglec-11 in the inflammatory processes *in vivo* a Siglec-11 transgenic mouse model (created by Dr. Yiner Wang) was used. For characterization of the Siglec-11 expression in the mice, RT-PCR and flow cytometry analysis was performed.

Tissue samples originating from brain, spinal cord, liver, spleen, bone marrow and blood of Siglec-11 transgenic mice and littermate controls were harvested. Transcripts of Siglec-11 were detected in the brain, liver and spleen tissue but not in the spinal cord, bone marrow or blood of Siglec-11 mice. None of the samples from the control mice showed any kind of Siglec-11 transcription (Figure 3.15 A).

For the flow cytometry experiments full organ cell homogenate was created and stained against Siglec-11. Here again, cells from brain, spleen and liver tissue but not spinal cord, bone marrow or blood presented a shift when tested for presence of Siglec-11. Like in the PCR experiments no proof for the presence of Siglec-11 on protein level was detected in cells originating from the littermate control animals (Figure 3.15 B).

A

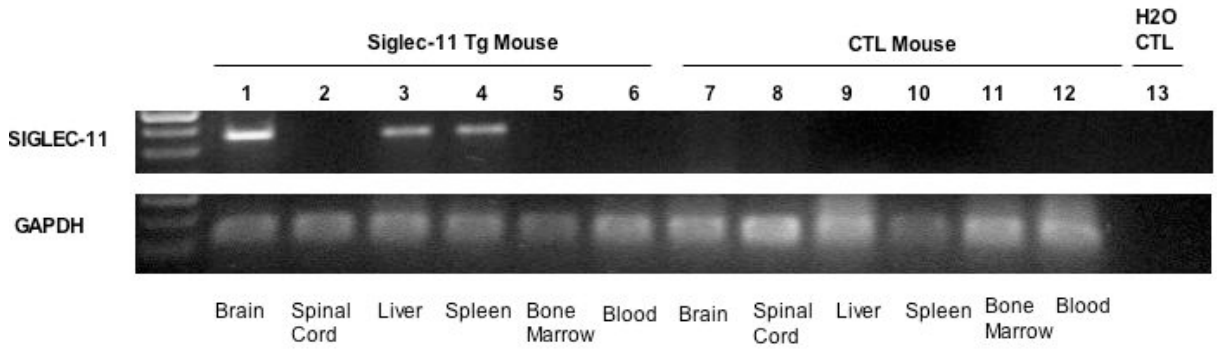

B

Siglec-11 transgenic mouse

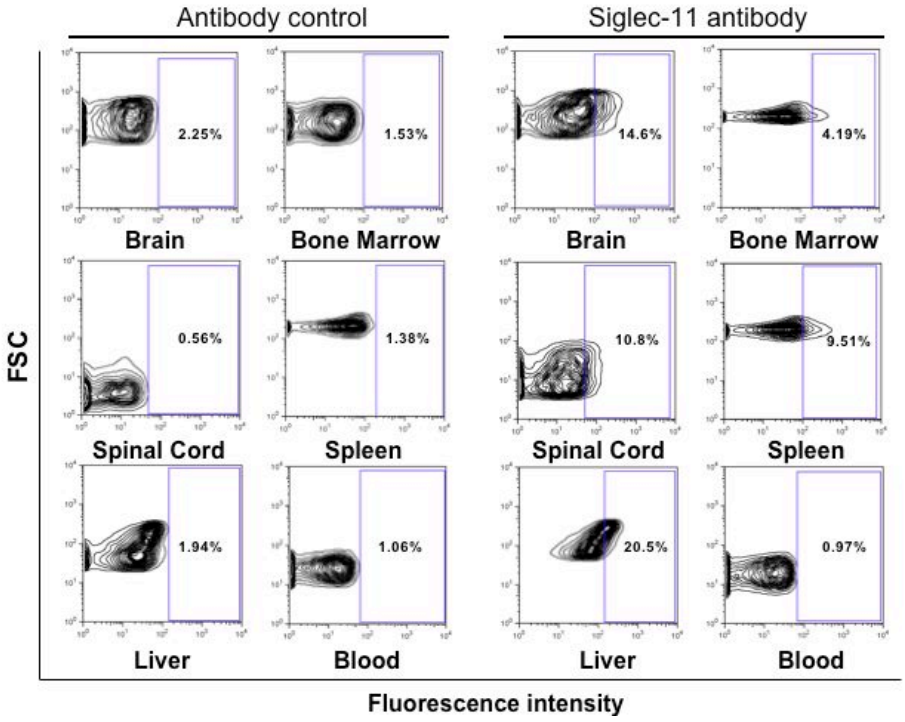

Littermate control mouse

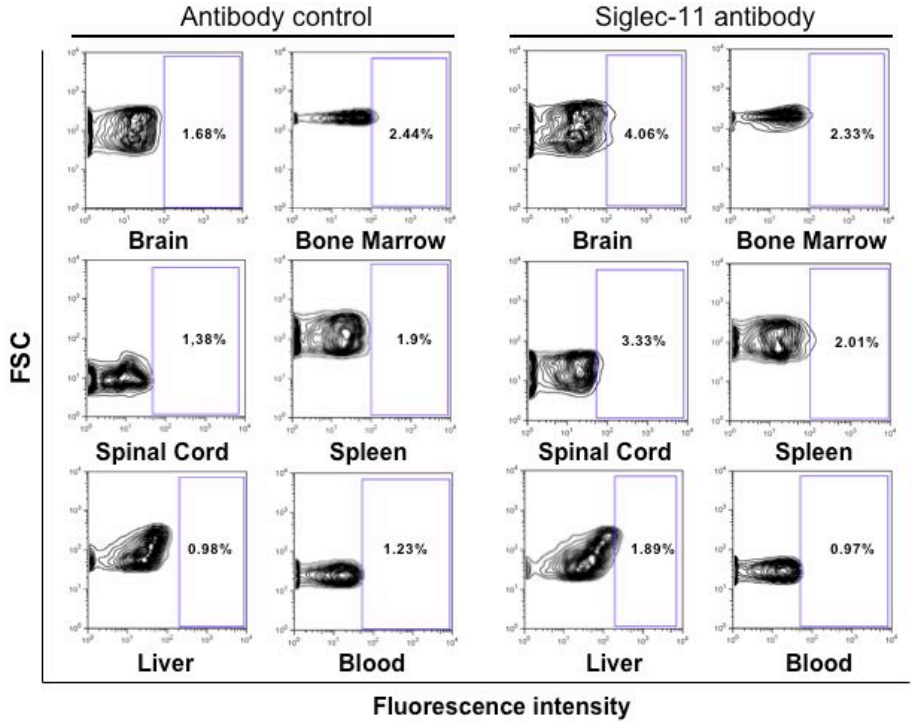

C

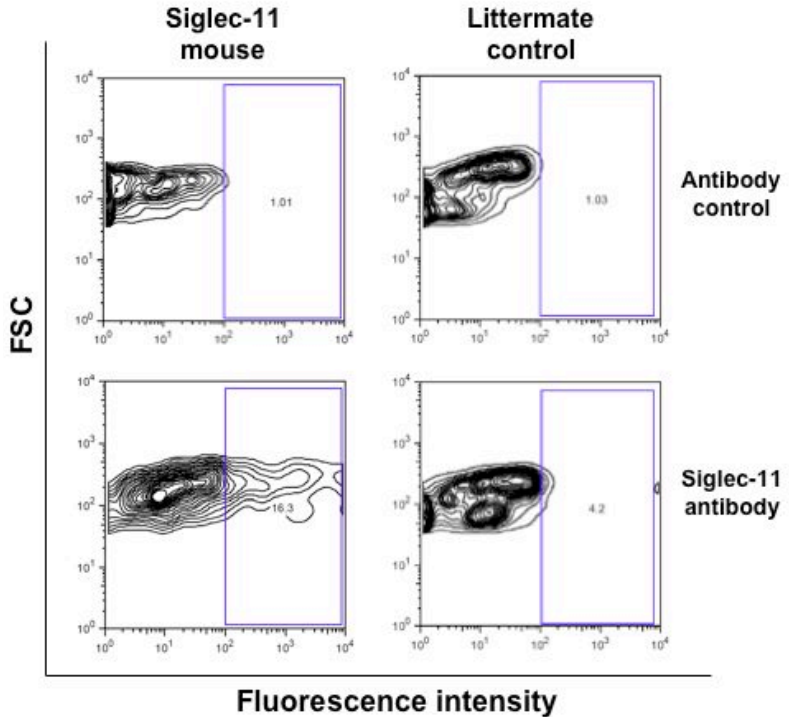

Figure 3.15 Siglec-11 expression in a transgenic mouse model: A Detection of Siglec-11 in brain, liver and spleen samples from Siglec-11 transgenic mice but not Bl6 control mice via RT-PCR. GAPDH was used as internal control. Brain, liver and spleen samples of Siglec-11 mice showed transcripts of Siglec-11. **B** Flow cytometry based detection of Siglec-11 in a mouse model. Siglec-11 is present on the cell surface of brain, liver and spleenocytes of Siglec-11 transgenic mice. No positive signal was found in the control mice. **C** Detection of primary microglia originating from Siglec-11 transgenic and littermate control mice via flow cytometry. Siglec-11 is found on microglia cells from the Siglec-11 transgenic mice. The results shown in A, B and C are representative for 3 individual experiments. The mice used in the experiments were generated by Dr. Yiner Wang (*107*).

3.2.10 PSA-20 treated Siglec-11 transgenic mice show reduced expression of inflammatory markers after LPS application

To investigate the effect of PSA-20 *in vivo* a Siglec-11 transgenic mouse line was used in a model of systemic inflammation. Therefore, Siglec-11 transgenic mice and littermate control mice received 4x PBS, LPS and/or PSA-20 LPS or (1 µg/g bodyweight) 4 days in a row with 24 hours between each treatment. 24 hours past the last injection the animals were sacrificed and brain and spleen samples were taken for

further investigation. Brain and spleen tissue were used for RNA isolation and subsequent qRT-PCR analysis. The cytokines of interest for the experiments were TNF-α, IL1-β as well as the microglia/macrophage marker Iba1.

The Siglec-11 PBS controls in brain and spleen showed no up-regulation of the inflammatory cytokines during the duration of the experiments and levels were equal to the PBS littermate controls. The Siglec-11 positive brain samples from mice that received LPS treatment but no PSA-20 showed reduced lower transcription levels of TNF-α and IL1-β compared to the LPS treated littermate controls. The Iba1 regulation of those samples was similar to the LPS control mice.

A

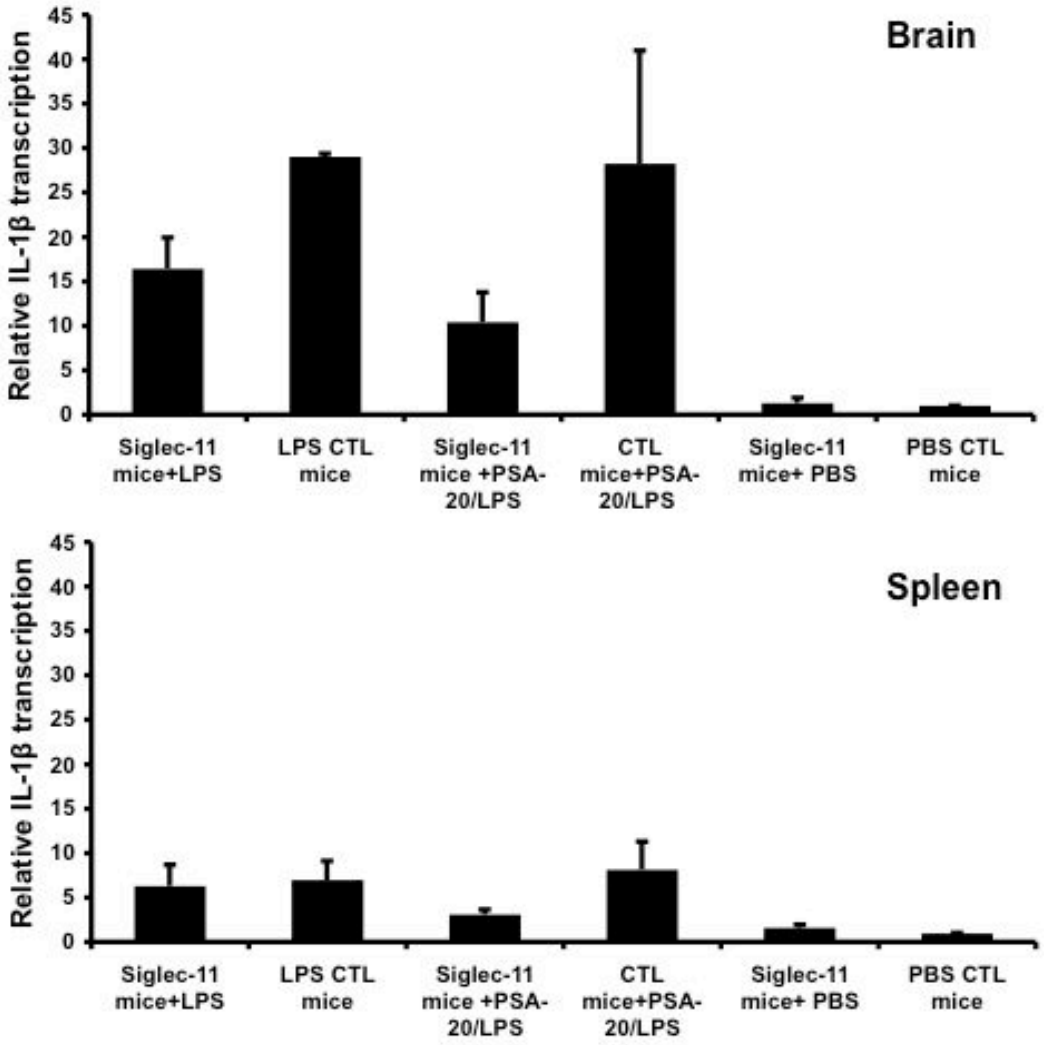

B

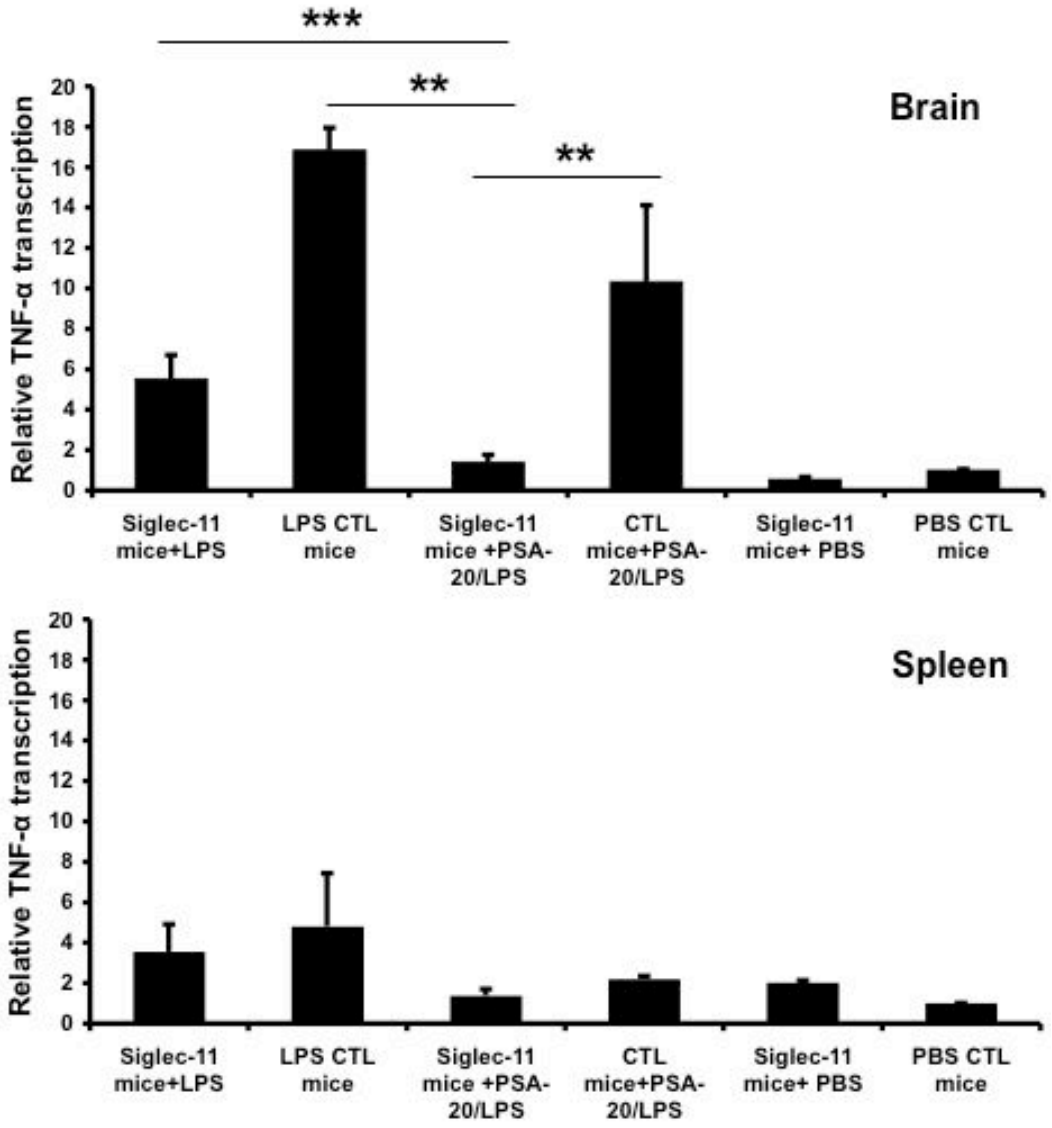
***
**
**
Brain
Relative TNF-α transcription
20
18
16
14
12
10
8
6
4
2
0
Siglec-11 mice+LPS
LPS CTL mice
Siglec-11 mice +PSA-20/LPS
CTL mice+PSA-20/LPS
Siglec-11 mice+ PBS
PBS CTL mice
Spleen
Relative TNF-α transcription
20
18
16
14
12
10
8
6
4
2
0
Siglec-11 mice+LPS
LPS CTL mice
Siglec-11 mice +PSA-20/LPS
CTL mice+PSA-20/LPS
Siglec-11 mice+ PBS
PBS CTL mice

C

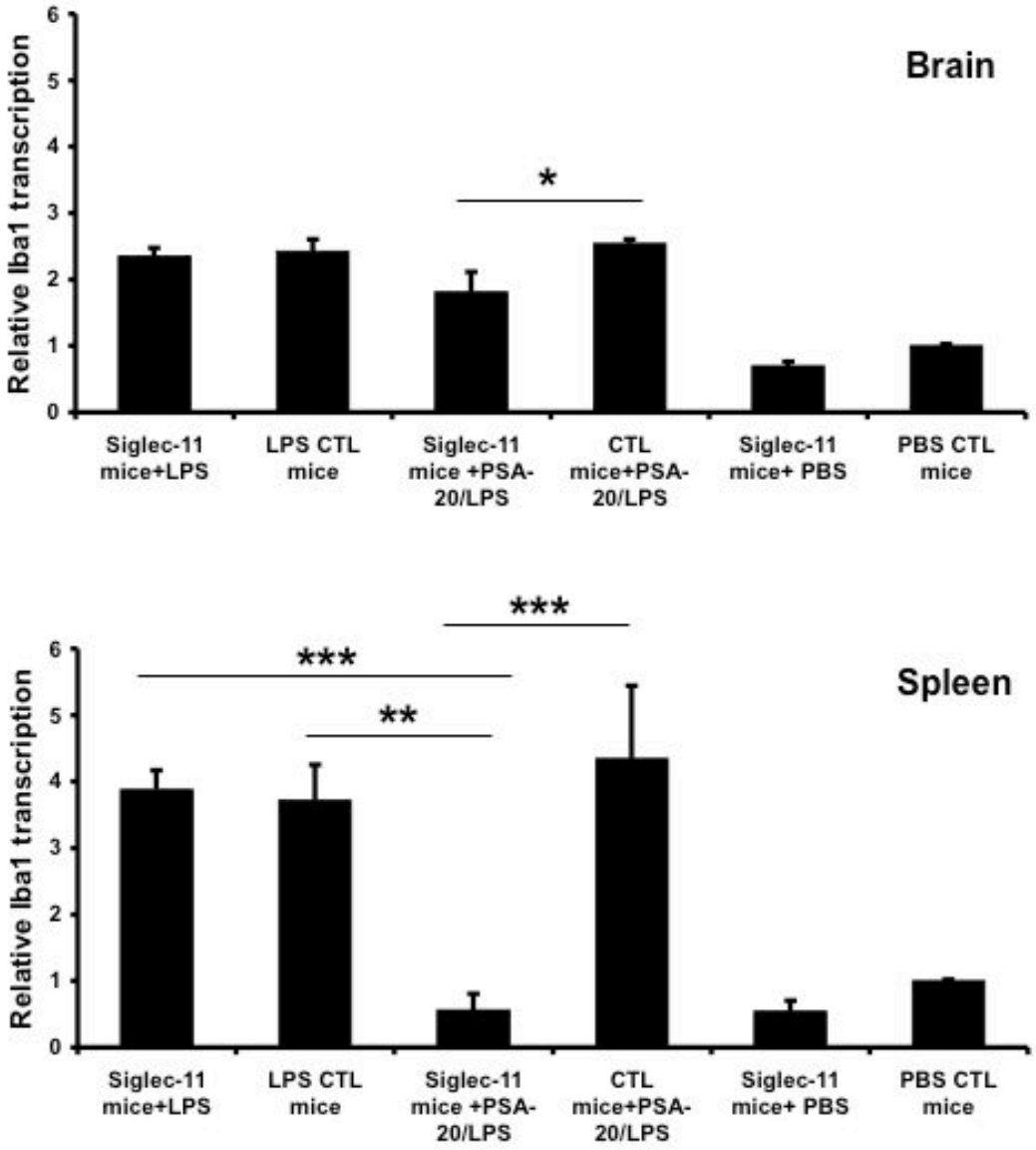

Figure 3.16 PSA-20 treated Siglec-11 transgenic mice show reduced leverls of inflammatory markers after LPS application : Quantification of IL1-β **(A)**, TNF-α **(B)** and Iba1 **(C)** transcription in mouse brain and spleen tissue via qRT-PCR. The mice used in the experiments were generated by Dr. Yiner Wang (*107*). Animals were injected 4x with 1 µg/gbw within 96 hous with a combination of LPS and PSA-20. Regulation of TNF-α, IL1-β and Iba1 was compared to PBS treated animals using GAPDH as internal control. Treatment of PSA-20/LPS showed significantly reduced level of TNF-α transcripts in the brain. Iba1 regulation was significantly reduced in brain and spleen past PSA-20/LPS treatment. Statistics were performed using SPSS software. Anova Bonferroni was chosen as test (✶=p≤0.05, ✶✶p≤0.01, ✶✶✶=p≤0.001). The values are given as mean plus SEM of n = 3-5 mice per condition. Adapted and modified from PCT/EP2014/055445, Neumann *et al*, 2014.

Notable differences in transcription levels of TNF-α, IL1-β and Iba1 were detected in the brain tissue of the animals challenged with the combination of LPS and PSA-20 (Figure 3.16 B and C).

The transcription of TNF-α in LPS/PSA-20 co-stimulated mice was significantly reduced compared to the LPS littermate ($p=0.006$) and LPS Siglec-11 ($p=0.001$) mice. Iba-1 transcription in the brain was impaired after LPS/PSA-20 treatment compared to the LPS/PSA-20 co-stimulated littermate control mice ($p=0.023$). The measurement of the spleen derived material showed different responses to the PSA-20 treatment. TNF-α and IL1-β levels were reduced but not significantly different in the LPS/PSA-20 treated mice. Values of Iba1 in Siglec-11 positive LPS/PSA-20 treated mice were significantly reduced against the LPS injected control ($p=0.003$) and Siglec-11 mice ($p=0.001$). The LPS/PSA-20 treated control mice presented decreased Iba1 transcription ($p=0.001$) as well (Figure 3.16 C).

4. Discussion

4.1 Importance of Siglecs

4.1.1 Siglecs in therapeutic approaches

This project was aiming to study Siglec mediated actions of microglial cells in neuroinflammation. Since Siglecs are linked to ITAM or ITIM structures one Siglec receptor of each kind was chosen. The potential of Siglec-11 and Siglec-H for therapy strategies was of particular interest for the investigation.

Due to their involvements in numerous essential regulatory processes, Siglecs are very important for the maintenance of homeostasis and orchestration of various cellular activities (*42*). Moreover, malfunctioning of Siglecs can also exaggerate inflammatory reactions which may among others foster autoimmune diseases (*35*). Therefore, it is not surprising that within the last years more and more approaches were initialized that are focusing on Siglecs as potential key targets for pharmacological strategies. Until now, the majority of projects involve antibody-based approaches. At the moment the most successful antibody therapy strategies are all aiming at inhibitory Siglecs.

Siglec-2 (CD22) was among the first to be studied. Since it is constitutively expressed on B-cells Siglec-2 offers a major potential for immunotherapy of B-cell malignancies and autoimmune diseases (*68, 69*). A line of clinical trails include toxin conjugated as well as naked antibodies (*68-70*). The humanized monoclonal antibody eratuzumab was shown to internalize into the cell after binding to the Siglec-2 receptor. These results brought about opportunities to carry out interesting experiments involving conjugation with toxins, cytotoxic drugs or radionucleotides (*71*). Currently, eratuzumab is tested with respect to treatment of non-Hodgkin lymphoma and systemic lupus erythematosus (*72*). Another Siglec that was identified as useful target was Siglec-3 (also called CD33). The receptor is constitutive expressed on cells belonging to the hematopoetic system. It is intensively investigated in relation to acute myeloid leukemia. However, despite a line of different phase III studies no antibody therapy based approach was found so far that showed a clear benefit for the patients

(*73-75*). In fact, several studies had to be discontinued due to developments of severe side effects or an outcome that was worse than that of the control group (*73, 74*).
Apart from the pure antibody therapy the novel technology of Siglec glycotargeting is gaining more attention. The underlying concept is called targeted drug or gene delivery (*76*). Carbohydrate-covered drugs or receptor blocking/crosslinking molecules can be applied to inhibit or foster Siglec functions. The induction of apoptosis of eosinophil granulocytes is currently under investigation and represents a promising approach to pharmacologically address allergic diseases (*77*). Although the proof of principle for this technology is given, it is at the moment far from being clinical applicable.
Despite substantial investment of money, time and the undeniable potential, only a minor part of the Siglec receptors are currently enrolled in studies including a therapy strategy. Furthermore, none of the ITAM associated Siglec receptors was until now seriously investigated in terms of being a target for therapy. Although some of the most advanced data available at the moment are derived from antibody based strategies they often fail to provide a clear benefit for the patient or are linked to severe side effects. Therefore, it is essential to extend the search for strategies on how to use the potential offered by the Siglec receptor family more efficiently.

4.2 Presence and function of Siglec-H on microglial cells

4.2.1 Siglec-H expression and regulation on microglia

Zang and co-workers first characterized the murine receptor Siglec-H in 2006 (*47*). Initially, it was considered to be a cell surface marker present on PDCs (*29, 46*). Later Siglec-H was also identified on subsets of macrophages in spleen and lymph nodes. Compared to other members of the receptor family Siglec-H is relatively small and lacks like Siglec-15 its own cytoplasmic signaling domain. Both receptors are mediating signaling via the ITAM linked adapter protein DAP12. No ligand could be determined for Siglec-H so far. However, experiments suggest an involvement of Siglec-H in endocytosis (*47*). When the interaction of PDCs with T-cells was investigated Siglec-H was found to participate in the orchestration of T-cell mediated inflammation and antigen delivery (*48, 78*).

Little is known about the role of DAP12 associated Siglecs in general and Siglec-H in particular regarding functions in innate immunity. Therefore, the basic idea was to investigate whether the receptor was detectable in the CNS on microglial cells. Furthermore, the study was aiming to receive additional insights in the functions of the protein in neuroinflammation. Siglec-H was found to behave different in microglial cells then in PDCs. It was not constantly expressed but up-regulated after defined stimuli. The microglia were challenged with pro-inflammatory factors in order to activate Siglec-H. From all reagents tested only IFN-γ or a combination of LPS and IFN-γ led to a detectable band. These findings were also confirmed on protein level via flow cytometry. Why the regulation is different between the PDCs and the microglia is an interesting question. It is possible that the answer lies in the two different locations of residence of both cell types. PDCs are present within the lymphatic organs or the blood stream. In those environments they are permanently exposed to pathogens and subsequently to T-cells during the process of antigen presentation. Microglia on the other hand are located in an immune privileged area were under normal conditions no or very little pathogens should be present. Thus, a constant presence of the receptor is maybe not necessary on the cell surface of the microglia. However, in case of sensed disorder that leads to the release of IFN-γ the up-regulation of Siglec-H possibly provides the microglial cell with an additional tool to deal with the source of the disorder.

4.2.2 Functions of Siglec-H

DAP12 associated receptors have been shown to play important roles in microglial phagocytosis (*79, 80*). More information is gathered with respect to the signaling cascade, ligands and functions of the receptors. Still little is known about the ligand and function of Siglec-H. In fact Siglec-H is the only member of this family that is not associated with any carbohydrate ligand so far (*47*).

The glycosylation pattern on the surface of cells varies dependent on cell type and activation state. Dramatic alterations of the glycostructure can be found on cells during tumor progression and malignancy (*81*). Recent studies reveal a connection between lectin–glycan interactions and the regulation of tumor microenvironments (*82*). One

characteristic of cancer cells is an increased expression of sialic acid residues on their cell surface (*83*). Furthermore, cancer cells express abnormal glycans on their surfaces, which are meanwhile in parts well characterized, and serve as biomarkers in cancer (*84, 85*). Some of these tumor-associated glycobiomarkers like the sialyl-Tn antigen, which is abnormally expressed in several types of cancer, is recognized by the DAP12 associated receptor Siglec-15 (*85*).

The performed experiments in this thesis now link Siglec-H with binding to glioma cells, but not to astrocytes or any other normal mouse cells tested. Although the function of Siglec-H in various aspects is unclear it has been previously described to execute the uptake of antigens (*46, 47*). Indeed Siglec-H on microglia showed the capability to specifically mediate engulfment of beads under pro-inflammatory IFN-γ stimulation in the performed experiments. In combination with the selective binding of the Siglec-H Fc fusion protein to glioma cells the data suggest that microglia can recognize and phagocytose malignant cells via the Siglec-H receptor. Although the precise molecular structures recognized on the glioma cells are unclear there are interesting similarities to human Siglec-15. Mouse Siglec-H and the structural similar human Siglec-15 appear both to recognize and fight of tumor cells. This would suggest an involvement of this DAP12 associated receptors in recognition and removal of cells that have undergone malignant changes. In this regard the fact that none of the regular α2-3, α2-6 or α2-8 linked sialic acids could be identified as ligands for Siglec-H is particularly interesting. It is very well possible that what they recognize is not a regular linked sialic acid but a variation caused by a mutation in the malignant cells that is not found in healthy cells.

Siglec-H is so far known for modulation of IFN-α release (*29, 86*). This new data provide solid hints regarding additional functions of ITAM signaling Siglec receptors. If confirmed in general these data would provide options for therapeutic strategies involving DAP12 associated Siglecs in cancer biology.

4.3 Siglec-11 interaction with sialic acids in neuroinflammation

4.3.1 PSA-20 a promising Siglec-11 ligand

Over the recent years increasing insights have been gained regarding the importance of glycobiology in various pathologies. Siglecs as receptors of sialic acids have been found to be involved not only in the maintenance of homeostasis but also in multiple immune relevant processes (*43*). Siglecs are also of high importance in all kinds of diseases including cancer, infectious or autoimmune reactions (*35, 85, 87*). As mentioned earlier, based on this knowledge substantial effort was initialized to develop therapeutic strategies involving Siglecs. However, most of the ideas follow conventional antibody based strategies, which often failed to provide beneficial results for the patients (*21*). No attempt aimed to make direct use of sialic acids as the natural ligand of the Siglec receptor family.

When Siglec-11 was discovered in 2002 low but distinct presence of Siglec-11 was detected via immuno-histochemical staining in a line of tissues. Expression of the protein was identified in microglial cells, Kupffer cells in the liver, intestinal lamina-propria macrophages, and perifollicular cells in the spleen, as well as in cells from tonsils and appendix (*23*). Recently, investigation of the ITIM exhibiting Siglec-11 was started with respect to neuroinflammation (*51*). Wang and co-workers used murine primary microglial cells that were transduced with a lentiviral vector to over-express a flag-tagged human Siglec-11 receptor variant. Stimulation of Siglec-11 by cross-linking with flag-specific antibodies led to the down-regulation of important pro-inflammatory cytokines in LPS treated microglia. Furthermore, neuroprotective effects of the Siglec-11 receptor were found in a neuron microglia co-culture system (*51*). The experimental approach used provided exciting data regarding the function Siglec-11 and highlighted it as promising target for therapy strategies. The disadvantage was that the flag-based approach was relative artificial.

To overcome this issue stimulation with soluble α2.8-linked PSA was chosen to further study the role of Siglec-11 in neuroinflammation (*23*). Microglia are, while patrolling the CNS, constantly exposed to sialic acids that represent an essential part of the cellular glycocalyx (*88*). In a healthy environment microglia should therefore constantly receive signals by sialic acid interactions with Siglec-11 that prevent them from getting

activated. Since sialic acids are regular participants in various cell-cell interactions (*3, 89*), contact to PSA could be considered by the immune cells as a sign of a not endangered area. Due to the receptor cross-linking data the assumption was that stimulation of Siglec-11 with PSA should initialize anti-inflammatory signaling.

The data generated *in vitro* highlight that different sizes of PSA do not have uniform effects on the cells. Short-chained sialic acids and PSA-20 are not affecting the cell metabolic activity in a negative way while PSA-60 and -180 reduced the metabolic activity of the cells. Apparently, the intensity of the signaling depends on the size of the sialic acids. It is more than likely that a certain concentration of larger sialic acid molecules is creating an amount of ITIM-linked signaling that has harmful consequences. This might occur via simultaneous activation of several Siglec-11 receptors by one sialic acid. If the inhibitory signals are too extensive the cell might shut down mechanisms, affecting the metabolic turnover like shown by the MTT assay. This would mean that cells are more capable to tolerate exposure to shorter sialic acids. To validate the PSA-20 effects observed in microglia a repetition of the metabolic turnover experiments using other Siglec-11 positive cells like macrophages should be performed.

Furthermore, not only metabolic activity but also inflammatory reactions were affected differently by sialic acids of various sizes. PSA-20 and PSA-60 counteracted the up-regulation of TNF-α transcripts in LPS stimulated microglia in a significant way. To a minor degree PSA-180 also showed this tendency. The fact that the mono-, tri- or hexa-sialic acids failed completely to dampen the LPS induced increase of TNF-α transcription suggests that also a minimum size is required to initialize a successful signaling. It is clear that the parameters investigated so far are not sufficient to cover the full spectrum of possible PSA reaction mechanisms appropriate. Nevertheless, the cell metabolic activity and TNF-α transcription data give evidence that the size of the PSA is a crucial point that has to be considered carefully if PSA is to be used for therapeutic purposes. Hence, for further experiments the short but still effective PSA-20 was the clear favorite.

4.3.2 PSA-20 a modulator of inflammation

The fact that stimulation of LPS co-treated microglia or macrophages with PSA-20 impaired the transcription of TNF-α was highly interesting with respect to treatment opportunities. Binding and downstream signaling of the cytokine with one of its cognate receptors, TNF-RI or TNF-RII, modulates fundamental processes in neuroinflammation including, gliosis, demyelination, blood–brain-barrier deterioration and neuronal cell death (*90, 91*). Furthermore, TNF-α has been shown to play an important role in systemic inflammation as well as in multiple sclerosis. Both pathologies are leading to severe cases of neuroinflammation and so far therapeutic approaches like TNF-α depletion often failed to provide satisfying results (*87*). In studies involving acute and chronic inflammation the effects of an anti-TNF-α therapy were not uniform as well. In sepsis a blockade of the cytokine worsened the conditions (*87*). On the other hand, it was found to be a very promising approach in rheumatoid arthritis (*92*). The potential of PSA-20 was revealed by the fact that it did not only affect TNF-α but was effective in a more general way. Since the reasons for the inflammation associated damage in diseases are rarely due to only one factor but often interact and enhance each other this feature is essential in order to have a certain treatment flexibility.

Experiments with microglia as well as with macrophages revealed that PSA-20 was significantly affecting phagocytosis as another key element of immune cell activation. Microglia can not only engulf apoptotic cells in inflamed tissues but also clear cellular debris/synapses during neuronal remodeling processes (*93*). Microglia are also capable to engulf stressed but viable neurons during inflammatory diseases (*93, 94*). Independently from each other several laboratories showed that in inflammation the ability of microglia to discriminate between living and dead neurons is impaired. As a consequence LPS or amyloid-β activated immune cells attacked healthy cells and reduced the numbers of neurons via phagocytosis (*95*). Administration of 1.5 µM PSA-20 was enough to decrease the transcription of TNF-α and the phagocytosis activity of microglia and macrophages significantly. Both cell types are highly involved in various inflammation-linked diseases within the CNS (*96*). If PSA-20 prevents uncontrolled exposure of neuronal structures to TNF-α and phagocytosis this could result in less damage to the cells. Since the dose used in the experiments is relative low there is also very little danger that the endogenous molecules cause negative effects by

themselves. Moreover, the sh-RNA based knock-down experiments proved a specific relation of PSA-20 binding to Siglec-11 and the observed impairment of inflammation. In summary the administration of PSA-20 to microglia and macrophages in cell culture experiments revealed substantial potential of the compound for anti-inflammatory treatment strategies.

4.3.3 Therapy of inflammation by sialic acids in disease models

Since the *in vitro* approach is always insufficient to test the potency of an experimental procedure animal models were required to further investigate the Siglec-11 interaction with PSA-20. In medicine bacterial sepsis, a systemic inflammatory response syndrome caused amongst others by LPS exposure is responsible for millions of deaths worldwide (*97*). Over time the inflammatory response caused by the invading pathogens gets out of balance leading to severe tissue damage (*98*). The longer pro-inflammatory markers persist the more harm they can cause. In case of TNF-α pathological alteration of lipid and glucose metabolism have been described (*99*).
A murine animal model of chronic inflammation induced by LPS injection was therefore an interesting tool to investigate the PSA-20 effect on TNF-α and other relevant inflammation markers like IL1-β and Iba1. The acquired data show a very strong suppression of TNF-α transcription levels in the brain while the spleen was not affected. IL1-β was neither modulated in the brain nor in the spleen in a notable way. Finally, Iba1 showed a decrease of transcripts that was exclusive to the spleen. The effect of PSA-20 on the regulation of the investigated genes was not uniform but selective and is therefore different to the effect of for example corticosteroids. The use of this inflammation-modulatory compound in sepsis is highly controversial since it is unclear when and under what circumstances it is beneficial. Additionally, corticosteroids act very unspecific and can present severe side effects (*100*). Hence, the application of PSA-20 could provide an option to modulate the TNF-α linked inflammatory processes during infectious events and chronic inflammation. Furthermore, the interference with the immune system would occur in a less stressful way then for example TNF-α depletion treatment (*99*).

Phagocytosis of healthy cells due to misjudgment during inflammation has been reported recently (*95*). Although, not investigated in our mouse model it is not far-fetched to speculate that the PSA-20 induced reduction of phagocytosis observed in cell culture experiments could also be happening *in vivo*. To allow a more qualified statement more inflammation relevant cytokines and receptors need to become investigated in the future to understand better what effects are restricted to the CNS and which are relevant for other organ sides. Furthermore, it is always important to keep in mind, that it is never possible to transfer *in vitro* data 1 to 1 to the *in vivo* situation. The selectivity of the PSA-20 treatment could allow very localized treatment without danger of offside effects.

4.3.4 Outlook

Besides the investigated model of systemic inflammation there are several other disease models that appear to be highly promising for PSA-20 testing. One of them is the model of experimental autoimmune encephalomyelitis (EAE). In previous EAE experiments including anti TNF-α approaches, application of anti-TNF-α or sTNF-α receptor antibodies attenuated the disease (*101, 102*). Studies have demonstrated that TNF-α is crucial in the early stages of EAE, whereas in later phases other mechanisms are dominating. According to literature, TNF-α may be more essential for initial leukocyte homing rather than progression of later stage disease (*103*). TNF-α levels measured in the CSF of patients suffering from multiple sclerosis were abnormally high and correlated with disease severity and progression (*104, 105*). TNF-α was found to be involved in myelin and oligodendrocyte deterioration, lymphocyte infiltration, astrocyte activation, and the up-regulation of MHC I and II molecules on CNS resident cells, thereby triggering T-cell responses. Despite the increasing knowledge about the beneficial effects of TNF-α suppression, all antibody-based studies tried so far were ineffective or had severe side effects. Therefore, tackling the problem from a different angle appears to be necessary. PSA-20 is an endogenous molecule that showed no harmful effects in cell culture systems. It should cause none of the undesired consequences observed in antibody-based therapies. Furthermore, the concentration of PSA-20 that was required to generate significant data in the different experimental

systems is quite low. This would mean that also the metabolism needs to be challenged with a dose that is easy to handle and so less stressful for the patient. One possible limitation of PSA-20 usage in multiple sclerosis is the fact, that TNF-α is only an essential factor in the beginning of the disease. It could be a very good treatment option if multiple sclerosis is recognized early enough. Measurement of TNF-α levels in PSA-20 treated EAE mice at different time points would be most interesting to determine the best time point for the application. Given that the undesired increase of the cytokine could be stopped milder clinical outcome in patients that received PSA-20 at the very onset of symptoms could be achieved. Later during the disease PSA-20 administration might be less effective. This is however a point that has to be investigated intensively in future experiments.

5 Summary

Sialic acid binding Siglecs are involved in various pathological processes. A minor fraction of Siglecs mediates activating signals via the ITAM linked DAP12 adaptor protein while the majority of Siglecs modulates inflammatory reactions via ITIM units. Siglec-11 and Siglec-H are both expressed on microglia cells but exhibit structural and functional differences. To get a better understanding about the function of Siglecs in microglia, one Siglec linked to ITAM and one linked to ITIM structures were studied.
In cell culture experiments the ITAM associated murine Siglec-H receptor was up-regulated after IFN-γ stimulation or IFN-γ/LPS co-stimulation in primary and cell line microglia. Microglial cells showed Siglec-H mediated engulfment of latex beads under pro-inflammatory conditions. Furthermore, a Siglec-H fc fusion protein bound to structures on two independent glioma cell lines while it did not bind control cells in *in vitro* experiments. Human Siglec-11 that exhibits an ITIM domain in its cytoplasmic tail is constitutively expressed on microglia and macrophages. The receptor was up-regulated after pro- and anti-inflammatory stimulation. Via heat mediated hydrolysis and subsequent separation using a HPLC system, α2-8 linked sialic acid molecules with a length of around 20, 60 and 180 sialic acid chains were generated. Treatment with the different sizes of sialic acids revealed a chain length of around 20 sialic acids (PSA-20) to not cause harmful effects on the metabolic activity at concentrations of 0.15 µM, 0.5 µM and 1.5 µM. Post stimulation with PSA-20, a down-regulation of TNF-α transcription and phagocytosis activity was detected in microglia and macrophage cell lines. For *in vivo* experiments a Siglec-11 transgenic mouse line expressing Siglec-11 in the brain, spleen and liver was used. When the Siglec-11 mice were used in a model of chronic inflammation, PSA-20 mediated suppression of TNF-α transcription in the brain was successfully detected. The data reveal sophisticated functions of the two investigated Siglecs regarding recognition of disturbances and modulation of inflammatory reactions in the CNS. Therefore, the Siglec receptors represent interesting research targets that can increase understanding of the Siglec mediated defense against malignant cells and the modulation of inflammation in the CNS.

6 References

1. K. Drickamer, M. E. Taylor, *Annu Rev Cell Biol* **9**, 237 (1993).
2. A. Varki, *Glycobiology* **3**, 97 (Apr, 1993).
3. A. Varki, T. Angata, *Glycobiology* **16**, 1R (Jan, 2006).
4. A. F. Williams, A. N. Barclay, *Annu Rev Immunol* **6**, 381 (1988).
5. P. R. Crocker, S. Gordon, *J Exp Med* **169**, 1333 (Apr 1, 1989).
6. P. R. Crocker, S. Gordon, *J Exp Med* **164**, 1862 (Dec 1, 1986).
7. I. Stamenkovic, B. Seed, *Nature* **345**, 74 (May 3, 1990).
8. P. R. Crocker *et al.*, *Embo J* **10**, 1661 (Jul, 1991).
9. I. Stamenkovic, D. Sgroi, A. Aruffo, M. S. Sy, T. Anderson, *Cell* **66**, 1133 (Sep 20, 1991).
10. L. D. Powell, D. Sgroi, E. R. Sjoberg, I. Stamenkovic, A. Varki, *J Biol Chem* **268**, 7019 (Apr 5, 1993).
11. W. A. Hamilton *et al.*, *Phys Rev Lett* **72**, 2219 (Apr 4, 1994).
12. S. Kelm *et al.*, *Curr Biol* **4**, 965 (Nov 1, 1994).
13. S. D. Freeman, S. Kelm, E. K. Barber, P. R. Crocker, *Blood* **85**, 2005 (Apr 15, 1995).
14. L. D. Powell, A. Varki, *J Biol Chem* **270**, 14243 (Jun 16, 1995).
15. P. R. Crocker *et al.*, *Glycobiology* **8**, v (Feb, 1998).
16. P. R. Crocker, J. C. Paulson, A. Varki, *Nat Rev Immunol* **7**, 255 (Apr, 2007).
17. T. Angata, E. H. Margulies, E. D. Green, A. Varki, *Proc Natl Acad Sci U S A* **101**, 13251 (Sep 7, 2004).
18. P. R. Crocker *et al.*, *Embo J* **13**, 4490 (Oct 3, 1994).
19. J. Q. Zhang, B. Biedermann, L. Nitschke, P. R. Crocker, *Eur J Immunol* **34**, 1175 (Apr, 2004).
20. J. Q. Zhang, G. Nicoll, C. Jones, P. R. Crocker, *J Biol Chem* **275**, 22121 (Jul 21, 2000).
21. C. Jandus, H. U. Simon, S. von Gunten, *Biochem Pharmacol* **82**, 323 (Aug 15).
22. J. Kopatz *et al.*, *Glia* **61**, 1122 (Jul).
23. T. Angata *et al.*, *J Biol Chem* **277**, 24466 (Jul 5, 2002).
24. H. Cao *et al.*, *Eur J Immunol* **38**, 2303 (Aug, 2008).
25. H. Cao, P. R. Crocker, *Immunology* **132**, 18 (Jan).
26. C. A. Lowell, *Cold Spring Harb Perspect Biol* **3** (Mar).

27. S. P. Paul, L. S. Taylor, E. K. Stansbury, D. W. McVicar, *Blood* **96**, 483 (Jul 15, 2000).

28. T. Avril, H. Floyd, F. Lopez, E. Vivier, P. R. Crocker, *J Immunol* **173**, 6841 (Dec 1, 2004).

29. A. L. Blasius, M. Cella, J. Maldonado, T. Takai, M. Colonna, *Blood* **107**, 2474 (Mar 15, 2006).

30. T. Angata, T. Hayakawa, M. Yamanaka, A. Varki, M. Nakamura, *Faseb J* **20**, 1964 (Oct, 2006).

31. T. Angata, Y. Tabuchi, K. Nakamura, M. Nakamura, *Glycobiology* **17**, 838 (Aug, 2007).

32. M. Ando, W. Tu, K. Nishijima, S. Iijima, *Biochem Biophys Res Commun* **369**, 878 (May 9, 2008).

33. N. Palaskas *et al.*, *Cancer Res* **71**, 5164 (Aug 1).

34. C. R. Boyd *et al.*, *J Immunol* **183**, 7703 (Dec 15, 2009).

35. T. Angata *et al.*, *Cell Mol Life Sci* (Mar 22).

36. T. Angata, A. Varki, *Chem Rev* **102**, 439 (Feb, 2002).

37. M. Cohen, A. Varki, *Omics* **14**, 455 (Aug).

38. A. Varki, T. K. Altheide, *Genome Res* **15**, 1746 (Dec, 2005).

39. C. E. Finch, *Proc Natl Acad Sci U S A* **107 Suppl 1**, 1718 (Jan 26).

40. M. Schwarzkopf *et al.*, *Proc Natl Acad Sci U S A* **99**, 5267 (Apr 16, 2002).

41. A. Varki, *Nature* **446**, 1023 (Apr 26, 2007).

42. A. Varki, R. Schauer, (2009).

43. A. Varki, *Glycobiology* **21**, 1121 (Sep).

44. Y. Liu, G. Y. Chen, P. Zheng, *Trends Immunol* **30**, 557 (Dec, 2009).

45. I. C. Schoenhofen, D. J. McNally, J. R. Brisson, S. M. Logan, *Glycobiology* **16**, 8C (Sep, 2006).

46. A. L. Blasius, M. Colonna, *Trends Immunol* **27**, 255 (Jun, 2006).

47. J. Zhang *et al.*, *Blood* **107**, 3600 (May 1, 2006).

48. H. Takagi *et al.*, *Immunity* **35**, 958 (Dec 23).

49. C. Liu *et al.*, *J Clin Invest* **118**, 1165 (Mar, 2008).

50. X. Wang *et al.*, *Mol Biol Evol* **29**, 2073 (Aug).

51. Y. Wang, H. Neumann, *J Neurosci* **30**, 3482 (Mar 3).

52. C. A. Janeway, Jr., R. Medzhitov, *Annu Rev Immunol* **20**, 197 (2002).

53. S. Akira, *Curr Opin Immunol* **15**, 5 (Feb, 2003).

54. D. M. Underhill, A. Ozinsky, *Annu Rev Immunol* **20**, 825 (2002).

55. U. K. Hanisch, H. Kettenmann, *Nat Neurosci* **10**, 1387 (Nov, 2007).

56. F. Ginhoux *et al.*, *Science* **330**, 841 (Nov 5).

57. Y. Z. Xu, M. Nygard, K. Kristensson, M. Bentivoglio, *Brain Behav Immun* **24**, 138 (Jan).

58. M. Griffiths, J. W. Neal, P. Gasque, *Int Rev Neurobiol* **82**, 29 (2007).

59. S. Gordon, *Nat Rev Immunol* **3**, 23 (Jan, 2003).

60. F. Gonzalez-Scarano, G. Baltuch, *Annu Rev Neurosci* **22**, 219 (1999).

61. U. G. Liebert, *Intervirology* **40**, 176 (1997).

62. H. Neumann, I. M. Medana, J. Bauer, H. Lassmann, *Trends Neurosci* **25**, 313 (Jun, 2002).

63. J. Vogt *et al.*, *Ann Neurol* **66**, 310 (Sep, 2009).

64. W. Li, M. B. Graeber, *Neuro Oncol* **14**, 958 (Aug).

65. P. Allavena, A. Sica, G. Solinas, C. Porta, A. Mantovani, *Crit Rev Oncol Hematol* **66**, 1 (Apr, 2008).

66. D. Aminoff, *Biochem J* **81**, 384 (Nov, 1961).

67. H. A. Goldberg, K. J. Warner, *Anal Biochem* **251**, 227 (Sep 5, 1997).

68. M. J. Townsend, J. G. Monroe, A. C. Chan, *Immunol Rev* **237**, 264 (Sep).

69. M. K. O'Reilly, J. C. Paulson, *Trends Pharmacol Sci* **30**, 240 (May, 2009).

70. J. P. Leonard, D. M. Goldenberg, *Oncogene* **26**, 3704 (May 28, 2007).

71. J. Carnahan *et al.*, *Clin Cancer Res* **9**, 3982S (Sep 1, 2003).

72. A. M. Jacobi *et al.*, *Ann Rheum Dis* **67**, 450 (Apr, 2008).

73. E. J. Feldman *et al.*, *J Clin Oncol* **23**, 4110 (Jun 20, 2005).

74. S. H. Petersdorf *et al.*, *Blood* **121**, 4854 (Jun 13).

75. F. Ravandi, *J Clin Oncol* **29**, 349 (Feb 1).

76. M. S. Wadhwa, K. G. Rice, *J Drug Target* **3**, 111 (1995).

77. Y. M. Park, B. S. Bochner, *Allergy Asthma Immunol Res* **2**, 87 (Apr).

78. J. Loschko *et al.*, *J Immunol* **187**, 6346 (Dec 15).

79. B. Linnartz, H. Neumann, *Glia* **61**, 37 (Jan).

80. S. Wakselman *et al.*, *J Neurosci* **28**, 8138 (Aug 6, 2008).

81. K. Ohtsubo, J. D. Marth, *Cell* **126**, 855 (Sep 8, 2006).

82. G. A. Rabinovich, D. O. Croci, *Immunity* **36**, 322 (Mar 23).

83. N. M. Varki, A. Varki, *Lab Invest* **87**, 851 (Sep, 2007).

84. K. Shida *et al.*, *Glycobiology* **20**, 1594 (Dec).

85. R. Takamiya, K. Ohtsubo, S. Takamatsu, N. Taniguchi, T. Angata, *Glycobiology* **23**, 178 (Feb).

86. F. Puttur *et al.*, *PLoS Pathog* **9**, e1003648.

87. K. Reinhart, W. Karzai, *Crit Care Med* **29**, S121 (Jul, 2001).

88. X. Wang *et al.*, *Glycobiology* **21**, 1038 (Aug).

89. S. Kelm, R. Schauer, *Int Rev Cytol* **175**, 137 (1997).

90. S. L. Montgomery, W. J. Bowers, *J Neuroimmune Pharmacol* **7**, 42 (Mar).

91. R. A. Heller, K. Song, N. Fan, D. J. Chang, *Cell* **70**, 47 (Jul 10, 1992).

92. P. Barrera *et al.*, *Rheumatology (Oxford)* **41**, 430 (Apr, 2002).

93. M. E. Tremblay *et al.*, *J Neurosci* **31**, 16064 (Nov 9).

94. J. J. Neher *et al.*, *J Immunol* **186**, 4973 (Apr 15).

95. M. Fricker *et al.*, *J Neurosci* **32**, 2657 (Feb 22).

96. G. C. Brown, J. J. Neher, *Nat Rev Neurosci* **15**, 209 (Apr).

97. R. C. Bone *et al.*, *Chest* **136**, e28 (Nov, 2009).

98. D. Annane, E. Bellissant, J. M. Cavaillon, *Lancet* **365**, 63 (Jan 1-7, 2005).

99. C. Popa, M. G. Netea, P. L. van Riel, J. W. van der Meer, A. F. Stalenhoef, *J Lipid Res* **48**, 751 (Apr, 2007).

100. G. P. Patel, R. A. Balk, *Am J Respir Crit Care Med* **185**, 133 (Jan 15).

101. K. Selmaj, C. S. Raine, A. H. Cross, *Ann Neurol* **30**, 694 (Nov, 1991).

102. D. Baker *et al.*, *Eur J Immunol* **24**, 2040 (Sep, 1994).

103. H. Korner *et al.*, *J Exp Med* **186**, 1585 (Nov 3, 1997).

104. J. Beck *et al.*, *Acta Neurol Scand* **78**, 318 (Oct, 1988).

105. M. K. Sharief, R. Hentges, *N Engl J Med* **325**, 467 (Aug 15, 1991).

106. H. Neumann *et al.*, PCT/EP2014/055445, (2014).

107. Y. Wang, urn:nbn:de:hbz:5N-18095, (2009)

7 List of Publications

7.1 Peer reviewed Journals

1. MacKinnon AC, Kopatz J, Sethi T. Br Med Bull. The molecular and cellular biology of lung cancer: identifying novel therapeutic strategies. 2010;95:47-61. doi: 10.1093/bmb/ldq023. Epub 2010 Jul 19. Review.

2. Linnartz B, Kopatz J, Tenner AJ, Neumann H. Sialic acid on the neuronal glycocalyx prevents complement C1 binding and complement receptor-3-mediated removal by microglia. J Neurosci. 2012 Jan 18;32(3):946-52. doi: 10.1523/JNEUROSCI.3830-11.2012.

3. Kopatz J, Beutner C, Welle K, Bodea LG, Reinhardt J, Claude J, Linnartz-Gerlach B, Neumann H. Siglec-h on activated microglia for recognition and engulfment of glioma cells. Glia. 2013 Apr 30. doi: 10.1002/glia.22501.

4. Linnartz-Gerlach B, Kopatz J, Neumann H. Siglec functions of microglia. Glycobiology. 2014 May 15. pii: cwu044. [Epub ahead of print] Review.

5. Neurodegeneration by activation of the microglial complement-phagosome pathway. Bodea LG, Wang Y, Linnartz-Gerlach B, Kopatz J, Sinkkonen L, Musgrove R, Kaoma T, Muller A, Vallar L, Di Monte DA, Balling R, Neumann H.
J Neurosci. 2014 Jun 18;34(25):8546-56. doi: 10.1523/JNEUROSCI.5002-13.2014.

7.2 Abstracts

1. Jens Kopatz and Harald Neumann, Induction of Siglec-H on microglia by interferon-γ and its involvement in phagocytosis, X European Meeting on Glial Cells in Health and Disease- Prague 2011, Neural Regeneration, Institute of Reconstructive Neurobiology, University Hospital Bonn, University Bonn, 53127 Bonn, Germany

2. Jens Kopatz, Clara Beutner, Johannes Ackermann, Harald Neumann,
M1-polarized microglia clear glioma cells via the Siglec-H receptor. 8th FENS Forum of Neuroscience - Barcelona 2012,
Neural Regeneration, Institute of Reconstructive Neurobiology, University Hospital Bonn, University Bonn, 53127 Bonn, Germany

3. Jens Kopatz, Clara Beutner, Johannes Ackermann, Harald Neumann,
Siglec-h on M1-polarized microglia antagonizes glioma cells growth, XI European Meeting on Glial Cells in Health and Disease –Berlin 2013,

Neural Regeneration, Institute of Reconstructive Neurobiology, University Hospital Bonn, University Bonn, 53127 Bonn, Germany

7.3 Submitted patent

1. Neumann H, Kopatz J, Sharaz A, Karlstetter M, Langmann T, Polysialic acid and use for treatment of neurodegenerative and neuroinflammatory diseases. PCT/EP2014/055445, 2014.

8. Declaration/Erklärung

Hiermit versichere ich, dass diese Dissertation von mir persönlich, selbständig und ohne jede unerlaubte Hilfe angefertigt wurde. Die Daten, welche im Rahmen einer Kooperation gewonnen wurden sind ausnahmslos gekennzeichnet. Die aus anderen Quellen übernommenen Daten, Abbildungen und Konzepte sind unter Angabe der jeweiligen Quelle gekennzeichnet. Die vorliegende Arbeit wurde an keiner anderen Hochschule als Dissertation eingereicht. Ich habe früher noch keinen Promotionsversuch unternommen.

Jens Christopher Kopatz,
Bonn, den 04.07 2014

9. Danksagung

Zuerst möchte ich mich bei Herrn Prof. Harald Neumann für die Möglichkeit der Promotion in seiner Arbeitsgruppe sowie die gute Förderung bedanken. Dies gilt besonders für die intensive und konstruktive Betreuung während der gesamten Zeit. Großer Dank gilt auch meinem Zweitgutachter Herrn Prof. Joachim Schultze welcher es schaffte mich zusätzlich zu motivieren. Mir ist bewusst, dass dieses Maß an Aufmerksamkeit und Interesse am Vorankommen des einzelnen Studenten seitens meiner beiden Betreuer nicht der Regelfall ist.

Ich möchte mich auch ausdrücklich bei sämtlichen ehemaligen und aktuellen Mitgliedern der Ag Neumann sowie meinen Kollegen am Institut für Rekonstruktive Neurobiologie für Ihre offene, hilfsbereite und freundliche Art bedanken. Ich habe die Arbeit mit euch immer als angenehm und motivierend empfunden.
Weiterhin möchte ich mich bei Prof. Gieselmann und seinen Mitarbeitern für die tolle Zusammenarbeit bedanken. Besonders Norbert Rösel war mir eine große Hilfe bei der Aufreinigung des PSAs. Herzlicher Dank gebührt Dr. Yiner Wang für das zur Verfügung stellen der Siglec-11 Maus Linie sowie Dr. Glas und Prof. Herrlinger für die GL261 und SMA560 Zellen.

Schließlich möchte ich mich bei meinen Eltern, meiner Schwester und meiner Freundin Lena für die unermüdliche Unterstützung bedanken. Ohne euch wäre ich nicht so weit gekommen.